

FORDAHL, STEVE, Ph.D. The Effect of Manganese Neurotoxicity on the γ -Aminobutyric Acid (GABA) Neurotransmitter System. (2013)
Directed by Dr. Keith M. Erikson. pp. 187

Manganese (Mn) is an essential metal that functions primarily as a cofactor for metalloenzymes contributing to numerous metabolic pathways. Exposure to excess environmental Mn overwhelms endogenous regulation, and deleterious effects disrupt neurotransmitter systems of the basal ganglia. The following studies examined the effects of Mn on γ -aminobutyric acid (GABA) using *in vivo* microdialysis, metabolomic analysis, and primary astrocyte cell culture. Microdialysis experiments in Sprague-Dawley rats revealed that 6-week exposure to Mn (1g Mn/L drinking water) significantly elevated extracellular GABA compared to controls. Using nipecotic acid to antagonize GABA transport proteins (GATs), we identified that Mn disrupted GABA homeostasis by inhibiting GAT mediated GABA clearance. Concurrently, metabolomic analysis of Mn exposed rats uncovered drastically altered lipid metabolism highlighted by a 12- and 15-fold increase in oleic and palmitic acids compared to control, respectively. Brain Mn accumulation was accompanied by abnormal stereotypy and was significantly correlated with plasma homogentisic, chenodeoxycholic, and aspartic acids, identifying biomarkers that correspond with Mn neurotoxicity. To elucidate mechanisms driving Mn induced changes in GABA uptake, primary astrocytes were exposed to Mn with or without oleic or palmitic acid. ^3H -GABA uptake was significantly reduced by Mn and exacerbated by oleic or palmitic acids. Plasma membrane levels of GAT3 were unaltered by Mn or fatty acids

despite increased regulatory protein kinase C (PKC) phosphorylation; however, fatty acid treatments augmented Mn accumulation at the plasma membrane of astrocytes. Moreover, control cells exposed to Mn exclusively during the experimental uptake had significantly reduced ³H-GABA uptake, and the addition of 50 μM GABA blunted cytosolic Mn accumulation. These data indicate that reduced GAT3 function in astrocytes is not driven by PKC signaling, but is likely influenced by Mn and fatty acids interacting with the plasma membrane, thereby inhibiting GABA uptake via GAT3. Together these studies improve our understanding of how Mn alters GABA neurotransmission upon overexposure. Furthermore, these data provide candidate biomarkers to improve early detection of Mn intoxication prior to irreparable damage.

THE EFFECT OF MANGANESE NEUROTOXICITY ON THE γ -AMIMOBUTYRIC
ACID (GABA) NEUROTRANSMITTER
SYSTEM

by

Steve Fordahl

A Dissertation Submitted to
the Faculty of the Graduate School at
The University of North Carolina Greensboro
in Partial Fulfillment
of the Requirements for the Degree
Doctor of Philosophy

Greensboro
2013

Approved by

Committee Chair

APPROVAL PAGE

This dissertation has been approved by the following committee of the Faculty of the Graduate School at the University of North Carolina at Greensboro.

Committee Chair _____
Committee Members _____

Date of Acceptance by Committee

Date of Final Oral Examination

ACKNOWLEDGEMENTS

This research was supported by the National Institutes of Health R15 NS061 309-01, North Carolina Biotechnology Center #2007-BRG-1253, Wake Forest University, and a Regular Faculty Grant from the University of North Carolina at Greensboro.

TABLE OF CONTENTS

	Page
LIST OF TABLES	vii
LIST OF FIGURES	viii
CHAPTER	
I. INTRODUCTION	1
II. REVIEW OF LITERATURE	5
Introduction	5
Manganese Exposure	7
Dietary	7
Environmental	8
Manganese Transport	9
Neurochemical Changes with Manganese Exposure	13
Manganese, Dopamine, and Neurodegeneration	13
Manganese and Dopamine Transporters	14
Manganese and Dopamine Receptors	16
Manganese and Dopamine Summary	18
Manganese and GABA Neurotransmission	20
Manganese and GABA Transporters	21
Manganese and GABA Receptors	23
Manganese and GABA Summary	24
Mechanisms Regulating GABA and Dopamine Transporters	27
Manganese Neurotoxicity	28
Mechanisms	28
Diagnosis	29
Proposed Therapies for Manganese Neurotoxicity	31
Chelation Therapy	31
Bioactive Food Components	32
Conclusion	34
III. MANGANESE EXPOSURE INHIBITS THE CLEARANCE OF EXTRACELLULAR GABA AND INFLUENCES TAURINE HOMEOSTASIS IN THE STRIATUM OF DEVELOPING RATS	35

Abstract.....	35
Introduction	36
Materials and Methods.....	40
Animals.....	40
Cell Cultures.....	40
³ H-Taurine Uptake.....	41
Stereotaxic Surgery	42
Microdialysis.....	43
CE-LIF Analysis.....	44
RNA Isolation and cDNA Synthesis.....	45
Quantitative PCR.....	46
Metal Analyses	46
Statistical Analyses	47
Results	47
Manganese and Iron concentrations	47
Extracellular concentrations of Taurine, GABA, and Glycine	49
³ H-Taurine Uptake.....	53
Gene Expression of Taurine Transporter	53
Discussion.....	58
Acknowledgements	63

IV. WATERBORNE MANGANESE EXPOSURE ALTERS PLASMA, BRAIN, AND LIVER METABOLITES ACCOMPANIED BY CHANGES IN STEREOTYPIC BEHAVIORS..... 64

Abstract.....	64
Introduction	65
Materials and Methods.....	69
Animals.....	69
Hematology	70
Behavior Analysis	71
Metal Analyses	72
Liquid Chromatography-Time of Flight Mass Spectrometry (LC-TOFMS).....	72
Gas Chromatography-Time of Flight Mass Spectrometry (GC-TOFMS).....	75
Data Analyses	77
Results	78
Body Weight and Hematology	78
Metal Analysis	79
Metabolomic Analyses	81
Behavioral Observations	91

Discussion.....	94
Funding	100
V. MANGANESE ACCUMULATION IN MEMBRANE FRACTIONS OF PRIMARY ASTROCYTES IS ASSOCIATED WITH DECREASED γ -AMINOBUTYRIC ACID (GABA) UPTAKE, AND IS EXACERBATED BY OLEIC ACID AND PALMITATE	
	101
Abstract.....	101
Introduction	102
Materials and Methods.....	106
Cell Isolation and Culture	106
^3H -GABA Uptake	107
Cell Fractionation	108
Western Blot Analysis	109
Metal Analysis	110
Statistical Analyses	111
Results.....	111
Manganese Decreases ^3H -GABA Uptake in a PKC Independent Manner.....	111
Membrane GAT3 May be Influenced by Cellular Manganese Localization.....	114
Oleic Acid and Palmitic Acid Exacerbate Manganese Accumulation Resulting in Decreased GABA Uptake.....	115
Iron Deficiency Decreases GABA Uptake	119
Extracellular Manganese and GABA Interact Reducing Their Transport Into Cells.....	121
Discussion.....	122
VI. EPILOGUE	128
REFERENCES.....	137
APPENDIX A. COPYRIGHT LICENSES	171

LIST OF TABLES

	Page
Table 3.1. Brain Tissue and Extracellular Metal Concentrations	49
Table 4.1. Body Weight and Hematology	78
Table 4.2. Metal Analysis of Brain, Liver, and Plasma.....	80
Table 4.3. Plasma Metabolites Altered with Mn Exposure.....	84
Table 4.4. Brain Metabolites Altered with Mn Exposure	85
Table 4.5. Brain Metabolites Correlated with Plasma Mn	86
Table 4.6. Liver Metabolites Altered with Mn Exposure	87

LIST OF FIGURES

	Page
Figure 2.1. Manganese Transport at the Blood Brain Barrier.....	12
Figure 2.2. Manganese Toxicity and Dopamine.....	19
Figure 2.3. Manganese Toxicity and GABA.....	26
Figure 3.1. Extracellular Amino Acid Concentrations.....	52
Figure 3.2. ³ H-Taurine Uptake in Primary Astrocytes.....	54
Figure 3.3. Taurine Transporter, Slc6a6, mRNA Levels.....	55
Figure 3.4. Working Model for Mn Induced GABA and Taurine Alterations.....	56
Figure 4.1. OPLS of Plasma Spectral Data.....	88
Figure 4.2. Relationships Between Brain Mn and Plasma Metabolites.....	89
Figure 4.3. OPLS of Brain Spectral Data.....	90
Figure 4.4. OPLS of Liver Spectral Data.....	91
Figure 4.5. Behavioral Analysis of Mn and Control Rats.....	93
Figure 5.1. ³ H-GABA Uptake and GAT3 Protein Levels in Mn Exposed Astrocytes.....	113
Figure 5.2. Astrocyte Mn Accumulation after Mn Exposure and ISO Pretreatment.....	115
Figure 5.3. ³ H-GABA Uptake and Western Blot Analysis of Astrocytes Exposed to Oleic and Palmitic Acids.....	117
Figure 5.4. Cytosolic and Plasma Membrane Metal Content of Astrocytes Exposed to Oleic and Palmitic Acids.....	118
Figure 5.5. Dose Response: Cytosolic and Membrane Mn Concentrations with Increasing Mn and GABA.....	120

Figure 5.6. Iron Deficiency Reduces ^3H -GABA Uptake in
Cultured Astrocytes 121

CHAPTER I

INTRODUCTION

Manganese (Mn) is an essential dietary metal critical for numerous cellular processes; however, overexposure to environmental Mn via industrial occupation or contaminated drinking water can lead to toxic brain Mn accumulation that has been associated with neurodegeneration (Cersosimo and Koller, 2006). Mn intoxication via inhalation has been reported over the past few decades and recently, cognitive deficits were reported in children drinking Mn contaminated well water (Wasserman et al., 2006). Symptoms of Mn neurotoxicity resemble idiopathic Parkinson's disease and similarly affect the dopamine-rich basal ganglia (Cersosimo and Koller, 2006); however, neurochemical changes due to Mn exposure extend beyond dopamine with recent data implicating γ -aminobutyric acid (GABA) as a target of Mn neurotoxicity.

Several models of Mn neurotoxicity have shown increased striatal GABA with various doses and duration of Mn exposure, but conflicting results have been reported on the effect of Mn on extracellular GABA (Takeda et al., 2002; 2003; Anderson et al., 2008). Proteins critical to synaptic regulation of GABA have been examined but minimal changes in gene expression or tissue protein levels were detected after Mn exposure. It is clear that Mn interferes with GABA

regulation; but specific mechanisms involved remain elusive. Identifying these mechanisms will aid in the development of treatments for Mn neurotoxicity.

Early detection of Mn neurotoxicity has proven difficult, with most cases of toxicity diagnosed after neurological symptoms are present. Additionally, few studies have focused on detecting early markers of Mn accumulation. There is a glaring need to develop biomarkers associated with disease progression, as well as prophylactic treatments that may benefit individuals with increased risk of Mn exposure.

The following studies were designed to elucidate the effect of Mn on GABA regulation and identify biomarkers associated with Mn neurotoxicity. The specific aims were as follows:

1. **Characterize the effect of Mn on extracellular GABA and GABA clearance mechanisms in the striatum of Mn exposed rats.** The hypothesis for this aim was that altered extracellular GABA observed with Mn exposure is due to Mn impeding GABA transporter (GAT) function. Recent studies have shown that Mn increases extracellular GABA without altering GAT protein or mRNA levels. We sought to elucidate whether Mn altered the function of GABA transport mechanisms.
2. **Identify biomarkers of Mn accumulation that correspond with behaviors indicative of neurotoxicity.** The hypothesis for this aim was that changes in metabolism due to Mn toxicity would create

detectable biomarkers that could be elucidated using metabolomics analysis. A shift in the metabolome of Mn exposed rats would not only provide candidates for testable biomarkers, but would identify global effects of Mn exposure that correspond with behaviors consistent with neurotoxicity.

3. **Identify the effect of cellular Mn localization on disturbances in GABA uptake.**

The central hypothesis for this aim was that the location of Mn accumulation within the cell affects how Mn interferes with GABA uptake. Identifying the burden of Mn accumulation in the cytosolic and membrane fractions of cells will help elucidate mechanisms by which Mn decreases GABA uptake.

4. **Test the efficacy of quercetin as a treatment for Mn neurotoxicity.**

The hypothesis for this aim was that pretreatment with a protein kinase C (PKC) inhibitor quercetin will stabilize GABA transport proteins on the plasma membrane preserving function. Mn is known to activate the PKC signaling pathway that regulates membrane recycling of GABA and dopamine transporters. Modulating Mn induced PKC signaling with quercetin will preserve normal transport function.

The overall hypothesis of these studies was that Mn exposure would impair GABA neurotransmission by disrupting synaptic uptake mechanisms and the changes in GABA uptake would correspond with Mn targeting the plasma membrane, inducing PKC signaling, and initiating GAT internalization.

Additionally, Mn accumulation would be associated with detectable metabolic changes, and some of the neurotoxic effects of Mn exposure could be modulated by pretreatment with the bioactive food component quercetin.

CHAPTER II

REVIEW OF LITERATURE

The section entitled *Neurochemical Changes with Manganese Exposure* including figures 2.2 and 2.3 were previously published by Springer Science in *Metal Ion in Stroke*, chapter 27: The Neurochemical Alterations Associated with Manganese Toxicity, pages 549 to 567, in 2012. The coauthors of the book chapter were Steven C. Fordahl and Keith M. Erikson. Kind permission from Springer Science and Business Media can be found in Appendix A. References from this article can be found in the Reference section.

Introduction

Manganese (Mn) is an essential dietary element that functions primarily as a coenzyme in several biological processes. These processes include, but are not limited to, macronutrient metabolism, bone formation, free radical defense systems, and in the brain, ammonia clearance and neurotransmitter synthesis. Although Mn has a diverse role in the human body, dietary requirements for this micronutrient have been modestly established at 1.8 and 2.3 mg per day for healthy adult women and men, respectively (National Academy of Science, 2002). This recommendation takes into account relatively low absorption rates of Mn ($\leq 5\%$) but still fulfills the biological requirements for this trace mineral. Because Mn is a ubiquitous metal found in a variety of foods (fruit, nuts, legumes, whole grains, and brewed tea) dietary Mn deficiency is not of public concern; however, because Mn is abundant in the earth's crust and is widely

used for industrial purposes, excessive exposure to Mn does happen and can lead to dire neurological consequences.

Overexposure to Mn most commonly happens via inhalation to excessive amounts of airborne Mn particulate, but has also been reported to occur after consumption of Mn polluted drinking water (ATSDR, 2008). Symptoms from these exposure routes manifest in a slightly different manner, which will be covered in further detail later in this chapter, but the end result is Mn accumulation in the brain (most notably the basal ganglia) interfering with neurotransmitter systems that result in cognitive and movement disorders similar to Parkinson's disease. Due to the occurrence and clinical relevance of Mn neurotoxicity, exposure thresholds have been established by the Environmental Protection Agency (EPA) and The World Health Organization (WHO) at 0.3 mg/L in drinking water and 0.2 mg/m³ for chronic air exposure (ATSDR, 2008). Even with these guidelines in place, Mn neurotoxicity still occurs predominantly in factory or mining industries where Mn is procured for welding, smelting, or battery manufacturing. Workplace guidelines for airborne Mn limits have been established for these settings; however, chronic exposure may still result in toxic accumulation. Similarly, populations that rely on well water from ground water sources with propensity for Mn contamination have reported learning impairment in children consuming unfiltered well water (Wasserman et al., 2006).

Manganese Exposure

Dietary

Mn is commonly found in the food supply but is particularly abundant in whole grains (oat bran and wheat), fruits (pineapple), vegetables (spinach), and red meats (USDA, 2002). The daily average intake of Mn has been estimated at 2-6 mg for adults with vegetarians consuming slightly greater amounts, estimated around 11 mg/day (Freeland-Graves and Turnlund, 1996; Gibson, 1994). These quantities are adequate for ideal health and fall slightly above the National Academy of Sciences recommended intakes. Fortunately, because absorptive mechanisms for Mn in the gut are tightly regulated, excess dietary Mn rarely results in toxicity. Absorption of dietary Mn is influenced by several different factors including intestinal pH, the presence of the divalent metal transporter (DMT1), other divalent metals competing for absorption (e.g. iron (Fe), copper (Cu), or zinc (Zn)), and chelating agents such as phytic acid (Aschner and Aschner, 2005; Hurrell, 2004). DMT1 is the primary metal transporter in the intestinal tract (Garrick et al., 2003), but DMT1 is also a key transporter allowing Mn to cross the blood brain barrier (BBB) (Erikson et al., 2005). In the gut, DMT1 expression is influenced primarily by systemic Fe status (Gunshin et al., 2001) with duodenal biopsy data showing increased protein levels of DMT1 correlating with decreased serum ferritin (Zoller et al., 1999). Serum ferritin levels were also associated with prolonged Mn retention in males but females with lower ferritin

levels had increased Mn absorption measured using the radio isotope ^{54}Mn (Finley, 2004). There is an inverse relationship between Fe and Mn with regard to absorption and tissue distribution where, generally, iron deficiency (ID) increases Mn absorption (Finley, 1999), and in cases of Mn overexposure, ID accelerates tissue Mn accumulation (Anderson et al., 2008).

Environmental

Occupational exposure to Mn is the most common cause of Mn neurotoxicity. Several cases of neurotoxicity have been linked to Mn exposure within mining, manufacturing, and welding industries (Hochberg et al., 1996; Crossgrove and Zheng, 2004). Inhalation of dense Mn particulate, up to 100-fold higher than established safe limits, has been reported workers who display neurological symptoms (Crossgrove and Zheng, 2004). While acute exposure manifests neurotoxic symptoms in a fairly quick manner, chronic exposure to low dose airborne Mn in the form of methylcyclopentadienyl manganese tricarbonyl (MMT) or Mn contaminated drinking water may present future health concerns. This is particularly true in vulnerable infant and iron deficient populations where chronic low grade exposure to Mn has been associated with cognitive impairments (Wasserman, 2006; Sahni et al., 2007). In Bangladesh, children drinking from wells with a high Mn content (793 $\mu\text{g/L}$, compared to the Environmental Protection Agencies (EPA) established safe limit of 300 $\mu\text{g/L}$) had significantly reduced verbal scores and overall intellectual performance

compared to children consuming water Mn concentrations under the EPA's established safe limit (Wasserman, 2006).

Manganese Transport

Under normal conditions Mn homeostasis is tightly regulated by the body with excess Mn excreted through the biliary system. Increased exposure to exogenous Mn, however, can overwhelm systemic regulation and result in peripheral tissue accumulation, most notably in the brain (Gianutsos et al., 1985). Systemic distribution of Mn to extrahepatic tissues is handled by transport proteins including albumin, β -globulin, and transferrin (Critchfield and Keen, 1992). Accumulation of Mn in the brain is well documented (specifically in the iron-rich basal ganglia Uchino et al., 2007)), but involves transport systems capable of bypassing the blood brain barrier (BBB). To date several transport mechanism have been discovered, but the mechanism engaged depends largely on Mn speciation, divalent (Mn^{2+}) or trivalent (Mn^{3+}), and plasma concentrations. Entrance of Mn via the cerebral spinal fluid at the choroid plexus tends to favor high plasma concentrations, whereas cerebral capillary transport at the BBB predominate under lower physiologic concentrations (Aschner et al., 2007). It is thought that the majority of Mn is chaperoned into the brain by Mn^{3+} bound to transferrin or uptake of Mn^{2+} by divalent metal transporter DMT-1 (Aschner et al., 2007). Ancillary Mn transport across the BBB also occurs through active transport, leak pathways, in the form of Mn^{2+} citrate, and through store-operated

calcium channels (Aschner and Gannon, 1994; Crossgrove et al., 2003; Crossgrove and Yokel, 2005).

DMT-1 is a known transporter of Mn and Fe that is expressed on the apical wall of endothelial cells, cerebral capillaries, on foot processes of astrocytes (integral to the BBB), and choroid epithelia of the blood-CSF barrier (Garrick et al., 2003). A study by Chua and Morgan, (1997) helped characterize the role of DMT-1 in Mn transport using homozygous Belgrade (b/b) rats with a defective DMT-1 allele. Mn and Fe transport into the brain was impaired in b/b rats compared to heterozygous (+/b) and Wistar rats indicating the importance of DMT-1.

Mn bound to transferrin represents another mechanism by which Mn crosses the BBB. Transferrin can bind to transferrin receptors at the cerebral capillaries for endocytosis into the capillary endothelium (Fishman et al., 1987). Within the endothelial cell, Mn is liberated from systemic transferrin to complex with brain synthesized transferrin for transport into the brain. A small amount of Mn in the blood is bound to citrate, this Mn-citrate complex is thought to cross the BBB through monocarboxylate transporter (MCT) (Aschner et al., 2007). Other small scale transport mechanisms include the zinc family transporter (ZIP) and leak pathways (Aschner et al., 2007). The mechanisms by which Mn travels within the brain are still largely undefined; however, transferrin is thought to play a role.

Lastly, Mn transport to the brain has also been demonstrated to occur along olfactory neurons (Dorman et al., 2002). Solubility of the Mn species appears to play a role in transport, with more soluble MnCl_2 and MnSO_4 concentrations peaking rapidly compared to less soluble MnHPO_4 (Dorman et al., 2001; Dorman et al., 2002; Brenneman et al., 2000). Inhaled Mn concentrates primarily in the olfactory bulb, but the mechanism governing Mn relocalization once it has entered the brain has yet to be fully elucidated (Leavens et al. 2007).

Figure 2.1. Manganese Transport at the Blood Brain Barrier.

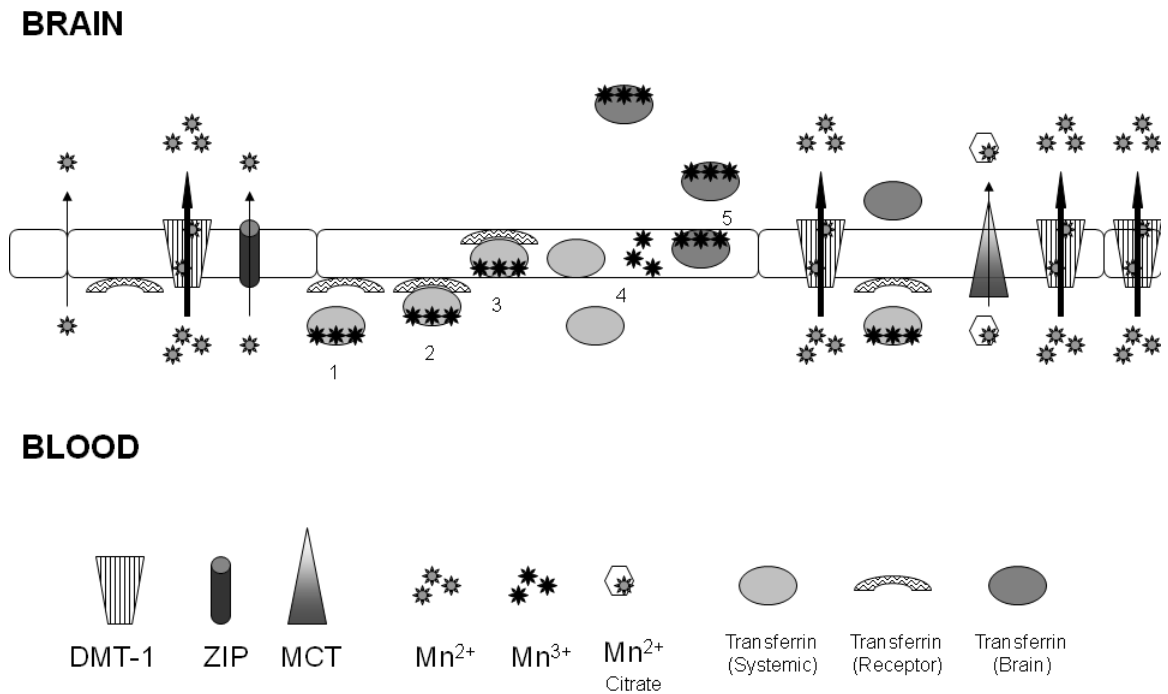


Figure 2.1. Manganese Transport at the Blood Brain Barrier. – The above figure is a schematic of the Mn transport mechanism across the BBB. Primary transport routes (DMT-1 and transferrin endocytosis) are depicted with more abundant BBB density and bold arrows compared to the other transport mechanism (ZIP, Mn^{2+} -Citrate, and leak pathways). Endocytosis of Mn-bound transferrin 1) Mn bound to systemic transferrin reaches the BBB. 2) Mn-bound transferrin binds to transferrin receptor. 3) Endocytosis of the receptor bound complex 4) Mn is liberated from systemic transferrin and binds to 5) brain-produced transferrin where it is transferred across the basolateral surface of the capillary endothelium into the brain.

Neurochemical Changes with Manganese Exposure

Manganese, Dopamine, and Neurodegeneration

Much of the early evidence linking Mn overexposure to alterations in neurochemical functioning has focused on dopamine biology within the basal ganglia (Neff et al., 1969; Mustafa and Chandra, 1971; Barbeau, 1984).

Dopamine input to the striatum from the substantia nigra works in concert with GABA and glutamate to modulate voluntary movements and fine motor control.

The effect of Mn accumulation on the dopaminergic activity of the basal ganglia results in extrapyramidal movement disorders similar to Parkinson's disease.

This Mn-induced condition termed manganism is characterized by bradykinesia, rigidity, dystonia, and a cock-like gait (Cersosimo and Koller, 2006). Movement abnormalities are often accompanied by behavioral alterations associated with the dopaminergic system including anxiety, diminished libido, apathy, and

emotional instability (Pal et al., 1999). While manganism and Parkinson's disease

are clinically distinct, their phenotypes are driven largely by alterations in

dopamine biology. The maintenance of normal dopamine biology is dependent

upon rapid recycling of extracellular dopamine into presynaptic neurons (Iversen,

1971). Since this dopamine reuptake is dependent upon a properly functioning

dopamine transporter protein, several recent studies have examined the effect of

Mn exposure on dopamine transporter biology.

Manganese and Dopamine Transporters

The dopamine transporter (DAT) is a member of the solute carrier (SLC) protein family (SLC6a3) that requires co-transport of two Na⁺ and one Cl⁻ per molecule substrate. DAT is a transmembrane protein regulated by phosphorylation, ubiquitination, and glycosylation that is expressed on presynaptic neuronal membranes and by most glial cell types, primarily astrocytes (Robinson, 2002). DAT clears excess dopamine from the synapse against its concentration gradient for repackaging into neuronal vesicles or for degradation. The interaction between Mn and DAT is dual-faceted. Evidence of impaired dopamine transport has been reported with Mn neurotoxicity suggesting impedance of DAT function (Kern et al., 2010); however, DAT has also been shown to aid in Mn transport (Anderson et al., 2007). Whether Mn competes with dopamine as a substrate for DAT or alters DAT density by influencing membrane trafficking remains unknown.

Magnetic resonance imaging (MRI) and positron emission tomography (PET) technologies using Fluorine-18-L-dihydroxyphenylalanine (¹⁸F-DOPA) have been used to identify brain Mn accumulation and DAT functionality in human subjects. A case study of two Taiwanese welders (the first, 12 yrs removed from 1 yr of Mn exposure; the second, 10 days removed from 8 yrs of exposure) used T1-weighted MRI to identify brain Mn accumulation and ¹⁸F-Dopa to monitor dopamine uptake (Kim et al., 1999). The first subject showed no

indication of Mn accumulation and exhibited normal dopamine uptake in the striatum. The second subject had high MRI signal intensities in the globus pallidus (GP), indicating Mn accumulation, and significantly reduced ¹⁸F-dopa uptake in the striatum. A 6 month follow up of the second individual showed a reduction of GP Mn approaching normal levels. Similar PET scan studies using ¹⁸F-DOPA to identify dopamine uptake in the striatum report a decrease in striatal dopamine uptake in Parkinson's disease (Brooks 2004), but normal uptake with Mn accumulation (Kim, et al. 1998). The fact that the second subject in the case study exhibited decreased uptake 10 days post Mn exposure, but both had normal uptake once removed from exposure, suggests that Mn inhibits DAT-mediated dopamine uptake in a transient nature. Findings from a study by Huang et al. (2003) corroborate these data, identifying a slight decrease in striatal DAT density in Mn exposed smelters compared to controls, though still significantly higher than Parkinson's disease patients.

Animal models of Mn toxicity support impaired DAT function observed in human subjects. Increased DAT binding potential, followed by decreased DAT function and motor deficits have been reported in non-human primates exposed to intravenous MnSO₄ (10-50 mg/kg) (Chen, et al. 2006; Guilarte, et al., 2006). Moreover, oral administration of Mn (750 µg/day) to rat pups PND 1-21 decreased striatal DAT density up to two months post treatment, impaired dopamine uptake, and modified learning behavior (McDougall, et al., 2008). Decreased striatal DAT has also been associated with hyperactivity in similarly

aged Mn exposed rats (Kern et al., 2010). Coupled with clinical and case reports from human subjects, these data suggest that Mn initiates a decline in dopamine neurotransmission that is characterized by a decrease in DAT function, which contributes to movement and behavior abnormalities seen with Mn over-exposure.

Additional studies exploring the Mn/DAT relationship discovered that DAT may have a functional role in brain Mn transport. Ingersoll et al., (1999) noted decreased ventral pallidum Mn accumulation when DAT reuptake blockers cocaine and reserpine were given to rats exposed to Mn (Ingersoll et al., 1999). This finding was substantiated when Mn accumulation was attenuated in striatopallidal tissue from DAT knockout mice (Erikson et al., 2005) and rats given the DAT inhibitor GRB12909 (Anderson et al., 2007a). These studies suggest that DAT aids in Mn accumulation leading to functional DAT decline.

Manganese and Dopamine Receptors

Dopamine receptors are divided into two different families, D₁-like and D₂-like, which are both G-protein coupled; however, D₁-like receptors increase cellular cyclic adenosine monophosphate (cAMP), while D₂-like receptors inhibit cAMP production. D₂-like receptors also tend to be presynaptic and function as auto receptors to modulate dopamine release.

A case report on a subject with manganism 40yrs post exposure using PET to detect ¹⁸F-methylspiperone binding to D₂ receptors showed a decrease in

D₂ density, possibly indicative of neurodegeneration (Kessler et al., 2003).

Another individual with non-Mn-induced liver encephalopathy showed increased Mn in the GP via T1-weighted MRI also exhibited decreased D₂ binding potential (Butterworth et al., 1995). Conversely, primates chronically exposed to Mn (0.1g per month for 26 months) had normal D₂ density but decreased binding of the D₁ agonist ³H-SCH 23,390 compared to control (Eriksson et al., 1992). The density and function of D₂ is essential in regulating dopamine function, but has also been shown to regulate the release of glutamate at cortical/striatal nerve terminals (Calabresi et al., 2001). Regulating glutamate input into the striatum is critical to regulate GABAergic projections from the striatum. Rodent models have repeatedly shown an increase in dopamine receptor activity. C57BL/6 mice receiving 20-40 mg MnCl₂/kg/d for 5 days had increased striatal D₂ protein and mRNA levels, which were associated with decreased motor coordination (Nam and Kim, 2008). Early Mn exposure in postnatal rats (PND 1-21) has also been linked with elevated striatal D₂ expression and increased D₂ binding sites (McDougall et al., 2011), and increased D₁ and D₂ receptor levels in the nucleus accumbens and prefrontal cortex (Kern and Smith, 2011). Some of the changes seen in early Mn exposure may also persist later in life (Kern and Smith, 2011), thus even short term Mn exposure during critical developmental periods may have a deleterious long term effect. Chronic Mn exposure later in life seems to differentially alter dopamine receptors. Rats exposed to solubilized Mn containing welding fumes for 7 weeks had decreased D₂ mRNA expression in the

striatum and midbrain for up to 35 days after exposure ceased (Sriram et al., 2010). These studies suggest that dopamine receptor functioning in the developing brain is more vulnerable to Mn exposure than the mature brain.

Manganese and Dopamine Summary

Unlike Parkinson's disease pathology, Mn induced changes in dopamine may be a function of altered transport or receptor proteins rather than dopaminergic neuron loss. Whether or not Mn antagonizes DAT through direct binding, competitive inhibition, or some other mechanism is not known. Altered striatal DAT function, with a concomitant decline in dopamine receptors levels, produces deficits in motor control and may contribute to some of the behavior changes (e.g. hyperactivity) observed with Mn neurotoxicity.

Figure 2.2. Manganese Toxicity and Dopamine.

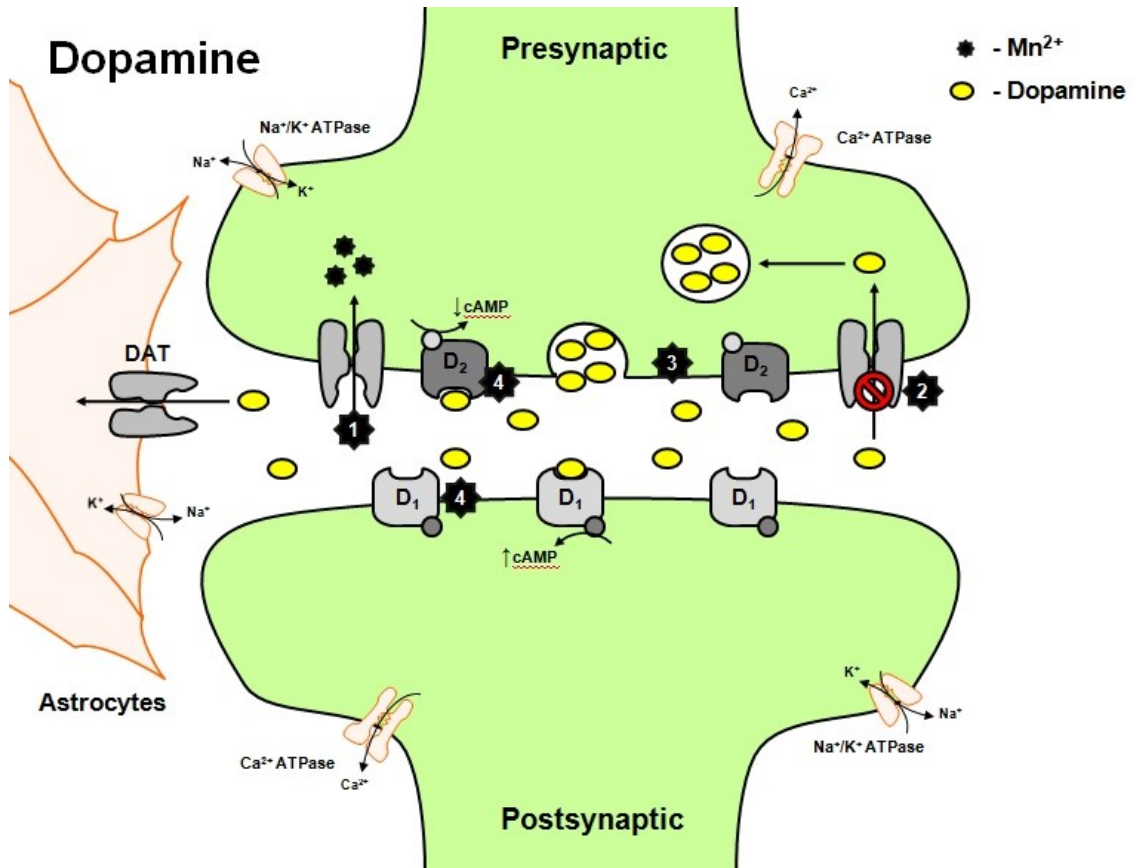


Figure 2.2. Manganese Toxicity and Dopamine. – Schematic of the effects of Mn on dopamine biology. **1)** Dopamine transporter (DAT) facilitates the transport of Mn into the cell aiding in accumulation (Erikson et al., 2005). **2)** There is a short initial increase in DAT binding potential followed by decreased DAT function and density (Kern et al., 2010). **3)** Mn decreases the density and binding potential of dopamine auto receptor D₂ (Butterworth et al., 1995). **4)** Increased expression and activity has been reported in both D₁ and D₂ receptors (Kern et al., 2010; McDougall et al., 2011).

Abbreviations – Na⁺:sodium, K⁺: potassium, Ca²⁺: calcium, Mn²⁺: manganese, DAT: dopamine transporter, D₁: metabotropic postsynaptic dopamine receptor, D₂: metabotropic presynaptic dopamine autoreceptor, cAMP: cyclic adenosine monophosphate.

Manganese and GABA Neurotransmission

Dense populations of GABAergic neurons are found in the basal ganglia primarily located in the striatum and GP. The inhibitory effect of GABA in these regions counteracts excitatory glutamate projections from the cortex, and along with dopamine input, helps regulate motor control. Similar to dopamine, evidence has shown that Mn toxicity alters GABA biology within the basal ganglia; however, conflicting results have been reported. Mn exposure has been linked with both increased and decreased GABA levels in the brain. Early studies identified increased striatal GABA in rats exposed to 10 mg MnCl₂/ml drinking water for two months (Bonilla, 1978), and after six months of exposure to dietary MnCl₂ (4% Mn diet) (Gianutsos and Murray, 1982). It is important to note that Gianutsos and Murray did not observe a change after 1-2 months of exposure. Shorter term, lower-dose exposure (6mg Mn/kg/d), however, decreased whole brain GABA concentrations (Chandra et al., 1982). Multiple factors may contribute to these differential findings such as age of subject and length and route of exposure. More recently, similar inconsistencies have been noted. Increased GABA was detected in striatal tissue of weanling rats receiving 20 mg Mn/kg/d for 30 days (Lipe et al., 1999), after intraperitoneal (i.p.) injection of 4.8 mg MnCl₂/kg/3x week for 5 weeks (Gwiazda et al., 2002), and in rat pups (post natal day 21) after nursing from Mn exposed dams (Garcia et al., 2006), but an inverse correlation was found between brain Mn levels and striatal GABA in normal, dietary iron deficient, and Mn exposed rats (Erikson et al., 2002). While

ex vivo detection of tissue GABA identifies brain regional changes that may perturb neurotransmission, it does not delineate between GABA sequestered in cell bodies versus physiologically relevant extracellular GABA in the synapse. Monitoring extracellular GABA during Mn exposure capitulates how Mn alters GABA neurotransmission, specifically by elucidating the effects of Mn on GABA transport.

Manganese and GABA Transporters

There are four different isoforms of the GABA transporter (GAT) -1, -2, -3, and -4 all members of the solute carrier transport family SLC6. In the brain, presynaptic neurons express GAT1 and astrocytes largely express GAT3, both of which function to clear GABA from the synapse (Minelli et al., 1995). The effect of Mn on GABA transporters has been observed directly by measuring ³H-GABA uptake or indirectly with *in vivo* microdialysis to monitor transient changes in extracellular GABA during or after Mn treatment.

Microdialysis studies, similar to tissue analysis of GABA, have reported opposing effects of Mn on GABA in the extracellular space. Two studies by Takeda et al., (2002; 2003) used microdialysis to examine the response of extracellular neurotransmitters when perfused with 200 nM MnCl₂. Direct delivery of Mn into the striatum and hippocampus of rats significantly reduced extracellular GABA (Takeda et al., 2002; 2003). These animals had not been exposed to any other form of exogenous Mn prior to direct probe injection

representing the immediate effect of extracellular Mn on a synapse. To help characterize the effect of Mn neurotoxicity on extracellular GABA a study by Anderson et al. (2008) measured extracellular GABA in rats with sub-chronic Mn exposure. Anderson et al. (2008) reported increased extracellular GABA in the striatum during the sixth week of oral Mn exposure (1g Mn/L drinking water); however, no changes in GAT1 protein levels were detected compared to control animals, which implied that Mn was impeding the function of GAT1 thereby decreasing GABA uptake. These data also corroborate previous evidence of decreased ^{14}C -GABA uptake in primary striatal cells and ^3H -GABA uptake in striatal synaptosomes after Mn exposure (Defazio et al., 1996; Anderson et al., 2007b, respectively). To confirm whether or not GAT1 function is impaired due to Mn exposure, *in vivo* microdialysis was performed on Mn exposed rats (1g Mn/L drinking water) using nipecotic acid, a potent GAT inhibitor, to pharmacologically probe GAT functioning. Perfusion of nipecotic acid into the striatum induced a 228% increase of extracellular GABA in control rats, an effect that was absent in Mn exposed rats (Fordahl et al., 2010). Mn exposure appears to block GABA uptake via decreased GAT functioning, but future experiments are warranted to identify the mechanism of action on GAT inhibition. Two putative factors contributing to Mn induced GAT inhibition are: 1) altered regulation of protein kinase C (PKC), or 2) taurine mediated feedback via GABA auto-receptor activation. PKC activation has been reported with Mn exposure (Latchoumycandane et al., 2005), linked to phosphorylation and subsequent

internalization of GAT1 (Gadea and Lopez-Colome, 2001), and shown to decrease ^3H -GABA uptake (Sato et al., 1995). Additionally, taurine homeostasis is disrupted with Mn exposure (Fordahl et al., 2010); because taurine is a known modulator of GABA receptors (Namima et al., 1982), alterations in extracellular taurine may contribute to the Mn-induced changes in GAT function.

Manganese and GABA Receptors

There are two different classes of GABA receptors expressed on either pre- or postsynaptic plasma membranes. Primarily, GABA_A receptors conduct inhibitory current on post synaptic neurons via the opening of Cl⁻ ion channels, while GABA_B receptors modulate release of GABA from the presynaptic terminal through activation of G-protein linked signal transduction and therefore are considered autoreceptors. To date, it remains unclear if accumulated brain Mn due to exposure interferes with GABA receptor activation/density, but due to its role in attenuating the functional capacity of GAT1, it is plausible.

Little data has been collected on the relationship between Mn and GABA receptors. Chronic exposure (26 weeks and 7-59 days) to varying Mn concentrations in primates has shown no effect on GABA_A density in two different studies (Eriksson et al., 1992; Burton et al., 2009). In rats, however, waterborne Mn exposure alters both GABA_A and GABA_B protein and mRNA expression in a heterogeneous fashion (Anderson et al., 2008). Specifically, Mn exposure increased GABA_A protein levels in the GP and hippocampus, although GABA_A

mRNA levels were unchanged in all regions except a decrease in the substantia nigra (Anderson et al., 2008). Decreased GABA_B protein levels were found in the GP, hippocampus, and substantia nigra accompanied by decreased mRNA in the hippocampus, substantia nigra, and the striatum. Decreased GABA_B levels may explain the increased extracellular GABA levels observed during Mn exposure (Anderson et al., 2008; Fordahl et al., 2010) due to this loss of autoreceptor-mediated GABA release. The hyperactivity associated with Mn exposure (Kern et al., 2010; Fordahl et al., 2012) could also be linked to decreased GABA_B levels as GABA_B null mice have hyper-locomotion and increased striatal dopamine (Vacher et al., 2006).

Manganese and GABA Summary

Mn neurotoxicity disrupts tissue and extracellular GABA by altering normal transport and receptor function, which impairs the ability of GABA to counteract the excitatory neurotransmission of glutamate in the basal ganglia. It is important to note that when examining GABA biology due to Mn neurotoxicity, there are clearly species differences (e.g., minimal effect in primates but robust effects in rodents); differences due to the developmental age (e.g., developing brains are more vulnerable than developed brains); as well as differences due to exposure length (acute versus chronic) and delivery method (i.e., enteral versus parenteral). When all of these factors are considered, it is evident that enteral, subchronic Mn exposure in the developing brain causes elevated striatal

extracellular GABA which is related to attenuated GAT functioning. Additionally, this Mn exposure paradigm is linked with heterogeneous alterations in GABA receptor levels in the basal ganglia which likely accounts for the hyperlocomotion associated with Mn neurotoxicity.

Figure 2.3. Manganese Toxicity and GABA.

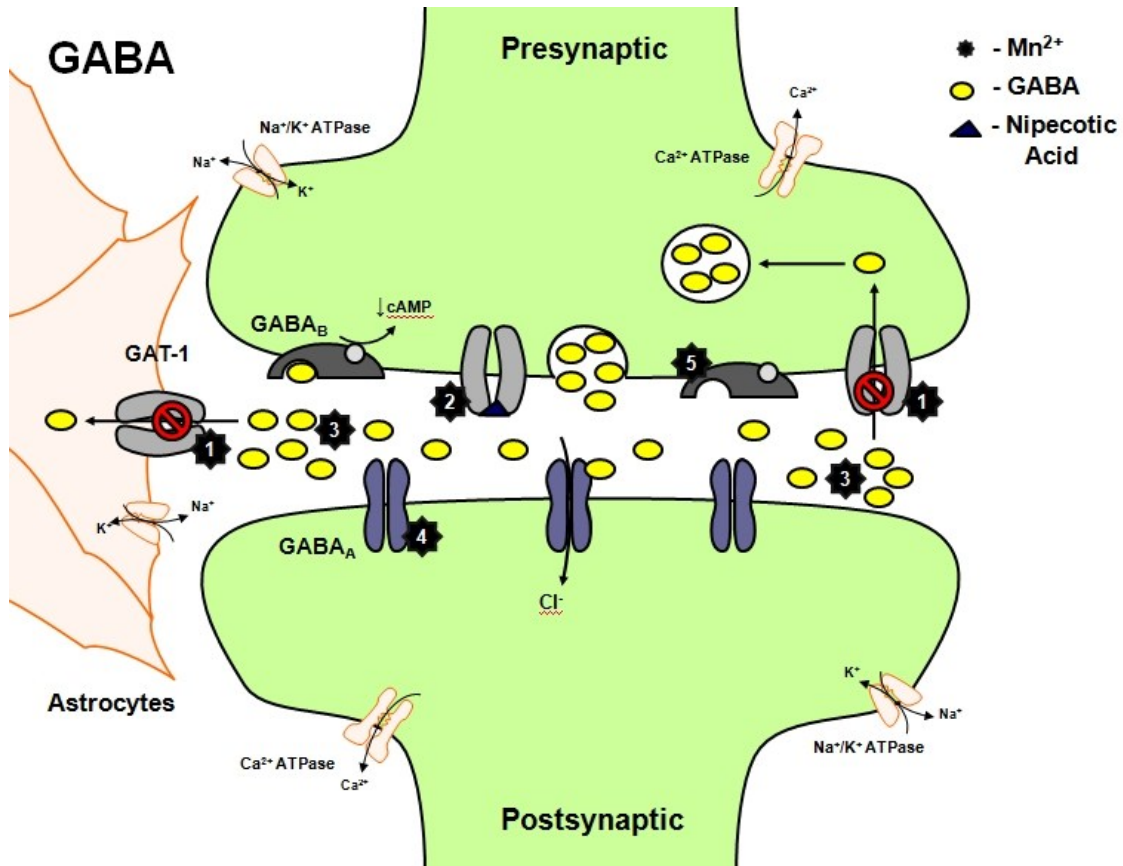


Figure 2.3. Manganese Toxicity and GABA. – Schematic of the effects of Mn on GABA biology. **1)** Mn exposure has been linked with decreased GAT1 gene expression and impaired GABA uptake in astrocytes and synaptosomes (Anderson et al., 2007;2008). **2)** *In vivo* microdialysis using GAT inhibitor nipecotic acid revealed that Mn interferes with GAT mediated GABA clearance (Fordahl et al., 2010) resulting in **3)** increased extracellular GABA. **4)** Increased GABA_A protein levels have been reported in Mn exposed animals as well as **5)** decreased GABA_B protein and mRNA levels (Anderson et al., 2008) which may alter inhibitory feedback mechanisms necessary for maintaining proper extracellular GABA concentrations.

Abbreviations – Na⁺:sodium, K⁺: potassium, Ca²⁺: calcium, Mn²⁺: manganese, Cl⁻: chloride, GABA: γ-aminobutyric acid, GAT-1: GABA transporter, GABA_A: ionotropic GABA receptor, GABA_B: metabotropic GABA receptor, cAMP: cyclic adenosine monophosphate.

Mechanisms Regulating GABA and Dopamine Transporters

Cellular regulation of GAT1 and DAT by Mn is poorly understood. Understanding how these proteins are regulated by Mn will help us identify how neurochemical communication within the basal ganglia may influence neurodegenerative pathologies. Normally GATs and DAT are recycled to and from the plasma membrane in response to membrane depolarization, cellular calcium levels, or feedback mechanism from pre-synaptic auto-receptor activation (Melikian, 2004 for review). Membrane recycling occurs at approximately 10%/min for GAT1 (Whitworth and Quick, 2001) and 3-5%/min for DAT (Loder and Melikian, 2003), and once internalized the transporters reside within endosomes for quick redistribution to the plasma membrane. Mounting evidence identifies PKC as an upstream mediator of GATs and DAT internalization (Torres et al., 2003; Copeland et al., 1996; Melikian and Buckley, 1999; Beckman et al., 1999; Sato et al., 1995; Quick et al., 1997; Quick et al., 2004). It is thought that phosphorylation of GATs and DAT by PKC is the first step in the endocytic process, tagging the protein, for subsequent internalization (Mortensen et al., 2008). Cellular phosphatases such as dual specificity phosphatase 6 (DUSP6) have been shown to play a role in this process (Mortensen et al., 2008) demonstrating the complexity of membrane trafficking; however, PKC activation and phosphorylation of membrane transporters remains the initial step in this process. Mn has been associated with increased PKC δ

activation (Kitazawa et al., 2005), but not the neuron specific isoform PKC γ .

Moreover, the events leading up to this activation remain unclear.

Manganese Neurotoxicity

Mechanisms

Proposed mechanisms of Mn neurotoxicity range from functional changes in neurotransmission, to cellular organelle damage, and oxidative stress caused by Mn accumulation. The effect of Mn on the brain is also influenced by route of exposure and magnitude of accumulation. Inhalation of Mn is generally associated with oxidative stress and increased neuronal apoptosis (Seo et al., 2013), whereas ingestion of Mn has more of a subtle effect altering neurochemistry and cognition (Gwiazda et al., 2002; Fitsanakis et al., 2006; Wasserman et al., 2006).

Excess Mn is primarily sequestered in astrocytes (Aschner et al. 1999). Dysfunction is thought to occur when excess Mn burden on astrocytes and other glial cells disrupts their ability to modulate the neuronal environment. This leaves neurons vulnerable to excitotoxicity, reactive oxygen species (ROS), and other toxic byproducts generally processed by astrocytes. Mn is known to localize the mitochondria of cells where its cytotoxic properties have been linked to inhibition of complex I and II of the electron transport chain (Zhang et al., 2004), increased production of ROS (Ali et al., 1995), disruption of mitochondrial membrane potential (Rao and Norenberg, 2004), and caspase 3 activation leading to

apoptosis (Oh et al., 2006). Other than energy production, one of the key physiologic functions of the mitochondria is to sequester cellular calcium (Gunter et al., 2004), a function shared with the endoplasmic reticulum (ER) (Koch, 1990). Similarly, Mn has been shown to induce ER stress (Chun et al., 2001) which is associated with the release of calcium into the cytosol (Verkhraatsky, 2004; Arduino et al., 2009). Altered cytosolic calcium may in turn trigger caspase-3 mediated apoptosis (Tantral et al., 2004). Additionally, increased ROS produced by Mn has also been associated with lipid peroxidation (Milatovic et al., 2007). These data display the breadth of damage instilled by Mn on several cellular compartments. Cells (astrocytes or neurons) damaged by Mn have an undoubtedly hampered ability to respond to the brains dynamically changing environment. Linking mechanistic changes (due to Mn) to functional outcomes of toxicity is the next step in understanding the progression of Mn neurotoxicity.

Diagnosis

Early symptom identification and removal from Mn exposure can improve the prognosis of Mn neurotoxicity. The use of magnetic resonance imaging (MRI) has been demonstrated to accurately reflect brain Mn deposits (Dorman et al., 2006; Fitsanakis et al., 2008), and when used in conjunction with positron emission tomography (PET) can identify biological alterations in neurotransmission (Kim et al., 1999). While MRI and PET technologies have advanced the identification of Mn neurotoxicity, the practical application and cost

of these tools may preclude widespread use. Moving forward, it is important to establish cost effective diagnostic measures that correspond with brain Mn accumulation similar to MRI. Identifying biomarkers of Mn neurotoxicity in biological fluids may provide an alternative solution to confirm the extent of brain Mn accumulation.

To date, few reliable markers exist to measure the extent of brain Mn accumulation. Prospective compounds such as lymphocytic manganese superoxide dismutase (MnSOD) and arginase were suggested as biomarkers over a decade ago; however, each possessed diagnostic limitations (Davis and Greger, 1992; Brock et al., 1994). More recently, Dorman et al. (2008) screened for potential Mn exposure biomarkers using a liquid chromatography-mass spectrometry method to identify metabolomic changes in the blood and urine of monkeys exposed to airborne MnSO₄. Of the 27 metabolites significantly altered by Mn, three blood metabolites corresponded with Mn accumulation in the globus pallidus: phenylpyruvate, disaccharides, and guanosine (Dorman et al., 2008). While these markers show promise, additional studies are needed to confirm their potential as consistent biomarkers.

The study of metabolomics is emerging as a reliable approach to identify potential biomarkers in diseased states including cancer (Kim et al., 2008) and amyotrophic lateral sclerosis (Pradat and Dib, 2009), among other potential applications (Oresic et al., 2006). Methods using liquid and gas chromatography,

coupled with mass spectrometry (LC-MS, GC-MS), enable the detection of thousands of metabolites in a biological sample (Halket et al., 2005). These methods are ideal for monitoring changes in metabolite byproducts due to altered cellular metabolism in either a diseased state or after application of selected therapies.

Proposed Therapies for Manganese Neurotoxicity

Chelation Therapy

Few treatment options have been proposed for Mn neurotoxicity. Removal from the Mn toxic environment is the first course of action, but only two clinical treatments have been tested; calcium disodium EDTA (CaNa_2EDTA) and para-Aminosalicylic Acid (PAS), each yielding success in a small sample cohort. CaNa_2EDTA is a synthetic compound used in detergents and food preservatives that is known to bind divalent and trivalent metal ions. A study by Hernandez et al. (2006) used CaNa_2EDTA to treat seven welder/foundry workers presenting Mn induced Parkinson's symptoms. Five of the seven workers showed improvement in muscle rigidity and postural tremor. The use of PAS as treatment for Mn intoxication was investigated in a case study of a 50 year old woman who had been exposed to airborne Mn for 21 years. All Mn-induced symptoms were significantly alleviated upon receiving PAS therapy, and the patient presented close to normal clinical, neurologic, MRI and handwriting scores in a follow up examination 17 yrs post treatment (Jiang et al., 2006).

Though CaNa_2EDTA and PAS treatments have shown positive results, the sample sizes in these studies are small, and to date no progress has evolved from these putative therapies. Additionally, these treatments are intended to relieve or improve symptoms secondary to Mn toxicity when neuronal damage may have already occurred. It is imperative that treatment strategies shift to prevent the onset of Mn neurotoxicity rather than the treatment of its symptoms. Recently, the use of bioactive food components in cancer and cardiovascular research fields has gained notoriety as a preventative treatment (Kris-Etherton et al., 2002). Bioactive food components are non-nutritive compounds found in foods that have immunoprotective properties within the plants themselves. These compounds are frequently pigments of plants and provide protection from free radical damage and other environmental insults. Emerging evidence suggests that a specific subclass of these bioactive components, the polyphenolic compounds, may have additional neuroprotective properties (See Kovacsova et al., 2010 for mini-review).

Bioactive Food Components

Quercetin is the most abundant polyphenolic compound in the American diet, particularly abundant in onions and blueberries (Scalbert and Williamson, 2000). With the ability to cross the blood brain barrier, quercetin has emerged as a new compound in neuroprotection. Rats ingesting quercetin in the form of blueberry extract had decreased hippocampal neuron loss in a model of

excitotoxic neurodegeneration (Duffy et al., 2008). Similar decreases in hippocampal neuron loss and improvement in learning and memory were observed in an Alzheimer's disease rodent model receiving quercetin in an inhaled liposome (Tong-un et al., 2010). Quercetin is also known to inhibit PKC activation, and to decrease inositol-3-phosphate activity (Ferriola et al., 1989; Natsume et al., 2009). These properties of quercetin make it a candidate for neuroprotection due to the role of PKC activation in GAT and DAT internalization.

Once ingested, quercetin is metabolized by the liver and other tissues to form several bioactive variants. Isorhamnetin (ISO) is a methylated quercetin metabolite that is capable of crossing the BBB (de Boer et al., 2005). In a study where rats and pigs were administered oral quercetin and examined for quercetin metabolite content in plasma and various tissues, ISO was the predominant metabolite in the brain with concentrations reported at 200 nM (de Boer et al., 2005). Plasma ISO levels were reported around 15 μ M (de Boer et al., 2005). While ISO is a slightly less potent PKC inhibitor than quercetin, (Ferriola et al., 1989) ISO has superior bioavailability and tissue distribution (Paulke et al., 2012).

Identifying a specific dietary food component of protective value against neurodegeneration would change the approach of therapeutic interventions. Until now treatments for Mn toxicity and neurodegenerative diseases have focused on treatments after the onset of symptoms. A dietary treatment utilizing a relatively

ubiquitous bioactive food component could be a proactive approach to mitigate disease prevention. Alternatively, quercetin may also provide an answer for therapeutic intervention alternative to pharmaceutical administration in progressing neurodegenerative disease.

Conclusion

It is well documented that brain Mn accumulation has a profound effect on the neurochemistry of the basal ganglia. Symptoms of Mn neurotoxicity are driven by changes in dopamine and GABA biology, where Mn is thought to impair synaptic proteins that govern these systems. There is a lack of evidence, describing mechanisms by which Mn interferes with these synaptic proteins to dysregulate signal conductance. Elucidating the effect of Mn on GABA neurotransmission is especially important because it is an early event in Mn neurotoxicity. Understanding how Mn alters GABA may prevent changes in other neurotransmitter systems that result in cognitive and movement abnormalities. Collecting data to help characterize the progression of Mn neurotoxicity will aid in the development of early treatments prior to irreparable damage.

CHAPTER III

**MANGANESE EXPOSURE INHIBITS THE CLEARANCE OF
EXTRACELLULAR GABA AND INFLUENCES TAURINE HOMEOSTASIS IN
THE STRIATUM OF DEVELOPING RATS**

Reprinted from *NeuroToxicology* , volume 31, Steve C. Fordahl, Joel G. Anderson, Paula T. Cooney, Tara L. Weaver, Christa L. Colyer, and Keith M. Erikson, Manganese Exposure Inhibits the Clearance of Extracellular GABA and Influences Taurine Homeostasis in the Striatum of Developing Rats, pages 639 to 646, in 2010, with permission from Elsevier to use the article in its entirety as notated in Appendix A. References from this article can be found in the Reference section.

Abstract

Manganese (Mn) accumulation in the brain has been shown to alter the neurochemistry of the basal ganglia. Mn-induced alterations in dopamine biology are fairly well understood, but recently more evidence has emerged characterizing the role of γ -aminobutyric acid (GABA) in this dysfunction. The purpose of this study was to determine if the previously observed Mn-induced increase in extracellular GABA (GABA_{EC}) was due to altered GABA transporter (GAT) function, and whether Mn perturbs other amino acid neurotransmitters, namely taurine and glycine (known modulators of GABA). Extracellular GABA, taurine, and glycine concentrations were collected from the striatum of control (CN) or Mn-exposed Sprague-Dawley rats using in vivo microdialysis, and the

GAT inhibitor nipecotic acid (NA) was used to probe GAT function. Tissue and extracellular Mn levels were significantly increased, and the Fe:Mn ratio was decreased 36-fold in the extracellular space due to Mn exposure. NA led to a 2-fold increase in GABAEC of CNs, a response that was attenuated by Mn. Taurine responded inversely to GABA, and a novel 10-fold increase in taurine was observed after the removal of NA in CNs. Mn blunted this response and nearly abolished extracellular taurine throughout collection. Striatal taurine transporter (Slc6a6) mRNA levels were significantly increased with Mn exposure, and Mn significantly increased 3H-Taurine uptake after 3-minute exposure in primary rat astrocytes. These data suggest that Mn increases GABAEC by inhibiting the function of GAT, and that perturbed taurine homeostasis potentially impacts neural function by jeopardizing the osmoregulatory and neuromodulatory functions of taurine in the brain.

Introduction

An essential trace element and a cofactor for several enzymes (Hurley and Keen, 1987), manganese (Mn) is involved in immune function, regulation of metabolism, reproduction, digestion, bone growth, and blood clotting (see review by Aschner et al., 2005). While frank manganese deficiency has not been clinically observed in humans, Mn toxicity, in particular Mn neurotoxicity, is of concern (Aschner et al., 2005; Dobson et al., 2004). A recent study suggests that high levels of Mn in drinking water (>300 µg/L) are associated with reduced

intellectual function in children (Wasserman et al., 2006) likely due to altered neurochemistry (Garcia et al., 2006; Anderson et al., 2008, 2009) Manganese neurotoxicity shares similarities with the neurodegenerative disorder Parkinson's disease (Beuter et al., 1994; Calne et al., 1994; Pal et al., 1999), though the two are clinically distinct (Calne et al., 1994; Pal et al., 1999; Perl and Olanow, 2007). Due to the similarities of Mn neurotoxicity with Parkinson's disease, most research in the area of Mn neurotoxicity has focused on its effect on the biology of dopamine. Recently it has become clear that alterations in the biology of other neurotransmitters are involved in the etiology of Mn neurotoxicity, with the most evidence concerning γ -aminobutyric acid (GABA) (Anderson et al., 2007, 2008; Garcia et al., 2006; 2007; Gwiazda et al., 2002).

With the intriguing findings that striatal extracellular GABA (GABA_{EC}) concentrations are higher due to Mn exposure (Anderson et al., 2008), and uptake of ³H-GABA is attenuated by Mn-exposure in striatal synaptosomes (Anderson et al., 2007) despite no significant effect of Mn on GABA transporter (GAT) protein and mRNA levels (Anderson et al., 2008); we hypothesize that the functioning of the transporter is altered by Mn exposure leading to attenuation of GABA reuptake. Thus, we designed our current experiment to pharmacologically probe the functioning of GAT by administering a known uptake inhibitor, nipecotic acid (NA). NA has a high binding affinity for human GAT-1 and rat GAT-1 and -2, decreasing astrocyte and neuronal GABA uptake (Krogsgaard-Larsen 1980; Krogsgaard-Larsen et al., 2000). We can, therefore, test GAT function by

measuring the increase in GABA_{EC} concentrations in the striatum of Mn-exposed rats by comparing them to the controls. The use of NA is also advantageous because it does not block the transport of other amino acid neurotransmitters, most notably taurine (del Olmo et al., 2004).

Taurine is an abundant non-essential amino acid in the brain formed from cysteine. Traditionally, brain taurine is thought to function as an osmoregulator in cells (cell volume regulation), but has also been implicated in neuromodulation, possibly functioning as a neurotransmitter. Data exist suggesting that taurine functions as an anxiolytic agent (Kong et al., 2006) and interacts with the GABA_A receptor (Jia et al., 2008). These data make sense given that it has long been recognized that taurine and GABA are structurally similar and may share transporters in the brain.

We chose to look at the taurine/GABA relationship in the striatum because it is a known region for Mn accumulation (Erikson et al., 2005; Liu et al., 2000) and because the GABAergic medium spiny neurons of the striatum help orchestrate dopaminergic activity in the basal ganglia (Ade et al., 2008), where dysfunction is known to contribute to movement abnormalities during Mn neurotoxicity (Carlsson and Carlsson, 1990). Microdialysate fractions collected from the striatum of rats revealed that taurine release was higher than glutamate and glycine, and that overall the striatum is very rich in taurine (Molchanova et al., 2004). To date, however, the effect of Mn exposure on extracellular taurine

(Tau_{EC}) in the striatum is unknown. Therefore, we sought to determine if Mn exposure effects Tau_{EC} concentrations in the striatum possibly as it relates to GABA biology.

In addition to GABA and taurine, we felt it was prudent to examine the effect of Mn on another amino acid neurotransmitter, glycine. Glycine is an abundant inhibitor neurotransmitter, similar to GABA, and it is known that taurine is a glycine receptor agonist (Xu et al., 2006). Although previous studies have not shown Mn to have an effect on extracellular glycine (Gly_{EC}) levels in the striatum (Takeda et al., 2003), it is possible that glycine levels may be affected due to potential alterations in GABA or taurine concentrations driven by NA or Mn exposure.

Within the brain, astrocytes are the primary cells that maintain the composition of the extracellular fluid (Wang and Bordey, 2008). It is logical, therefore, that disturbances in GABA_{EC}, Gly_{EC} and Tau_{EC} caused by Mn exposure could be due to astrocyte dysfunction. Thus, our final goal of this study was to examine the effect of Mn exposure on amino acid biology in primary astrocyte cultures.

Materials and Methods

Animals

Male weanling (post-natal day 21) Sprague-Dawley rats (Harlan Sprague-Dawley, Indianapolis, IN) (n=8 for microdialysis study; n=6 for PCR gene expression and metal analysis studies) were randomly divided into two dietary treatment groups used in previous studies (Anderson et al., 2007, 2008): control (CN; 35 mg Fe/kg, 10 mg Mn/kg diet & d.i. water) and Mn-exposed (Mn; control diet & 1 g Mn (as MnCl₂)/L d.i. water). Diets were obtained from Bio-Serv (Frenchtown, NJ) and certified for metal content. Rats had free access to food and water 24 hr/day, with the lights off between 1800 and 600 h and room temperature maintained at 25 ± 1° C. The University of North Carolina at Greensboro Animal Care and Use Committee approved all of the animal procedures.

Cell Cultures

Rat primary cortical astrocyte cultures were purchased from Invitrogen (Carlsbad, CA) and certified for purity with > 95% staining positive for the astrocytic marker glial fibrillary acidic protein (GFAP). Cells were grown in Dulbecco's Modified Eagle Media (D-MEM) with 15% fetal bovine serum (FBS), and maintained in a humidified atmosphere of 95% air/5% CO₂ at 37°C. Manganese treatments were delivered using 0, 100, or 300 µM Mn in the form of MnCl₂. These dose concentrations are based on previous studies in non-human

primates reporting clinical symptoms of Mn neurotoxicity at brain concentrations of 300 μM , while 100 μM concentrations appeared to be asymptomatic (Suzuki et al., 1975). For this reason 300 μM was used to examine the effect of toxic Mn accumulation on Taurine uptake, while 100 and 300 μM were used for the mRNA experiments to examine if there is a change in expression of Scl6a6 from moderate non-symptomatic levels (100 μM) to known toxic accumulation (300 μM).

³H-Taurine Uptake

Uptake of tritiated taurine (³H-Taurine) was measured as described by Erikson and Aschner (2002). Astrocytes (cultured for 3-4 weeks, seeded 2 x 10⁵ in 6-well plates, and grown to confluence) were incubated overnight at 37°C with treatment media containing 0 or 300 μM MnCl₂. The next day, cells were washed 3X with HEPES buffer [122 mM NaCl, 3.3 mM KCl, 0.4 mM MgSO₄, 1.3 mM CaCl₂, 1.2 mM KH₂PO₄, 10 mM glucose, and 25 mM N-2-hydroxyethylpiperazine N'-2-ethansulfonic acid, pH 7.4] and incubated for 1, 3, or 6 minutes with HEPES buffer containing 0.5 μCi ³H-taurine (GE Healthcare Life Sciences, Piscataway, NJ). The reaction was stopped by aspirating the tritiated HEPES and washing the cells 4X with cold (4°C) 290 mM mannitol buffer containing 0.5 mM calcium nitrate to maintain cell adhesion to the substrate. Cells were solubilized in 1 mL RIPA lysis buffer (99 mL 1X PBS, 1 mL Nonidet 40, 0.1 g sodium dodecyl sulfate, 0.5 g sodium deoxycholate, pH 7.4) and 750 μL

aliquots were used for β -counting with a Beckman LS 3801 liquid scintillation analyzer (Beckman Instruments). The remaining 250 μ L was used for protein determination using the bicinchoninic assay (BCA, Pierce Chemicals).

Stereotaxic Surgery

After five weeks of dietary treatment and one week prior to microdialysis experiments, rats were anesthetized with ketamine-HCl (80 mg/kg) and xylazine (12 mg/kg) and maintained on a heating pad at 37° C. The heads of the rats were shaved and wiped with a 5% povidone-iodine solution to reduce risk of infection. Sterile instruments and gloves were used throughout the surgical procedure. The rats were secured in the stereotaxic frame and an incision was made perpendicular to the bregma. A guide cannula (CMA/12, CMA Microdialysis, Acton, MA) was implanted into the striatum using the following coordinates: 2.4 mm lateral to the midline, 7.5 mm anterior to the lambda. The cannula was lowered to a depth of 2.5 mm, positioning it in the medial area of the striatum (Paxinos and Watson, 1998). Anchoring screws were utilized to maintain the position of the cannula before being cemented into place using dental adhesive. Animals were given 0.9% sterile saline (0.5 mL/kg body weight, i.p.) to reduce fluid lost while under anesthesia and to aid in recovery time. Animals were also given the xylazine reversal agent Antisedan (Atapimazole) (0.1 mg/kg body weight, i.p.) (Allivet, Hialeah, FL) to reduce recovery time.

Animals were returned to shoebox cages with Tek-Fresh bedding (Harlan, Indianapolis, IN) and monitored daily until microdialysis experiments began.

Microdialysis

During week six of the dietary protocol, a microdialysis probe (CMA/12 Elite, CMA Microdialysis, Acton, MA) was inserted into the guide cannula and the rat was perfused with artificial cerebral spinal fluid (aCSF) (155 mM Na⁺, 0.83 mM Mg²⁺, 2.9 mM K⁺, 132.76 mM Cl⁻, 1.1 mM Ca⁺, pH 7.4) for one hour at a flow rate of 1 μ L/min. After perfusion, the flow rate was adjusted to 0.5 μ L/min and 30 minute fractions were collected in microtubes for a total of four and a half hours (9 samples per rat) in a refrigerated fraction collector (CMA Microdialysis, Acton MA). This protocol has been used successfully in previous studies with stable neurotransmitter recovery in the dialysate (Anderson et al., 2008; 2009). Probe recoveries measured using in vitro standards for GABA, taurine, and glycine were averaged for each amino acid over all probes; however, because tissue diffusion may affect in vivo probe recovery no correction was made for total recovery as in previous studies (Anderson et al., 2008; 2009; Beard et al., 1994; Chen et al., 1995; Nelson et al., 1997). The microdialysate samples analyzed were collected at 0, 60, 120, 180, and 240-minute time-points with NA administration (100 μ M in aCSF) just prior to the 60-minute collection. This time course identifies baseline values (0 min), the response of extracellular amino acid concentrations to decreased GAT function (60 min), their recovery after

removal of NA and re-perfusion with aCSF (120 min), and renormalization (180 and 240 min). Samples were stored at -80° C until analysis of the dialysate fraction. Rats were then returned to their home cage, and, the following day, were euthanized, brains removed, and probe placement verified post mortem.

CE-LIF Analysis

A protocol by Chen et al. (2001) allowing for detection of amino acids and biogenic amines at nanomolar concentrations, modified to accommodate the needs of our previous studies (Anderson et al., 2008, 2009), was utilized in the current study as well. The advantages of applying CE analysis to neuroactive compounds include minimal required sample volumes, speed of analysis, and high separation efficiency (Powell and Ewing, 2005). Briefly, on the day of sample analysis, 5 µL of microdialysate sample were derivatized at 40°C by the addition to 100 nmol ATTO-TAG™ FQ fluorogenic reagent (Molecular Probes, Eugene, OR) and 10 µL of a 10 mM borate (Fisher, Fair Lawn, NJ)/ 25 mM KCN (Fluka) solution (pH 9.18). The total sample volume was adjusted to 20 µL using HPLC grade methanol (G.J. Chemical Company, Newark, NJ). After a minimum reaction time of 90 min., 1 µL of an FQ derivatized homoserine (Sigma, St.Louis, MO) internal standard solution was added to the derivatized microdialysate sample and analyzed. CE-LIF conditions leading to high efficiency peaks for microdialysate samples were 10 kV for 10 min with sample injections at 10 psi/sec. Uncoated silica capillary (Polymicro, Arizona) with an i.d. of 25 µm, o.d.

of 361 μm , and effective/total lengths of 25.4/30.0 cm was used. The run buffer was 15 mM sodium borate (Fisher), pH 9.0, with 45 mM sodium dodecyl sulfate (Pierce, Rockford, IL), 5 mM sodium cholate (Anatrace, Maumee, OH), and 4% (v/v) 2-propanol (Fisher). Three replicates were analyzed for each sample, with calibration curves for neurotransmitters of interest constructed each day of sample analysis using three points with a concentration range of 0.1 μM to 5 μM . GABA (Sigma), glycine (Sigma), taurine (Sigma), and homoserine standard solutions used for construction of calibration curves were prepared in ACSF with the same composition as that used in the microdialysis studies. The ratio of neurotransmitter peak height to internal standard (homoserine) peak height for each sample was used to determine the concentration of the neurotransmitter based on the calibration curve response.

RNA Isolation and cDNA Synthesis

Total RNA was isolated from astrocyte monolayers and the striatum of control and Mn exposed rats for quantitative PCR analysis. Tissue samples were stored in 1 mL of RNeasy lysis solution (Qiagen, Crawfordsville, IN) and kept at -80°C until analysis. Astrocytes were cultured in 6-well plates, then treated for 24 hrs with media containing 0, 100, or 300 μM Mn. Astrocytes were harvested in 500 μL Denaturation Solution (Ambion Inc., Austin, TX). Tissue and cell culture RNA isolation was performed using the ToTALLY RNA™ system (Ambion Inc., Austin, TX), following manufacturer's instructions. RNA concentration and purity were

determined by spectrophotometric analysis before carrying out cDNA synthesis. Synthesis of cDNA was performed using the High Capacity cDNA Reverse Transcriptase Kit (Applied Biosystems, Foster City, CA), following manufacturer's instructions.

Quantitative PCR

Quantitative real-time PCR analysis was utilized to determine differential mRNA expression between control and Mn treated tissue or cell samples of the solute carrier family taurine transporter Slc6a6 (Applied Biosystems, Foster City, CA; Rn00567962_m1, Chr. 4 - 125875817 – 125945795). Triplicate aliquots of cDNA were analyzed on 96-well plates using TaqMan® Gene Expression assays (Applied Biosystems, Foster City, CA). Values of cDNA expression were normalized relative to the expression of β -actin (Rn00667869_m1, Chr. 12 - 12047070 – 12050040) analyzed from the same sample on the same plate and reported as percent of control.

Metal Analyses

Mn, Fe, and copper (Cu) concentrations were measured with graphite furnace atomic absorption spectrometry (Varian AA240, Varian, Inc., USA). Brain tissue from the striatum was digested in ultra-pure nitric acid (1:10 w/v dilution) for 48-72 hours in a sand bath (60° C). A 50 μ L aliquot of digested tissue was brought to 1 mL total volume with 2% nitric acid for analysis. The extracellular striatal samples obtained via microdialysis were not diluted due to the small

volume (20 μ L) and the likelihood that this biological compartment has a low concentration of metals. Bovine liver (NBS Standard Reference Material, USDC, Washington, DC) (10 μ g Mn/g; 184 μ g Fe/g; 80 μ g Cu/g) was digested in ultrapure nitric acid and used as an internal standard for analysis (final concentration 5 μ g Mn/L; 92 μ g Fe/L; 10 μ g Cu/L).

Statistical Analyses

Data were analyzed using SPSS v14 for Windows (Microsoft, Redmond, WA). Metal, baseline microdialysis, and ^3H -Taurine uptake data were analyzed using paired samples *t*-tests to examine the difference between Mn treated samples and controls. Independent sample *t*-tests were used to examine time-point percent change differences in the microdialysis data, time-point ^3H -Taurine uptake changes, and significance between Mn exposed versus control mRNA expression of *Scf6a6*. A p-value of < 0.05 was considered significant.

Results

Manganese and Iron concentrations

Mn exposure resulted in significant alterations in compartmental metal concentrations. As expected, tissue Mn levels were significantly higher in Mn exposed rats versus control ($p = 0.001$) (Table 1). Cu levels were slightly increased with Mn exposure, and no appreciable difference was observed in Fe levels between the two groups; however, there was a significant reduction ($p =$

0.002) in the Fe:Mn ratio in the Mn exposed group (Table 1). Examining Fe and Mn as a ratio may portray metal toxicities more accurately. The use of an Fe:Mn ratio has recently emerged as a reliable diagnostic criteria for metal neurotoxicities, as levels of one divalent cation may alter the availability or functionality of the other (Chua and Morgan, 1996; Cowan et al., 2009; Fitsanakis et al., 2008).

Collected fractions of microdialysate were analyzed for Fe and Mn to assess changes in extracellular metal levels as a consequence of oral Mn exposure. Extracellular Mn within the striatum was significantly increased in the Mn exposed rats, while Fe levels significantly decreased, compared to controls ($p = 0.021$ and 0.001 , respectively) (Table 1). Differences in extracellular metal concentrations between Mn exposed and control groups revealed a significant ($p = 0.020$), 36-fold, decrease in the extracellular Fe:Mn ratio due to increased Mn (Table 1).

Table 3.1. Brain Tissue and Extracellular Metal Concentrations.

	Extracellular (μM)			Ratio
	Mn	Fe	Cu	Fe:Mn
Control	0.023 \pm 0.006	4.071 \pm 0.510	-	5044:1
Manganese	0.104 \pm 0.030*	1.526 \pm 0.304*	-	137:1*

	Caudate Putamen (nmol/mg Protein)			Ratio
	Mn	Fe	Cu	Fe:Mn
Control	0.185 \pm 0.029	3.896 \pm 0.106	0.177 \pm 0.034	25:1
Manganese	0.477 \pm 0.059*	3.329 \pm 0.407	0.426 \pm 0.037*	9:1*

Table 3.1. Brain Tissue and Extracellular Metal Concentrations. –

Compartmental metal concentrations represented in the striatum of Mn exposed rats. Extracellular metal concentrations represent Mn and Fe levels measured in microdialysate fractions of extracellular fluid collected from the rat striatum (n=4). Striatal Mn, Fe, and Cu levels represent metal concentrations of brain tissue (n=6). The Fe:Mn ratio depicts metal homeostasis changes due to Mn accumulation. A significant increase in extracellular Mn accompanied by significant decreases in both Fe levels and the Fe:Mn ratio were observed in rats exposed to Mn treatment. No significant changes in tissue Fe levels were observed; however, a significant reduction in the Fe:Mn ratio indicates altered metal homeostasis. * = $p < 0.05$, ‡ = $p \leq 0.001$ versus control according to paired-sample *t*-test analysis.

Extracellular concentrations of Taurine, GABA, and Glycine

Extracellular amino acid concentrations are differentially altered by Mn exposure. Baseline levels of taurine and glycine were more abundant than GABA in the extracellular space, though Mn does not have a statistically significant effect on their levels compared to control (Figure 1). Mn exposure, however, did significantly increase ($p = 0.017$) baseline GABA concentrations over control (Figure 1A), corroborating our previous findings (Anderson et al. 2007, 2008). While GABA_{EC} was more concentrated in the striatum of Mn-

exposed rats, the rise in NA-induced GABA levels was not as profound in Mn-exposed versus control rats (Figure 1C). Administration of NA caused a significant 228% increase in the GABA_{EC} levels of the control ($p = 0.015$) but not in the Mn exposed group ($p = 0.233$) (Figure 1C). After the removal of NA and a 60-minute perfusion with aCSF, GABA levels returned to baseline and remained unchanged at the 180- and 240-minute time-points (data not shown).

No significant difference in baseline taurine levels were found between control and Mn exposed animals (Figure 1A). In control animals administration of NA caused a modest 75% decline in Tau_{EC} from baseline, followed by a significant ($p = 0.010$) 1000% increase after removal of NA at the 120 minute time-point (Figure 1B). The decrease in Tau_{EC} was similar in the Mn exposed group due to NA administration; however, no rise in Tau_{EC} was observed after removal of NA, as observed in the control rats (Figure 1B). In control and Mn exposed animals, taurine levels returned to and maintained levels similar to baseline at the 180- and 240-minute time-points (data not shown).

Gly_{EC} levels were similar in control and Mn exposed groups, and no significant percent changes were observed between time-points within either control or Mn groups (Figure 1 D).

Limits of detection of the CE-LIF method employed for each neurotransmitter were found by serial dilution of derivatized standards until no discernable analyte peak could be obtained. Accordingly, limits of detection for

GABA, glycine, and taurine were 6.9 ± 1.7 nM, 24 ± 5 nM, and 42 ± 21 nM, respectively, with linear dynamic ranges of 3.6 decades, 3.1 decades, and 3.3 decades, respectively.

Figure 3.1. Extracellular Amino Acid Concentrations.

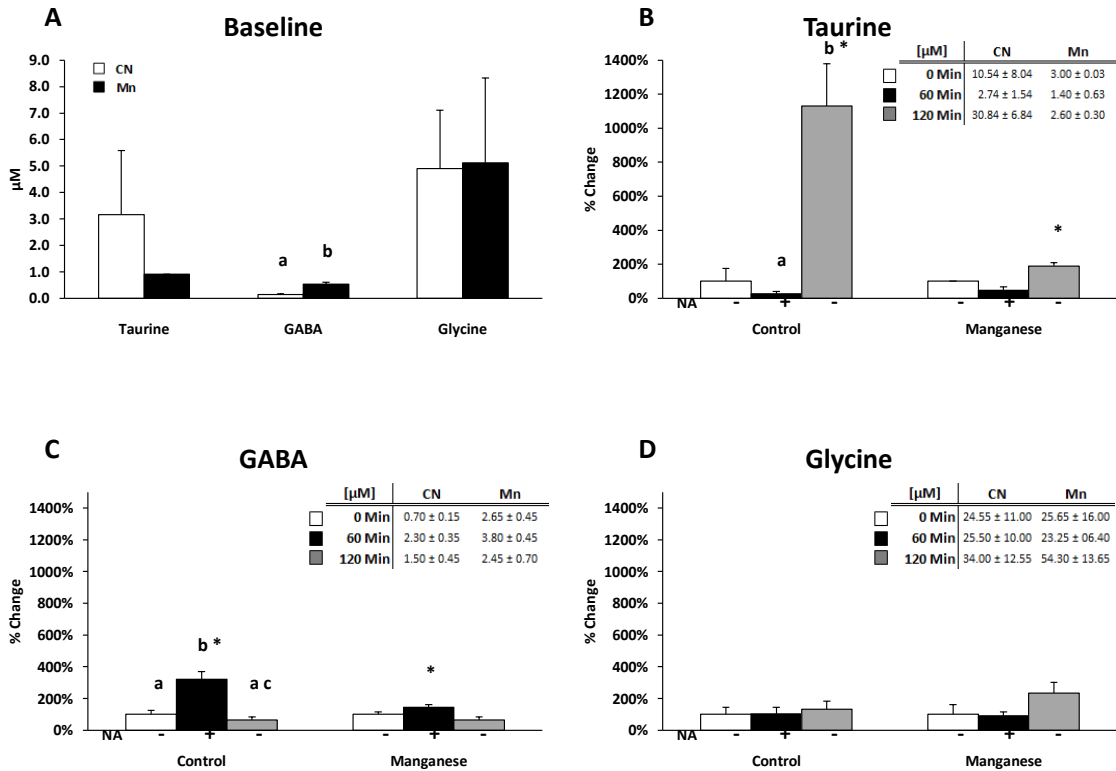


Figure 3.1. Extracellular Amino Acid Concentrations. – Microdialysate fractions from the striatum of control (n=4) and Mn-exposed (n=4) rats were analyzed for taurine, GABA, and glycine concentrations at baseline, 60 minutes, and 120 minutes. Nipecotic Acid (NA) was administered prior to the 60-minute time-point. Graph values are expressed as percent change ± SEM; inset data are μM concentrations ± SEM. A) Baseline concentrations of each amino acid at onset of sample collection (0 Min) in both control and Mn-exposed rats. Percent change in amino acid concentration was calculated from baseline (100%) to post-NA administration, then post-NA to 120-minute recovery period for B) Taurine, C) GABA, and D) Glycine to observe the effect of Mn on extracellular amino acid levels. Superscript letters denote significant within-group differences (bars with different letters are significantly different from one another, bars that share a letter are not significant from one another), while * denote significance between groups.

a, b, c, and * = $p < 0.05$ via independent samples t -test within or between groups.

³H-Taurine Uptake

Mn exposure results in increased ³H-Taurine uptake in astrocytes. After observing the unique effects of Mn-exposure on Tau_{EC} in the striatum of rats in vivo, we decided to examine the effect of Mn exposure on ³H-Taurine uptake in primary rat astrocytes in vitro. Primary astrocytes exposed to Mn revealed a slight (30%) decrease in taurine uptake after 1 minute, followed by a significant (219%) increase after 3 minutes (p = 0.034) (Figure 2). Six minute ³H-Taurine retention in Mn exposed cells was similar to that of controls. Uptake of ³H-Taurine in control cells remained consistent around 0.4 pmol/mg protein at each time-point (Figure 2 inset). To examine whether or not 24 hr Mn exposure had an effect on taurine transporter expression in astrocytes, we next evaluated Mn induced alterations in the taurine transporter, Slc6a6.

Gene Expression of Taurine Transporter

Mn exposure increased taurine transporter gene expression in the rat brain, but not cultured astrocytes. Quantitative RT-PCR analysis was conducted on primary astrocytes and striatal brain tissue to determine whether or not taurine transporter (Slc6a6) gene expression reflected the observed Mn induced alterations in Tau_{EC} and ³H-uptake. Chronic Mn exposure caused a significant (p = 0.045) increase in striatal Slc6a6 mRNA levels compared to control (Figure 3). Alternatively, acute Mn exposure (100 and 300 μM Mn) had relatively little effect on astrocyte Slc6a6 mRNA levels (Figure 3).

Figure 3.2. ³H-Taurine Uptake in Primary Astrocytes.

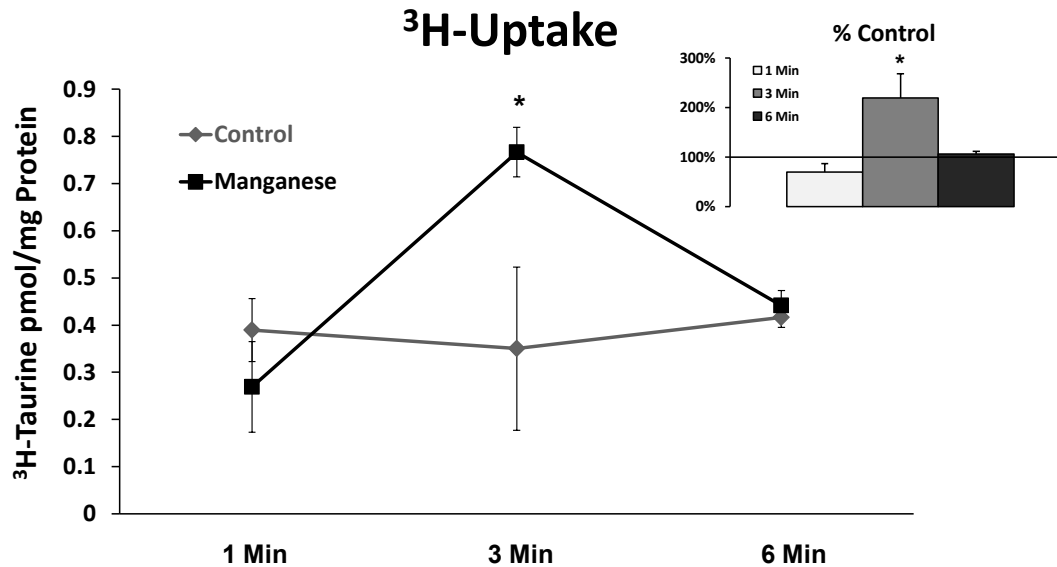


Figure 3.2. ³H-Taurine Uptake in Primary Astrocytes. – Primary astrocytes, seeded 2×10^5 in 6-well plates (n=6) then grown to confluence, were cultured with either Mn-treated (300 μ M MnCl₂) or control media. After 24hrs cultures were exposed to ³H-Taurine for 1, 3, or 6 minutes and analyzed for ³H-Taurine retention. The inset represents percent change in uptake due to Mn exposure expressed as percent control \pm SEM. A significant ($p = 0.034$) increase in ³H-Taurine uptake was observed after 3mins of exposure in the Mn treated astrocytes versus control.

* = $p < 0.05$ via independent samples *t*-test between Mn and control treatment groups at each time-point.

Figure 3.3. Taurine Transporter, Slc6a6, mRNA Levels.

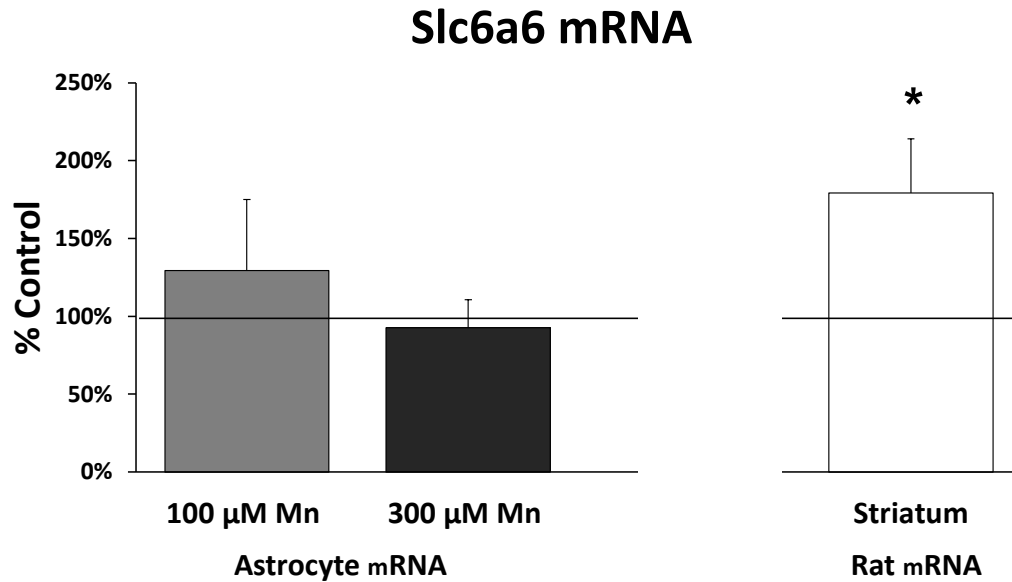


Figure 3.3. Taurine Transporter, Slc6a6, mRNA Levels. – Quantitative RT-PCR results for taurine transporter, Slc6a6, in Mn exposed astrocytes (n=6) and the striatum of Mn exposed rats (n=6). Values are expressed as percent control \pm SEM, with control values representing no Mn exposure. Minimal alterations in Slc6a6 levels were observed in astrocytes treated with either 100 or 300 μ M MnCl₂. Mn exposure did, however, significantly increase Slc6a6 mRNA levels within the caudate putamen, versus matched control animals.

* = $p < 0.05$ via independent samples T-Test between Mn and control treatment groups.

F). We hypothesize this lack of response in Mn-exposed rats is driven by decreased GABA transporter (GAT-1) function. **(A)** The control panel displays $GABA_{EC}$ and Tau_{EC} under normal conditions, representing baseline microdialysis measurements. All percent change (% change) comparisons in subsequent panels are based on the % change from baseline levels, represented in the control panel. Under normal conditions $GABA_{EC}$ binds to $GABA_A$ receptors ($GABA_A$ -R) allowing chloride ion (Cl^{2-}) movement for inhibitory hyperpolarization of postsynaptic neurons, while presynaptic binding to $GABA_B$ -receptors ($GABA_B$ -R) regulates GABA release (Kamisaki et al., 1993) through slow G-protein-linked inhibitory tone via $GABA_B$ activation (Chen and van den Pol, 1998). GAT-1 functions normally to clear excess GABA from the synapse as Tau_{EC} modulates pre- and post-synaptic transmission (Namima et al., 1982; 1983). **(B)** Administration of NA, a GAT specific inhibitor, blocks GABA reuptake substantially increasing $GABA_{EC}$ while decreasing Tau_{EC} . Additionally, NA activates $GABA_A$ -like Cl^{2-} channels (Barrett-Jolley, 2001) in addition to GAT binding, increasing the pre- and post-synaptic inhibitory tone. **(C)** Upon removal of the NA, $GABA_{EC}$ returns to normal; however, a 10-fold increase in Tau_{EC} ensues. We speculate that the taurine efflux is a compensatory response to regulate GABA release through $GABA_B$ activation (Chen and van den Pol, 1998). Elevated Tau_{EC} may also function to stabilize the inhibitory tone achieved in the striatum due to increased $GABA_A$ activation (del Olmo et al., 2000; Jia et al., 2008). Tau_{EC} slowly returns to control levels over the next two hours (data not shown), indicating the acute nature of this response. **(D)** During Mn-exposure, $GABA_B$ expression is decreased (Anderson et al., 2008) and GABA reuptake via GAT-1 is attenuated, resulting in higher $GABA_{EC}$ and lower Tau_{EC} (Figure 1B and C) compared to control. We hypothesize that this alteration in GAT-1 function is regulated by Mn activation of protein kinase C (PKC) (Latchoumycandane et al., 2005) causing phosphorylation of GAT-1 and subsequent internalization (Gadea and Lopez-Colome, 2001). This internalization decreases synaptic density of GAT-1 and attenuates GABA reuptake. Additionally, decreased $GABA_B$ expression alters auto-receptor feedback resulting in significantly higher $GABA_{EC}$ compared to normal conditions. **(E)** Mn exposure significantly attenuates the effects of NA, potentially via decreased synaptic availability of GAT-1. The attenuated rise in $GABA_{EC}$ coupled with decreased auto-receptor expression results in less $GABA_A$ and $GABA_B$ activation leading to reduced inhibitory tone compared to control. **(F)** Removal of NA in Mn-exposed rats led to $GABA_{EC}$ returning to pre-NA levels (Panel D); however, the taurine efflux was absent compared to control (refer to Figure 1B). We interpret the dramatically decreased taurine efflux observed with Mn exposure as a function of altered auto-receptor biology (Anderson et al., 2008). Altered feedback regulation in conjunction with a modest rise (40%) in $GABA_{EC}$, compared to the normal feedback regulation and significant rise (228%) in $GABA_{EC}$ observed in control rats, leads to an uncoupling of the taurine efflux response due to Mn-exposure. Our studies suggest that Mn exposure disrupts extracellular conditions within the

striatum, altering neurochemical coordination with other brain regions. Elucidating the mechanism involved in this response will further the development of pharmacological therapies aimed at susceptible populations.

Discussion

The purpose of this study was to examine the effect of Mn on GAT-mediated GABA uptake. Knowing that glycine and taurine are important amino acid neurotransmitters that are known to modulate GABA neurochemistry (Namima et al., 1982; Hernandez and Troncone, 2009), it was logical that we measure them in the dialysate too. We found that GAT function is attenuated by Mn exposure, and that the resulting increase in GABA_{EC} alters taurine but not glycine homeostasis. Specifically, we observed a 10-fold increase in Tau_{EC} upon removal of NA in the control animals but not in the Mn exposed, implicating a critical neurotransmitter function of Tau_{EC} that Mn alters (discussed in more detail below and in Figure 4).

Mn, Fe, and Cu levels were analyzed in the striatum of Mn exposed rats and non-exposed controls to ascertain homeostatic changes due to Mn accumulation. As expected, Mn exposure led to significant Mn accumulation in the striatum (Table 1). Striatal Cu levels were slightly higher with Mn exposure, but tissue Fe levels were unaffected. These data are consistent with striatal Fe levels reported in previous studies with Mn exposure (Anderson et al., 2009; Erikson et al., 2004; Fitsanakis et al., 2008). However, there was a near three-fold decrease in the Fe:Mn ratio with Mn exposure, suggesting altered metal

homeostasis. While tissue levels of Fe remained relatively unchanged, extracellular Fe was significantly decreased by Mn accumulation, with a 36-fold drop in the Fe:Mn ratio. Previously, Mn driven decreases in extracellular Fe have been positively correlated with extracellular norepinephrine levels and inversely associated with GABA_{EC} (Anderson et al., 2008, 2009), but no significant changes in tissue Fe levels were observed. The disparity between tissue and extracellular Fe:Mn ratios suggest the synaptic environment may be subject to drastic changes in metal homeostasis. Moreover, these changes may leave the extracellular compartment vulnerable compared to striatal tissue, in which Fe and Mn levels appear to be more tightly regulated.

We specifically selected the striatum to examine the effect of Mn on GABA_{EC} and GAT function because it is a known region for Mn accumulation (Erikson et al., 2005; Liu et al., 2000), and due to its high density of GABAergic cell bodies (Oertel and Mungnaini, 1984). Mn exposure has been associated with increased GABA_{EC} concentrations in the striatum, and decreased ³H-GABA uptake has been reported in striatal synaptosomes (Anderson et al., 2007, 2008). While these studies reported little effect on GAT protein and mRNA levels with Mn exposure, the implications of these data on GAT functionality prompted us to pharmacologically probe GAT function with NA. We hypothesized that Mn exposure alters GAT function as indicated by the attenuation of increased GABA_{EC} concentrations in the presence of NA. Results from the microdialysis experiment indicate that this is indeed the case. NA in the striatum of control rats

caused a 228% increase in GABA_{EC}; however, in Mn-exposed rats NA only increased GABA_{EC} by 43%. The use of NA in the current study identifies GAT as a target for Mn toxicity, and provides an explanation for the observed increase in GABA_{EC} with Mn accumulation. Exactly how Mn regulates GAT function warrants further investigation; however, decreased GAT function may be regulated through protein kinase C (PKC) activation. Mn exposure has been shown to activate PKC in N27 mesencephalic cells (Latchoumycandane et al., 2005), and PKC activation has been demonstrated to decrease ³H-GABA transport by GAT (Sato et al., 1995). Moreover, phosphorylation of GAT-1 via PKC (Mandela and Ordway, 2006) may lead to internalization of GABA transporters (Gadea and Lopez-Colome, 2001). This could explain why Anderson et al. (2008) found increased GABA_{EC} despite no decrease in GAT-1 protein levels (as detected by western blot analysis which would measure both plasma membrane and internalized GAT-1 levels). It is also possible that Mn may alter some sort of feedback mechanism such as an autoreceptor (e.g., GABA_B or GABA_A). Being that taurine is a known modulator of GABA receptors (del Olmo et al., 2000; Kamisaki et al., 1993; Jia et al., 2008; Namima et al., 1982, 1983), perturbations in taurine biology may play a role in GABA homeostasis.

A novel finding from our study was that control rats responded to cessation of NA with a 10-fold increase of Tau_{EC} in the striatum, an effect that was absent in the Mn exposed rats. Changes in Tau_{EC} coincided inversely with alterations in GABA (Figure 1A, B), presumably due to its role in osmoregulation.

These results suggest that alterations in GABA uptake may dictate taurine release due to a hyperosmotic environment. Alternatively, the 10-fold increase in taurine after removal of NA may be a compensatory response to help decrease GABA_{EC} concentrations. Taurine binding to GABA_A receptors (del Olmo et al., 2000; Jia et al., 2008) and GABA_B autoreceptors (Kamisaki et al., 1993; Namima et al., 1982, 1983), may help to regulate GABA release. Enhanced taurine efflux observed in control animals after NA administration could functionally decrease GABA release by activating GABA_A and GABA_B receptors thereby normalizing GABA_{EC}. Additionally, there is evidence that NA activates GABA_A-like ion channels (Barrett-Jolley, 2001). Taurine efflux may be an adaptive response to facilitate GABA_A activation compensating for the loss of inhibitory tone due to NA cessation. Whether the taurine response observed in the control rats is due to its role in regulating striatal neurochemistry or through a secondary osmoregulatory effect, the lack of this response in the Mn-exposed rats may have profound consequences (See Figure 4).

Because Mn alters GAT function and GAT transport proteins are in the solute carrier protein family Slc6 (shared by the taurine transporter, Slc6a6), it is reasonable to assume that Mn may influence taurine movement by altering the function of the taurine transporter. In cultured astrocytes we measured ³H-Taurine uptake and found that while Mn initially decreased taurine uptake by 30%, it was followed by a significant 219% increase in uptake before normalizing to control levels (Figure 2). Uptake of ³H-Taurine in control cells remained

consistent around 0.4 pmol/mg protein at each time-point, suggesting that fluctuations in taurine uptake in vitro is probably due to osmoregulation or altered transporter kinetics. Taurine transporter Slc6a6 mRNA levels were not altered in cultured astrocytes exposed to 100 or 300 μ M Mn. Similar results were found by Erikson and Aschner (2002), with Slc6a6 expression significantly increasing in astrocytes only when exposed to 500 μ M Mn. It is important, however, to remember that taurine transport may also occur via volume-sensitive organic osmolyte anion channels (VSOAC) (Mongin et al., 1999). VSOACs allow the transport of Na⁺, K⁺, Cl⁻, and organic osmolytes (e.g. taurine) under conditions of cell shrinkage or swelling (Lang, 2007). Without directly inhibiting Slc6a6, controlling osmolarity, and taking into account Cl⁻ influx due to GABAA activation we cannot confirm the functionality of Slc6a6 in the presence of Mn. Interestingly, Slc6a6 mRNA levels are increased in the striatum of Mn exposed rats, compared to control (Figure 3). The contradiction of in vivo and in vitro Slc6a6 expression may be a product of chronic (6 week) exposure to Mn in vivo versus acute (24 hr) exposure in vitro. Additionally, Slc6a6 gene expression is increased in the absence of sufficient taurine, and decreased when taurine is in excess (Bitoun and Tappaz, 2000; Lambert, 2004). Therefore, it is likely that altered taurine homeostasis in the striatum due to Mn exposure influences striatal Slc6a6 expression similarly.

Collectively, our data show that the GABA_{EC} and Tau_{EC} are indeed influenced by Mn accumulation and altered GAT function. Moreover, Mn virtually

abolished Tau_{EC} and dramatically blunted the taurine rebound observed during the post NA recovery period (Figures 2B and 4), indicating a serious disconnect in taurine homeostasis in the Mn-exposed rat striatum. Moving forward, it is essential to understand the effect of Mn toxicity on taurine movement in the brain. Characterizing the role of Mn on GABA and taurine may help depict the multifaceted etiology of Mn neurotoxicity, and provide insight into some of the behavioral changes observed with Mn accumulation.

Acknowledgements

The authors thank Dr. Jan Albrecht (Polish Academy of Sciences) for sharing his expertise. This research was supported by the National Institutes of Health R15 NS061309-01 (KME), and by the North Carolina Biotechnology Center #2007-BRG-1253 and Wake Forest University (TLW and CLC).

CHAPTER IV

**WATERBORNE MANGANESE EXPOSURE ALTERS PLASMA, BRAIN, AND
LIVER METABOLITES ACCOMPANIED BY CHANGES IN STEREOTYPIC
BEHAVIORS**

Reprinted from *Neurotoxicology and Teratology*, volume 34, Steve C. Fordahl, Paula T. Cooney, Yunping Qiu, Guoxiang Xie, Wei Jia, and Keith M. Erikson, *Waterborne Manganese Exposure Alters Plasma, Brain, and Liver Metabolites Accompanied by Changes in Stereotypic Behaviors*, pages 27 to 36, in 2012, with permission from Elsevier to use the article in its entirety as notated in Appendix A. References from this article can be found in the Reference section.

Abstract

Overexposure to waterborne manganese (Mn) is linked with cognitive impairment in children and neurochemical abnormalities in other experimental models. In order to characterize the threshold between Mn exposure and altered neurochemistry, it is important to identify biomarkers that positively correspond with brain Mn accumulation. The objective of this study was to identify Mn induced alterations in plasma, liver, and brain metabolites using liquid/gas chromatography-time of flight-mass spectrometry metabolomic analyses; and to monitor corresponding Mn induced behavior changes. Weanling Sprague-Dawley rats had access to deionized drinking water either Mn free or containing 1g Mn/L for six weeks. Behaviors were monitored during the sixth week for a continuous 24h period while in a home cage environment using video surveillance. Mn

exposure significantly increased liver, plasma, and brain Mn concentrations compared to control, specifically targeting the globus pallidus (GP). Mn significantly altered 98 metabolites in the brain, liver, and plasma; notably shifting cholesterol and fatty acid metabolism in the brain (increased oleic and palmitic acid; 12.57 and 15.48 fold change (FC), respectively), and liver (increased oleic acid, 14.51 FC; decreased hydroxybutyric acid, -14.29 FC). Additionally, Mn altered plasma metabolites homogentisic acid, chenodeoxycholic acid, and aspartic acid correlated significantly with GP and striatal Mn. Total distance traveled was significantly increased and positively correlated with Mn exposure, while nocturnal stereotypic and exploratory behaviors were reduced with Mn exposure and performed largely during the light cycle compared to unexposed rats. These data provide putative biomarkers for Mn neurotoxicity and suggest that Mn disrupts the circadian cycle in rats.

Introduction

Overexposure to environmental manganese (Mn) is known to have neurological consequences with symptomology similar to Parkinson's disease (PD) (Pal et al., 1999; Cersosimo and Koller, 2006; Perl and Olanow, 2007). Both are characterized by alterations in the dopaminergic system of the basal ganglia, producing movement abnormalities and cognitive deficits (Pal et al., 1999; Cersosimo and Koller, 2006). Mn neurotoxicity is clinically distinct from PD in that onset may occur at earlier ages, movement symptoms occur bilaterally as

opposed to unilaterally in PD, and the lack of response to levo-Dopa treatment (Cersosimo and Koller, 2006). Cases of Mn neurotoxicity have been reported due to occupational contact (e.g., mining, battery manufacturing, and welding) and contaminated drinking water (Crossgrove and Zheng, 2004; Wasserman et al., 2006). Challenges exist in diagnosing Mn neurotoxicity, and factors such as length or route of exposure may differentially affect symptom onset. Inhalation of Mn species leads to rapid brain Mn accumulation and is associated with increased biomarkers of oxidative stress (Erikson et al., 2007); whereas, ingested Mn accumulates in the brain at slightly lower concentrations and is associated with neurochemical alterations (Garcia et al., 2006; Anderson et al., 2008; Fordahl et al., 2010) and cognitive decline (Wasserman et al., 2006; Bouchard et al., 2011).

Mn-neurotoxicity has been linked with changes in dopamine, γ -aminobutyric acid (GABA), and glutamate (Fitsanakis et al., 2006 for review). Mn induced changes in these neurochemicals, specifically dopamine, have been associated with hyperactivity in rodents (Kern et al., 2010), and learning/memory deficits accompanied by changes in stereotypic behaviors in primates (Schneider et al, 2006; Kern et al., 2010). Similar symptoms have been reported in Mn-exposed children (Bouchard et al., 2007; Farias et al., 2010), and it is imperative to identify symptoms of toxicity early during this critical stage of growth and neurological development.

Early symptom identification and removal from Mn exposure can improve the prognosis of Mn neurotoxicity. The use of magnetic resonance imaging (MRI) has been demonstrated to accurately reflect brain Mn deposits (Dorman et al., 2006; Fitsanakis et al., 2008), and when used in conjunction with positron emission tomography (PET) can identify biological alterations in neurotransmission (Kim et al., 1999). While MRI and PET technologies have advanced the identification of Mn neurotoxicity, the practical application and cost of these tools may preclude widespread use. Moving forward, it is important to establish cost effective diagnostic measures that correspond with brain Mn accumulation similar to MRI. Identifying biomarkers of Mn neurotoxicity in biological fluids may provide an alternative solution to confirm the extent of brain Mn accumulation.

To date, few reliable markers exist to measure the extent of brain Mn accumulation. Prospective compounds such as lymphocytic manganese superoxide dismutase (MnSOD) and arginase were suggested as biomarkers over a decade ago; however, each possessed diagnostic limitations (Davis and Greger, 1992; Brock et al., 1994). More recently, Dorman et al. (2008) screened for potential Mn exposure biomarkers using a liquid chromatography-mass spectrometry method to identify metabolomic changes in the blood and urine of monkeys exposed to airborne MnSO₄. Of the 27 metabolites significantly altered by Mn, three blood metabolites corresponded with Mn accumulation in the globus pallidus (GP): phenylpyruvate, disaccharides, and guanosine (Dorman et al.,

2008). While these markers show promise, additional studies are needed to confirm their potential as consistent biomarkers.

The study of metabolomics is emerging as a reliable approach to identify potential biomarkers in diseased states including cancer (Kim et al., 2008) and amyotrophic lateral sclerosis (Pradat and Dib, 2009), among other potential applications (Oresic et al., 2006). Methods using liquid and gas chromatography, coupled with mass spectrometry (LC-MS, GC-MS), enable the detection of thousands of metabolites in a biological sample (Halket et al., 2005). These methods are ideal for monitoring changes in metabolite byproducts due to altered cellular metabolism in either a diseased state or after application of selected therapies. The goal of this study was to identify potential biomarkers of Mn neurotoxicity, and to link any changes in the metabolome with biological alterations associated with Mn exposure. Additionally, we wanted to monitor any changes in behavior or locomotor activity indicative of neurotoxicity. While previous studies have examined the effects of Mn exposure on behavior over short observational periods, to date no study has examined the effects of Mn on locomotor and circadian behaviors longitudinally over a 24h period in a home-cage environment. A 24h time frame allows for analysis of diurnal and nocturnal behaviors not normally captured with other behavioral tests.

Materials and Methods

Animals

Male weanling (post-natal day 21) Sprague-Dawley rats (Harlan Sprague-Dawley, Indianapolis, IN) (n=12) were individually housed and randomly divided into two treatment groups: control (AIN-93G diet (35, 10, and 6 mg/kg Fe, Mn, and Cu, respectively) with deionized water) and Mn-exposed (AIN-93G diet with deionized water containing 1 g Mn (as MnCl₂) /L. Formulated diet was obtained from Dyets Inc. (Bethlehem, PA). This Mn-exposure protocol has been used previously in our lab to achieve consistent brain Mn accumulation producing neurochemical changes indicative of toxicity after 6 weeks of exposure (Anderson et al., 2007; 2008; Fordahl et al., 2010). Based on average water consumption for rats (10-12 ml per 100 g body weight (Harkness and Wagner, 1989)), Mn ingestion was approximately 100 mg/kg per day. Water levels were monitored to examine consumption, and no avoidance of Mn containing water was observed. Because intestinal Mn absorption in rodents is estimated at 1-5% (Hurley and Keen, 1987), the systemic Mn burden was approximately 1-5 mg. Human exposure to waterborne Mn has been reported at >700 µg/L in children (Wasserman et al., 2006) leading to cognitive impairment, and up to 14 mg/L in 25 Japanese adults (Kawamura et al. 1941) resulting in neurotoxicity (n=23) and death (n=2). Although 100 mg Mn/kg is considerably higher than documented human exposure, it should be noted that Sprague Dawley rats have a higher threshold for toxicity than humans withstanding Mn doses of 200 mg/kg/day for

2yrs and 2,251 mg/kg/day for 6 months before fatality (NTP, 1993; Gianutsos and Murray, 1982). Rats had free access to food and water 24 hr/day, with the lights off between 1800 and 600 h and room temperature maintained at $25 \pm 1^\circ\text{C}$. During the seventh week of the study, after an overnight fast with access to water, the rats were rendered unconscious in a CO_2 chamber, euthanized via decapitation, brains and liver tissue removed, and trunk blood was collected for analysis. Dissected tissues were immediately placed on dry ice then stored at -80°C until analysis. For metal analysis, sections of the globus pallidus (GP) and striatum, two regions known to accumulate Mn, were removed, and the remaining brain tissue was used for metabolomic analysis. The University of North Carolina at Greensboro Animal Care and Use Committee approved all of the animal procedures.

Hematology

Trunk blood from each rat was collected in heparinized tubes and stored on ice until processed. Hematocrit was determined by centrifugation of heparinized micro-hematocrit capillary tubes (Fisher Scientific, Waltham, MA). Remaining whole blood samples were centrifuged for 15 minutes at $1000 \times g$ to separate plasma for iron (Fe) status assays, metabolomic analysis and metal quantification. Plasma was stored at -80°C . Plasma ferritin and transferrin were determined using enzyme linked immunosorbent assay (ELISA) kits from (ICL, Inc., Newberg, OR) and (GenWay Biotech, Inc., San Diego, CA), respectively.

Behavior Analysis

Behavior analysis was conducted using Clever Systems Home Cage Scan (HCS) system (Reston, VA) rather than a rating scale system, which are generally time-consuming and provide ordinal data (Flagel and Robinson, 2007). The HCS system utilizes video images from the home cage acquired at 30 frames per second. Software algorithms then categorize the images into a set of behaviors by extracting the image of the animal movements. Based on the sequential postures of the animal and position of body parts in space, behaviors are assigned using pre-trained data sets as a reference (Flagel and Robinson, 2007). Agreement between behaviors identified by the HCS and manual assessments has been found to be $\geq 90\%$ (Steele et al., 2007). During weeks four, five, and six of the dietary protocol, animals were placed in individual shoebox cages with food, water, and minimal bedding. The animals were allowed to acclimate to the novel environment for a 24h period to ensure that any behavior alterations captured were treatment effects. After the acclimation period the animals were monitored by video surveillance and their behaviors were analyzed for an additional 24h period to capture the entire light and dark cycle. Cameras were mounted onto tripods and placed parallel to the shoebox cages. Red lighting was utilized during the dark phase to provide an appropriate background for the HCS system to analyze movement. Behaviors were scored by the HCS system and data exported to MS Excel 2007 for analysis. The

following behaviors were examined: total distance traveled, repetitive turning (turning), sniffing, rearing, and grooming.

Metal Analyses

Mn, Fe, and copper (Cu) concentrations were measured with graphite furnace atomic absorption spectrometry (Varian AA240, Varian, Inc., USA). Brain, liver, and plasma samples were digested in ultra-pure nitric acid (1:10 dilution for plasma, 1:10 w/v dilution for tissue) for 48-72 hours in a sand bath (60° C). A 50 µL aliquot of digested sample was further diluted 1:20 with a 2% nitric acid solution for analysis. Bovine liver (NBS Standard Reference Material, USDC, Washington, DC) (10 µg Mn/g; 184 µg Fe/g; 80 µg Cu/g) was digested in ultrapure nitric acid and used as an internal standard for analysis (final concentration 5 µg Mn/L; 92 µg Fe/L; 40 µg Cu/L). Metal data are expressed as µg/g tissue or µg/L plasma. Additionally, an Fe:Mn ratio was also used to address the relationship between these metals as levels of one may impact the functionality or availability of the other (Chua and Morgan, 1996; Cowan et al., 2009; Fitsanakis et al., 2008).

Liquid Chromatography-Time of Flight Mass Spectrometry (LC-TOFMS)

Plasma samples were thawed and centrifuged at 13,000 rpm for 5 min. A volume of 100 µL supernatant was mixed with 400 µL of a mixture of methanol and acetonitrile (5:3). The mixture was vortexed for 2 min, allowed to stand for 10 min, centrifuged at 13,000 rpm for 20 min, and then the supernatant was used

for LC-TOFMS. Liver and brain tissue (100 mg and 50 mg, respectively) was added to 500 μ L of a chloroform, methanol, and water mixture (1:2:1, v/v/v). These samples were then homogenized and centrifuged at 13,000 rpm for 10 min at 4°C. A 150 μ L aliquot of supernatant was transferred to a sampling vial. The deposit was re-homogenized with 500 μ L methanol followed by a second centrifugation. Another 150 μ L supernatant was added to the same vial for drying and then reconstituted in 500 μ L of ACN:H₂O (6:4, v/v) before separation.

An Agilent HPLC 1200 system equipped with a binary solvent delivery manager and a sample manager (Agilent Corporation, Santa Clara, CA, USA) was used with chromatographic separations performed on a 4.6 \times 150 mm 5 μ m Agilent ZORBAX Eclipse XDB-C18 chromatography column. The LC elution conditions are optimized as follows: isocratic at 1% B (0–0.5 min), linear gradient from 1% to 20% B (0.5–9.0 min), 20–75% B (9.0–15.0 min), 75–100% B (15.0–18.0 min), isocratic at 100% B (18–19.5 min); linear gradient from 100% to 1% B (19.5–20.0 min) and isocratic at 1% B (20.0–25.0 min). For positive ion mode (ESI+) where A = water with 0.1% formic acid and B = acetonitrile with 0.1% formic acid, while A = water and B = acetonitrile for negative ion mode (ESI-). The column was maintained at 30 °C as a 5 μ L aliquot of sample is injected. Mass spectrometry is performed using an Agilent model 6220 MSD TOF mass spectrometer equipped with a dual sprayer electrospray ionization source (Agilent Corporation, Santa Clara, CA, USA). The system was tuned for optimum sensitivity and resolution using an Agilent ESI-L low concentration tuning mix in

both positive (ES+) and negative (ES-) electrospray ionization modes. Agilent API-TOF reference mass solution kit was used to obtain accurate mass time-of-flight data in both positive and negative mode operation. The TOF mass spectrometer was operated with the following optimized conditions: (1) ES+ mode, capillary voltage 3500 V, nebulizer 45 psig, drying gas temperature 325 °C, drying gas flow 11 L/min, and (2) ES- mode, similar conditions as ES+ mode except the capillary voltage was adjusted to 3000 V. The TOF mass spectrometer is calibrated routinely in ES+ and ES- modes using the Agilent ESI-L low concentration tuning mix. During metabolite profiling experiments, both plot and centroid data are acquired for each sample from 50 to 1,000 Da over a 25 min analysis time. Data generated from LC-TOFMS were centroided, deisotoped, and converted to mzData xml files using the MassHunter Qualitative Analysis Program (vB.03.01) (Agilent). Following conversion, xml files are analyzed using the open source XCMS package (v1.16.3) (<http://metlin.scripps.edu>), which runs in the statistical package R (v.2.9.2) (<http://www.r-project.org>), to pick, align, and quantify features (chromatographic events corresponding to specific m/z values and elution times). The software is used with default settings as described (<http://metlin.scripps.edu>) except for xset (bw = 5) and rector (plotype = "m", family = "s"). The created .tsv file is opened using Excel software and saved as .xls file. The resulting 3-D matrix containing arbitrarily assigned peak index, retention time, and abundance value (.xls file) are further exported to SIMCA-P software 12.0 (Umetrics, Umeå, Sweden) for multivariate statistical analysis.

Compound identification was performed by comparing the accurate mass and retention time with reference standards available in our laboratory, or comparing the accurate mass with online database such as the Human Metabolome Database (HMDB).

Gas Chromatography-Time of Flight Mass Spectrometry (GC-TOFMS)

The GC-TOFMS analysis procedure was followed by our previous publications (Qui et al., 2009; Pan et al., 2010). For plasma samples (50 μ l for each sample), the metabolites were extracted by 150 μ l of mixture solvent (methanol: chloroform (3:1)). After centrifugation, an aliquot of the 170- μ L supernatant was transferred to a glass sampling vial to vacuum dry at room temperature. The tissue samples were prepared identically to those used in the LC-TOFMS without reconstitution in ACN:H₂O. Instead, the 150 μ l aliquot of supernatant was added to the same vial (containing 10 μ l heptadecanoic acid in methanol, 1 mg/ mL) to vacuum dry at room temperature. The residue of plasma and tissue samples was then derivatized by adding 80 μ L methoxyamine (15 mg/mL in pyridine) to the vial while holding at 30°C for 90 minutes, then 10 μ L retention index compounds (the mixture of C10-C40, 50 μ g/mL) and 80 μ L BSTFA (1%TMCS) were added into the reaction vials. Then the samples were subjected to a 70°C for 120 minutes derivatization reaction.

A 1 μ L aliquot of the derivatized solution was injected using splitless mode into an Agilent 7890N gas chromatograph coupled with a Pegasus HT time-of-

flight mass spectrometer (Leco Corporation, St Joseph, USA). Separation was achieved on a DB-5 ms capillary column (30 m × 250 µm I.D., 0.25-µm film thickness; Agilent J&W Scientific, Folsom, CA, USA), with helium as the carrier gas at a constant flow rate of 1.0 ml/min. The temperature of injection, transfer interface, and ion source was set to 260°C, 260°C, and 210°C, respectively. The GC temperature programming was set to 2 min isothermal heating at 80°C, followed by 10°C/min oven temperature ramps to 220 °C, 5 °C/min to 240°C, and 25°C/min to 290 °C, and a final 8 min maintenance at 290°C. Electron impact ionization (70 eV) at full scan mode (m/z 40-600) was used, with an acquisition rate of 20 spectra/second in the TOFMS setting. The acquired MS files from GC/TOFMS analysis were exported in NetCDF format by ChromaTOF software (v4.22, Leco Co., CA, USA). CDF files were extracted using custom scripts (revised Matlab toolbox hierarchical multivariate curve resolution (H-MCR), developed by Par Jonsson, et al.) in the MATLAB 7.0 (The MathWorks, Inc, USA) for data pretreatment procedures such as baseline correction, de-noising, smoothing, alignment, time-window splitting, and multivariate curve resolution (based on multivariate curve resolution algorithm). The resulting three dimension data set includes sample information, peak retention time and peak intensities. Internal standards and any known artificial peaks, such as peaks caused by noise, column bleed and BSTFA derivatization procedure, were removed from the data set. The resulting data was mean centered and unit variance scaled during chemometric data analysis in the SIMCA-P 12.0 Software package

(Umetrics, Umeå, Sweden). Compound identification was performed by comparing the mass fragments with NIST 05 Standard mass spectral databases in NIST MS search 2.0 (NIST, Gaithersburg, MD) software with a similarity of more than 70% and finally verified by available reference compounds.

Data Analyses

Metal, body weight, hematology, and behavior data were analyzed using SPSS v14 for Windows. Data were examined for normality of distribution using a one-sample Kolmogorov-Smirnov test and for the presence of outliers by boxplot analysis. Independent *t*-test analyses were conducted to identify changes between control and Mn exposed groups for metal, body weight, hematology, and behavior data. After Bonferroni correction for multiple comparisons, the significance level for metal and behavior *t*-tests was set at $p < 0.025$ and $p < 0.01$, respectively. Pearson's correlational analyses were then performed to examine relationships between metal concentrations, biomarkers, and behaviors, with a significance threshold set at $p < 0.05$.

Metabolomic LC/GC-TOFMS data was analyzed using principle component analysis (PCA) and OPLS analysis between groups. The differential metabolites were selected when they meet the requirements of variable importance in the projection (VIP) >1 in OPLS model and $p < 0.05$ from student *t*-test. The corresponding fold change shows how these selected differential metabolites varied from control. Final data analysis between control and Mn

exposed groups for each metabolite was conducted using independent *t*-test analysis with a $p < 0.05$ significance threshold.

Results

Body Weight and Hematology

Oral Mn-exposure alters systemic markers of iron status. Body weight measurements were completed three times per week to monitor growth. No significant change in body weight was observed between groups throughout the study, or in terminal body weight (Table 1). Because of the close relationship between biological Mn and Fe levels, we examined changes in hematological indicators of overall iron status due to Mn exposure. Mn-exposed rats had normal hematocrit levels but had significantly increased ($p = 0.016$) plasma transferrin accompanied by a trend toward reduced ferritin (Table 1) suggesting early stages of iron deficiency.

Table 4.1. Body Weight and Hematology.

Treatment	Body Wt. (g)	Hematocrit	Transferrin (mg/mL)	Ferritin (ng/mL)
Control	278.7 ± 6.3	0.50 ± 0.01	1.53 ± 0.06	425 ± 47.8
Manganese	263.3 ± 5.9	0.51 ± 0.01	2.21 ± 0.21*	299 ± 44.6

Table 4.1. Body Weight and Hematology. – Values are listed ± SEM and significance was established using independent *t*-tests to identify differences between the control (n=6) and Mn-exposed (n=6) groups. * = ($p \leq 0.05$)

Metal Analysis

Oral Mn exposure led to significantly elevated brain, liver, and plasma Mn concentrations. Mn, Fe, and Cu were quantified in dissected brain regions of Mn exposed rats and non-exposed controls. Mn accumulated significantly in the striatum and GP ($p = 0.003$; $p = 0.019$, respectively) of Mn-exposed rats compared to controls (Table 2). Brain Fe levels were largely unaffected by Mn exposure; however, due to Mn accumulation the Fe:Mn ratio was significantly lower in the striatum of Mn exposed animals compared to controls (Table 2). While Fe homeostasis in the GP was quite stable under Mn exposure, Cu levels were significantly elevated ($p = 0.05$) due to Mn (Table 2). Although the Fe:Mn ratio was significantly lower in many brain regions, stable Fe levels suggest that metabolic and behavioral changes are driven by Mn accumulation, not Fe deficiency.

Similar to the brain, significantly higher Mn content was found in the liver of Mn exposed rats compared to controls ($p = 0.002$) (Figure 2). Elevated liver Mn was accompanied by dramatically reduced liver Fe levels ($p = 0.012$) and Fe:Mn ratio ($p < 0.001$) due to Mn exposure. These data along with the transferrin and ferritin results indicate that Mn alters systemic Fe status leading to deficiency, without anemia. Liver Cu levels were comparable between Mn and control groups.

Plasma Mn concentrations were significantly increased in the Mn exposed group versus control ($p = 0.013$). Plasma Fe and Cu levels were similar between groups, but the Fe:Mn ratio was significantly lower in Mn exposed ($p = 0.003$), compared to control.

Table 4.2. Metal Analysis of Brain, Liver, and Plasma.

		Brain $\mu\text{g/g}$ Tissue			
		Mn	Fe	Cu	Fe:Mn Ratio
Striatum					
Control		0.34 \pm 0.06	6.1 \pm 1.2	1.5 \pm 0.2	21:1
Manganese		0.69 \pm 0.06*	6.4 \pm 1.3	1.5 \pm 0.2	9:1*
Globus Pallidus					
Control		0.57 \pm 0.06	7.5 \pm 1.8	0.9 \pm 0.2	12:1
Manganese		1.03 \pm 0.10*	9.5 \pm 0.9	1.3 \pm 0.1*	9:1
		Liver $\mu\text{g/g}$ Tissue			
		Mn	Fe	Cu	Fe:Mn Ratio
Control		2.31 \pm 0.06	256 \pm 31.1	4.3 \pm 0.3	111:1
Manganese		5.10 \pm 0.43*	92.6 \pm 21.3*	4.4 \pm 0.2	18:1**
		Plasma $\mu\text{g/L}$			
		Mn	Fe	Cu	Fe:Mn Ratio
Control		8.32 \pm 0.35	1543 \pm 112	838 \pm 19	186:1
Manganese		26.5 \pm 4.49*	1504 \pm 256	848 \pm 32	57:1*

Table 4.2. Metal Analysis of Brain, Liver, and Plasma. – Values are listed \pm SEM and data were analyzed using independent t-tests to identify differences in metal content between the Mn (n=6) and control (n=6) groups. * = ($p \leq 0.025$) ** = ($p < 0.001$)

Metabolomic Analyses

Mn exposure significantly altered plasma, brain, and liver metabolites indicating a shift in the metabolome compared to controls. Metabolomic analysis of these tissues using LC/GC-TOFMS identified 98 significantly altered metabolites due to Mn exposure. Significant changes were observed in each compartment: plasma (Table 3), brain (Table 4), and liver (Table 6), indicating changes in lipid and amino acid metabolism. Similarly, OPLS plots of plasma (Figure 1), brain (Figure 3), and liver (Figure 4) data identify a shift in the metabolome of animals exposed to Mn versus healthy controls.

Several plasma metabolites altered by Mn reflect amino acid breakdown. Markers of tryptophan metabolism, 3-indolepropionic acid and kynurenine, were significantly elevated (2.12 fold change (FC); $p = 0.026$ and 2 FC; $p = 0.041$, respectively). Similarly, arginine and homogentisic acid levels were increased due to Mn, while alanine and creatinine were significantly decreased (Table 3). Significant associations were also identified between regional brain Mn accumulation and select plasma metabolites (Figure 2). Positive correlations were found between plasma homogentisic acid and Mn levels in the striatum and GP ($r = 0.6980$, $p = 0.012$ and $r = 0.7155$, $p = 0.009$, respectively) (Figure 2A), as well as substantia nigra Mn, GP Cu, and GP Fe levels ($r = 0.7068$, $p = 0.010$; $r = 0.6973$, $p = 0.012$; and $r = 0.6355$, $p = 0.026$, respectively) (data not shown). Similarly, chenodeoxycholic acid was positively correlated with striatal and GP

Mn ($r = 0.7724$, $p = 0.003$ and $r = 0.7589$, $p = 0.004$, respectively) (Figure 2C). These changes were accompanied by negative correlations between plasma aspartic acid and Mn in the striatum and GP (Figure 2B). Additionally, correlations between metabolite changes and brain metals represent potential indices for brain metal homeostasis and Mn accumulation.

Mn altered brain metabolites indicative of compromised lipid metabolism and potential plasma membrane integrity including significant increases in cholesterol (4.42 FC; $p = 0.033$), desmosine (12.69 FC; $p = 0.007$), oleic acid (12.57 FC; $p < 0.001$), and palmitic acid (15.48 FC; $p < 0.001$) (Table 4). Changes in these lipids and several other brain metabolites were correlated with plasma Mn levels (Table 5). Alterations in oleic and palmitic acid may also suggest an impairment in fatty acid synthesis and energy metabolism, along with the significant increase in 2-butenedioic acid “Fumarate” (2.12 FC; $p = 0.030$). Mn caused a significant increase in urea (2.36 FC; $p = 0.025$) and decreased 2-pyrrolidone-5-carboxylic acid (-2.79 FC; $p = 0.029$), which could be linked to disrupted glutamine metabolism.

The largest effect Mn exposure had on liver metabolites pertained to lipid metabolism and ketone body formation; oleic acid (14.51 FC; $p = 0.003$) and hydroxybutyric acid (-14.29 FC; $p = 0.048$), respectively (Table 6). Mn also significantly decreased metabolites associated with energy metabolism including creatine (-3.13 FC; $p = 0.008$) and nicotinamide ribotide (-3.03 FC; $p = 0.031$),

and structural markers hydroxyglutaric acid, desmosine, and serine (6.47 FC, 5.25 FC, and 3.78 FC, respectively; $p < 0.002$) (Table 6). It is important to note that the liver metabolites altered by Mn-exposure were correlated with increased liver Mn concentrations and not decreased Fe levels (data not shown).

Table 4.3. Plasma Metabolites Altered with Mn Exposure.

Compound	FC	p
Cholesterol	1.35	0.008
2-Aminobutyric acid	1.24	0.043
2-ethyl-3-hydroxypropionic acid	1.54	0.015
3,4-Dihydroxybutanoic acid	1.46	0.001
3-Hydroxybutyric acid	1.48	0.015
3-Indolepropionic acid	2.12	0.026
4-Hydroxy-proline	-2.71	0.002
Alanine	-2.00	0.041
Arginine	2.39	0.009
Aspartic acid	-2.55	0.004
Chenodeoxycholic acid	2.98	0.000
Creatinine	-2.50	0.009
Histidine	1.36	0.035
Homogentisic acid	2.39	0.009
Isocitric acid	1.76	0.002
Keynurenine	2.00	0.041
Methionine	1.21	0.027
Methyl phosphate	1.63	0.003
Myo-Inositol, phosphate	1.52	0.005
Oxalic acid	1.29	0.043
Phenylalanine	1.34	0.017
Phosphate	1.83	0.014
Pseudo uridine	1.36	0.007
Uracil	1.31	0.023

Table 4.3. Plasma Metabolites Altered with Mn Exposure. – Listed is the fold change (FC) of each metabolite in the Mn exposed (n=6) compared to control (n=6) group, and its corresponding p-statistic. Independent *t*-tests were used to identify significance between Mn-exposed and control groups.

Table 4.4. Brain Metabolites Altered with Mn Exposure.

Compound	FC	p
2-Aminobutyric acid	1.28	0.010
2-Butenedioic acid	2.12	0.030
2-Pyrrolidone-5-carboxylic acid	-2.79	0.029
3-Hydroxybutyric acid	1.46	0.005
4-Guanidinobutanoic acid	1.23	0.025
Acetyl aspartate	3.11	0.011
Arabitol	1.63	0.048
Ascorbic acid	1.60	0.004
Aspartic acid	-1.10	0.024
Carnitine	-1.10	0.011
Cholesterol	4.42	0.033
Citric acid	1.31	0.031
Desmosine	12.69	0.007
Fructose	1.41	0.028
Glycocholic acid	-2.78	0.009
N-Acetyl-L-aspartic acid	1.55	0.004
Oleic acid	12.57	0.000
Palmitic acid	15.43	0.000
Phosphate	1.12	0.018
Proline	-1.84	0.027
Sarcosine	1.33	0.006
Uracil	1.35	0.028
Urea	2.36	0.025
Valine	1.55	0.024

Table 4.4. Brain Metabolites Altered with Mn Exposure. – Listed is the fold change (FC) of each metabolite in the Mn-exposed (n=6) compared to control (n=6) group, and its corresponding p-statistic. Independent *t*-tests were used to identify significance between Mn-exposed and control groups.

Table 4.5. Brain Metabolites Correlated with Plasma Mn.

Compound	<i>r</i>	<i>p</i>
2Butenedioic acid	0.8415	< 0.001
Cholesterol	0.6208	0.031
Desmosine	0.8197	0.001
Glycocholic acid	-0.6627	0.019
Oleic acid	0.8332	< 0.001
Palmitic acid	0.7589	0.004

Table 4.5. Brain Metabolites Correlated with Plasma Mn. – Relationships between plasma Mn and altered brain metabolites were identified using Pearson’s correlational analysis. *r* and *p* values are displayed for each metabolite significantly ($p < 0.05$) correlated with plasma Mn.

Table 4.6. Liver Metabolites Altered with Mn Exposure.

Compound	FC	<i>p</i>	Compound	FC	<i>p</i>
1,4-Diaminobutane	1.40	0.022	N-Acetyl glucosamine	1.22	0.042
1-Methyladenosine	1.37	0.001	Nicotinamide ribotide	-3.03	0.031
2-Aminobutyric acid	1.34	0.033	Norepinephrine	1.95	0.011
3-Hydroxy-n-valeric acid	1.52	0.015	Norleucine	1.28	0.045
Aminocaproic acid	1.15	0.013	Octadecanedioic acid	1.58	0.013
Aspartic acid	1.11	0.047	Oleamide	1.57	0.040
But-2-enoic acid	1.24	0.000	Oleic acid	14.51	0.003
Cadaverine	1.93	0.008	Pantothenic acid	1.25	0.007
Choline	-1.19	0.041	Proline	1.55	0.006
Citicoline	1.59	0.007	Pyridoxamine	1.20	0.013
Creatine	-3.13	0.008	Pyroglutamic acid	-1.13	0.045
Cytidine	1.24	0.030	Ribitol	1.67	0.050
Desmosine	5.25	0.002	Ribonic acid-1,4-lactone	2.19	0.000
Dihydrothymine	-3.03	0.012	Sebacic acid	1.15	0.018
d-Xylose-1-phosphate	-1.48	0.010	Serine	3.78	0.001
Ethylmalonic acid	2.30	0.040	Serotonin	1.27	0.034
Glycerophosphate	-1.56	0.002	S-Nitrosoglutathione	1.64	0.015
Homocitrulline	1.63	0.006	Stearic acid	-3.33	0.017
Hydroxybutyric acid	-14.29	0.048	Taurocholic acid	1.38	0.017
Hydroxyglutaric acid	6.47	0.001	Threonine	1.19	0.022
Isoleucine	2.62	0.030	Uracil	1.41	0.029
L-Cysteine	1.42	0.000	Urobilin	-1.75	0.020
L-Methionine	1.15	0.044	Valeric acid	1.22	0.050
Malonic acid	-1.32	0.014	Valine	1.17	0.048
N,N-Dimethylglycine	1.47	0.038	Xanthosine	1.53	0.002

Table 4.6. Liver Metabolites Altered with Mn Exposure. – Listed is the fold change (FC) of each metabolite in the Mn-exposed (n=6) compared to control (n=6) group, and its corresponding *p*-statistic. Independent *t*-tests were used to identify significance between Mn exposed and control groups.

Figure 4.1. OPLS of Plasma Spectral Data.

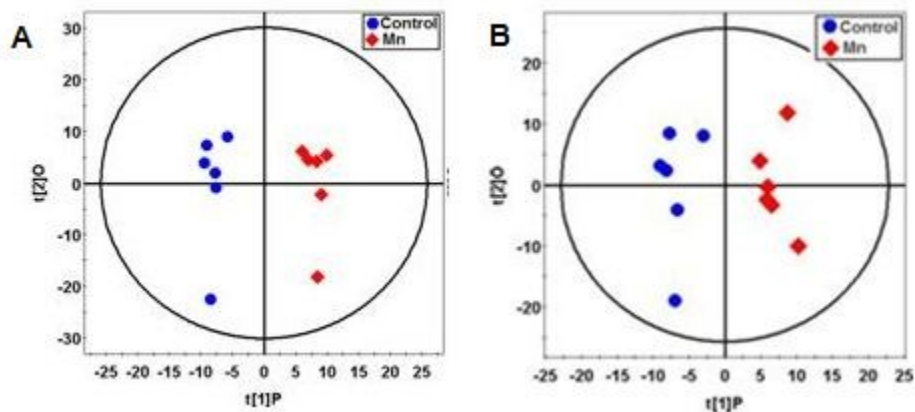


Figure 4.1. OPLS of Plasma Spectral Data. – A) Gas chromatography-time of flight-mass spectroscopy (GC-TOFMS) data represented by OPLS-DA scores plot between control and Mn-exposed groups. OPLS-DA Model: Control vs Mn, 1+2 components, R^2X (cum)=0.542, $R^2X_p = 0.152$, R^2Y (cum)=0.977, Q^2 (cum)=0.652. B) Liquid chromatography-time of flight mass spectroscopy (LC-TOFMS) data represented by the OPLS scores plot of the separation between healthy control and Mn-exposed rats. OPLS model: 2 component model, $R^2X=0.395$, $R^2Y=0.934$, Q^2 (cum)=0.554.

Figure 4.2. Relationships Between Brain Mn and Plasma Metabolites.

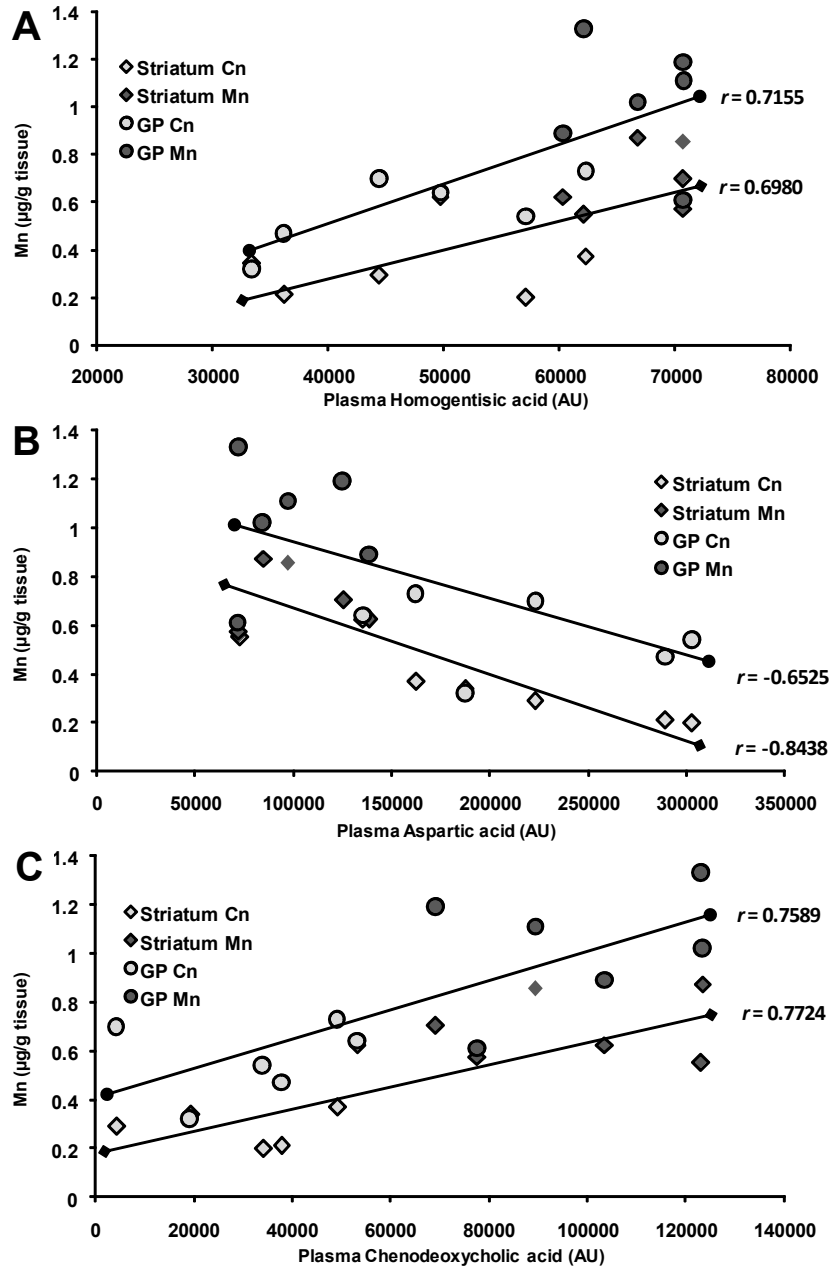


Figure 4.2. Relationships Between Brain Mn and Plasma Metabolites. – Pearson’s correlational analysis was conducted between plasma metabolites altered by Mn and Mn levels in the striatum and globus pallidus (GP). Significant relationships emerged between striatal and GP Mn levels with A) plasma homogentisic acid, B) aspartic acid, and C) chenodeoxycholic acid, represented by arbitrary units (AU), and depicted in scatterplot form with best fit trendlines

representing the Pearson's r value for each plasma metabolite and brain region's metal content. Control (Cn) ($n=6$) and Mn ($n=6$) groups were included in the analysis and are depicted by shades of gray on each plot.

Figure 4.3. OPLS of Brain Spectral Data.

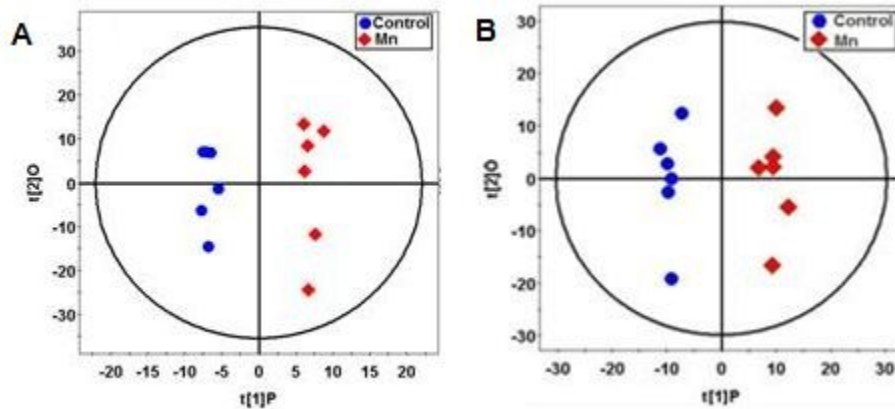


Figure 4.3. OPLS of Brain Spectral Data. – A) Gas chromatography-time of flight-mass spectroscopy (GC-TOFMS) data represented by OPLS-DA scores plot between control and Mn-exposed groups. OPLS-DA, Control vs Mn, 1+2 components, R^2X (cum)=0.462, $R^2X_p = 0.153$, R^2Y (cum)=0.978, Q^2 (cum)=0.526. B) Liquid chromatography-time of flight mass spectroscopy (LC-TOFMS) data represented by the OPLS scores plot of the separation between healthy control and Mn-exposed rats. OPLS model: 2 component model, $R^2X=0.500$, $R^2Y=0.979$, Q^2 (cum)=0.642.

Figure 4.4. OPLS of Liver Spectral Data.

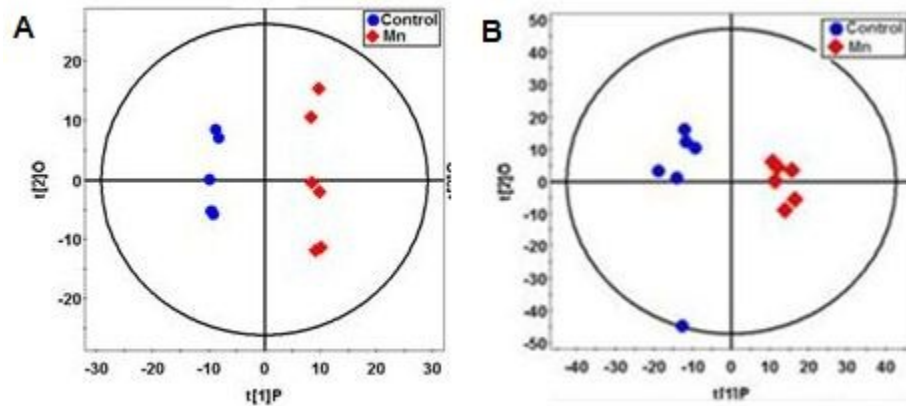


Figure 4.4. OPLS of Liver Spectral Data. – A) Gas chromatography-time of flight-mass spectroscopy (GC-TOFMS) data represented by OPLS-DA scores plot between control and Mn-exposed groups. OPLS-DA Model: Control vs Mn, 1+2 components, R^2X (cum)=0.454, $R^2X_p = 0.176$, R^2Y (cum)=0.996, Q^2 (cum)=0.695. B) Liquid chromatography-time of flight mass spectroscopy (LC-TOFMS) data represented by the OPLS scores plot of the separation between healthy control and Mn-exposed rats. OPLS model: 2 component model, $R^2X=0.391$, $R^2Y=0.964$, Q^2 (cum)=0.660.

Behavioral Observations

Mn exposure significantly increased locomotion and altered stereotypic activity associated with light and dark cycles. Because hyperactivity and altered locomotion has been previously associated with Mn exposure (Bouchard et al., 2007; Kern et al., 2010) we conducted behavioral analysis during the fourth, fifth, and sixth weeks of Mn exposure using 24h video surveillance to monitor Mn induced changes in activity. No changes in behavior occurred until the sixth week of exposure when total activity, measured as total distance traveled (TDT), was significantly greater ($p = 0.003$) in the Mn exposed group (Figure 5A); moreover, increased locomotion was strongly correlated with GP, striatal, and

plasma Mn levels ($r = 0.8027$, $p = 0.002$; $r = 0.7212$, $p = 0.008$; and $r = 0.6229$, $p = 0.030$, respectively) (Figures 5A1, 5A2, and 5A3). Analysis of individual behaviors identified a significant increase in repetitive turning ($p = 0.007$) during the light cycle of Mn exposed animals and a significant Mn induced decrease in rearing ($p = 0.006$) during the dark cycle (Figure 5B). Depicting behaviors as percent performed in the light cycle versus dark cycle revealed increased activity of Mn exposed animals in the light cycle, contradictory to the nocturnal activity of the controls (Figure 5C).

Figure 4.5. Behavioral Analysis of Mn and Control Rats.

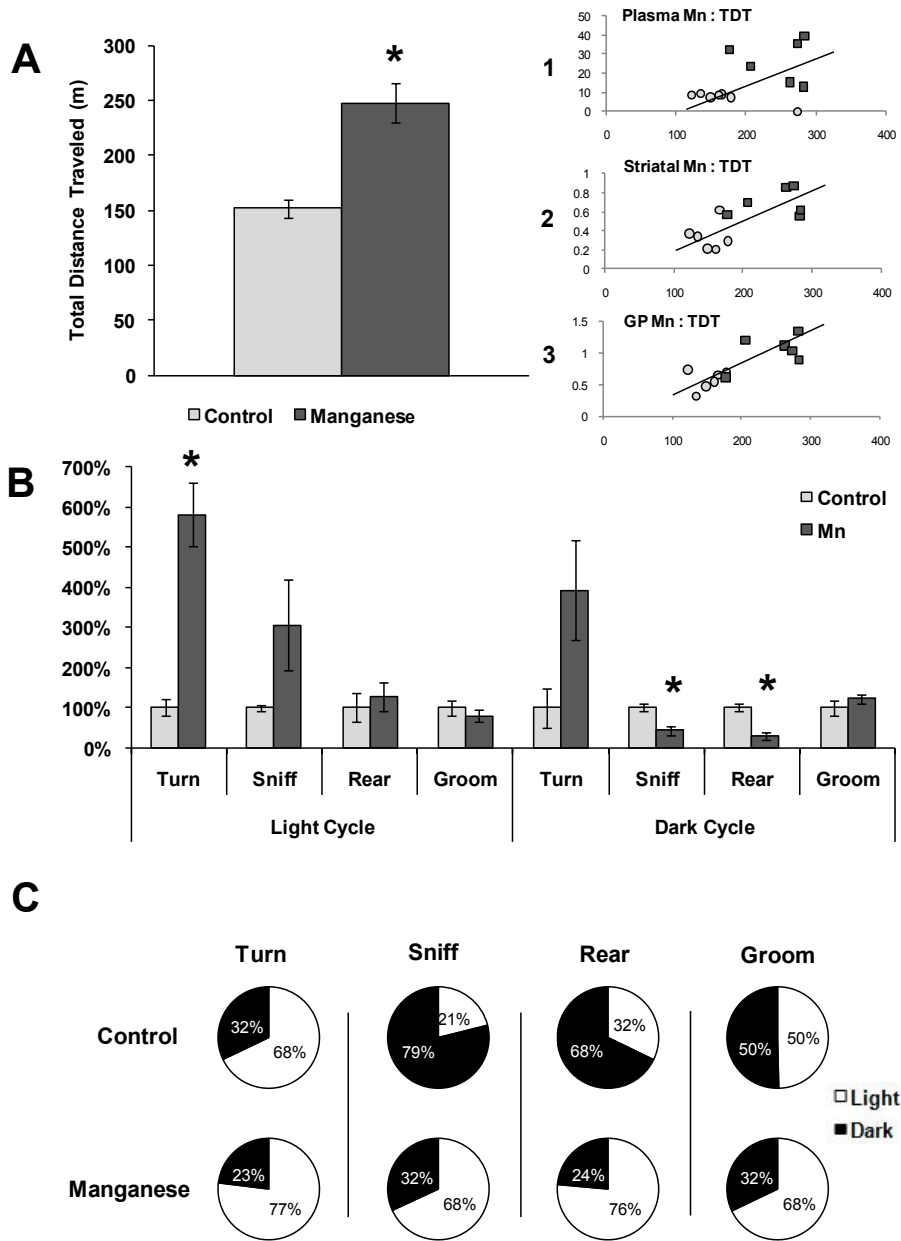


Figure 4.5. Behavioral Analysis of Mn and Control Rats. – Behaviors were monitored for 24 h using Home Cage Scan video surveillance during the sixth week of Mn exposure. A) Total distance traveled (TDT) in meters over the 24 h period for control and Mn exposed rats. Independent *t*-tests were used to identify differences between groups and data are expressed \pm SEM. Inset) Scatter plot

representation of Pearson's correlational analysis between TDT (in meters; x axis) and 1) plasma Mn ($\mu\text{g/L}$; y axis) ($r = 0.6229$), 2) striatal Mn ($\mu\text{g/g}$; y axis) ($r = 0.7212$), and 3) globus pallidus (GP) Mn ($\mu\text{g/g}$; y axis) ($r = 0.8027$). B) Total behaviors expressed as percent control during the light and dark cycles using independent t-tests to identify differences between groups data are expressed \pm SEM. ($* = p < 0.01$) C) Percentage of each behavior completed in the light or dark cycle for control and Mn exposed rats.

Discussion

The purpose of this study was to identify biomarkers of Mn toxicity that provide diagnostic information corresponding to brain Mn accumulation, and to monitor changes in rat home cage behaviors that accompany Mn accumulation. Using a LC/GC-TOFMS method of metabolomic analysis we were able to identify several potential biomarkers that corresponded with indices of Mn neurotoxicity in rats; including, altered metal homeostasis, amino acid metabolism, and markers of structural damage. Additionally, video surveillance identified altered behavior and activity consistent with previous observations in Mn exposure models; however, our 24h data collection period identified a previously unreported disturbance in circadian rhythm due to Mn toxicity.

Oral Mn exposure elevated brain Mn in all regions examined, primarily localizing in the GP. A novel increase in Cu was also observed in the GP, but it is unclear whether the elevation in Cu is a direct effect or an artifact of Mn exposure. For example, Mn can influence Fe homeostasis, evidenced by a decrease in the Fe:Mn ratio, which has been linked with elevated GP copper (Erikson et al., 2004). Similarly, liver and plasma Mn levels were increased with

Mn exposure. While Mn exposure did not drastically alter brain or plasma Fe levels, it did significantly lower liver Fe content. Decreased liver Fe was accompanied by decreased plasma ferritin and increased plasma transferrin indicating systemic Fe deficiency but not anemia (normal hematocrit) (Tables 1, 2). It is important to note that while systemic Fe status was significantly altered due to Mn exposure, the metabolic and behavior alterations that occurred were strongly associated with increased brain Mn content and not depleted systemic iron.

Locomotor activity (i.e. total distance traveled) is often used in neuroscience as an outcome measure for neurotoxic effects (O'Donoghue, 1996; Flagel and Robinson, 2007). In our study, increased overall activity, measured by TDT, was observed with Mn exposure, and was associated with plasma, striatal, and GP Mn levels (Figure 5A). Increases in the motor activity of rats as a result of Mn exposure have been reported previously (Calabresi et al., 2001; Kern et al., 2010), though these effects are often transient (Vacher et al., 2006). Repetitive turning was also observed in Mn exposed rats, which may contribute to the overall increased activity, but has also been associated with stereotypy linked to dopaminergic dysfunction, akin to obsessive compulsive disorders (de Haas et al., 2010). While repetitive turning was significantly elevated in Mn exposed rats the distribution of repetitive turning events was consistent with the circadian behavior of control animals, unlike rearing, sniffing and grooming (Figure 5C). Rearing and sniffing behaviors were markedly decreased during the

dark cycle of Mn exposed rats, consistent with previous reports (Witholt et al., 2000). Changes in these exploratory behaviors contradict typical nocturnal behavior (Scheer et al., 2003) and suggest that Mn exposure may disrupt the circadian clock. Sleep disturbances are common among Parkinson's disease patients (Suzuki et al., 2011), and reversal of the circadian rhythm has been observed in iron deficient rats and is attributed to alterations in dopaminergic and/or noradrenergic activity (Youdim et al., 1980). In addition to dopamine and norepinephrine, circadian rhythm is largely influenced by serotonin, GABA, and glutamate in the suprachiasmatic nucleus (Wagner et al., 2001; Reghunandanan and Reghunandanan, 2006), and circadian fluctuations in dopamine, glutamate, and GABA have been reported in the striatum of rats (Castaneda et al., 2004). Therefore, if the altered light/dark behaviors observed in this study are indeed alterations in circadian rhythm, they are likely driven by alterations in striatal dopamine, GABA and/or glutamate that have been linked with Mn exposure (Fitsanakis et al., 2006 for review). Further studies utilizing larger sample size with longer monitoring periods are needed to confirm Mn induced circadian reversal; however, these data suggest that Mn disrupts normal behaviors throughout the light/dark cycle as opposed to previously reported short observational periods (Youdim and Yehuda, 1985). While behavior is a valuable indicator of neurobiological function when assessing neurotoxicity; biochemical measures (e.g. metabolomics) are equally important to identify metabolic changes congruent with neurotoxicity, and to reveal potential biomarkers.

To our knowledge, the only other metabolomic analysis of Mn exposure was completed by Dorman et al., (2008) in monkeys exposed to airborne MnSO₄. While the Mn exposure protocol between the two studies differed, there were similarities in altered blood metabolites, specifically elevated arginine and glutamine derivatives. Our study corroborated these previous data and revealed a few new scenarios. Possibly the most compelling identified a substantial impact of Mn on fatty acid metabolism in the brain. Palmitic acid, the product of de novo lipogenesis, was detected in 15-fold greater concentrations in the brains of Mn exposed rats. Increased palmitate was accompanied by significant elevations in oleic acid, desmosine, and cholesterol (Table 4). Other than oleic acid, Mn did not have the same affect on these metabolites in the liver, which is interesting because Mn has been shown to increase lipogenesis in liver tissue despite high lipid availability (Baquer et al., 1974), possibly by inhibiting normal feedback mechanisms. Mn has also been linked to increased acetyl-CoA carboxylase activity, enhancing fatty acid synthesis (Scorpio and Masoro, 1970). Mn enhanced lipogenesis could account for the increased palmitic acid (found in the brain) and its potential downstream product oleic acid (increased in brain and liver). Alternatively, Mn has been implicated in endoplasmic reticular stress (Chun et al., 2001; Tjalkens et al., 2006), which may disrupt fatty acid elongation resulting in abnormally high palmitic acid content. Mn accumulation may also compromise liver function leading to liver damage or failure. Mn induced liver

failure will directly affect liver metabolites and may influence metabolite changes in other tissues including clearance and/or degradation.

Increased palmitic acid in the brain, along with elevated cholesterol, may introduce a scenario similar to what has been observed in Alzheimer's disease (AD). Palmitic acid has been linked to increase ceramide production in astrocytes (Patil et al., 2007) and implicated in the elevation of β -secretase (BACE1) activity and tau hyperphosphorylation (Patil et al., 2008). Additionally, elevated free cholesterol influences β - and γ -secretase activity enhancing amyloid β production (Shobab et al., 2005). Mn has also been directly linked to tau hyperphosphorylation in PC12 cells (Cai et al., 2011). Changes in lipid availability may also compromise membrane integrity by increasing fatty acid and cholesterol incorporation, thereby altering normal structure and dynamics. Continuity of vascular structure may also be compromised as elevated levels of desmosine, a marker of elastin breakdown (Ronchetti and Contri, 1997), were found in the Mn exposed group compared to control.

Evidence of compromised integrity existed in the brains of Mn exposed rats. We speculate, however, that markers of structural damage were not linked to neuronal death. Neuronal loss due to structural damage has been associated with decreased N-acetylaspartate (NAA) levels (Demougeot et al., 2001), and a previous study on Mn exposed primates observed decreases in NAA and the NAA:creatinine ratio suggesting neuronal integrity/density was altered (Guilarte et al., 2006). We observed minimal changes in brain creatine levels and increased

NAA due to Mn exposure, and when coupled with altered lipid metabolites likely signify altered membrane integrity rather than neuronal death.

To investigate potential biomarkers associated with Mn induced neurological dysfunction, we conducted correlational analyses between the plasma metabolites prominently altered by Mn with brain Mn concentrations in the striatum and GP. Notable plasma metabolites that were altered due to Mn were aromatic amino acids derivatives (Tryptophan: 3-indolepropionic acid and kynurenine; Tyrosine: homogentisic acid) (Table 3). Plasma homogentisic acid, aspartic acid, and chenodeoxycholic acid all correlated significantly with GP and striatal Mn accumulation (Figure 2). Increased chenodeoxycholic acid is consistent with altered bile acid regulation in the liver (Table 6). Because plasma Mn correlated significantly with GP Mn we also examined relationships between plasma Mn and altered brain and liver metabolites. Weak correlations were found between plasma Mn and liver metabolites associated with energy production (e.g. creatine and ribonic acid) (data not shown); however, plasma Mn was a better predictor of altered lipid metabolism (cholesterol, palmitate and oleate) and structural integrity (desmosine) in the brain. In this aspect, plasma Mn may be useful to monitor along with plasma metabolites (e.g., chenodeoxycholic acid or homogentisic acid) in order to gain a more complete picture of brain Mn accumulation and its resulting pathologies possibly leading to earlier intervention.

In conclusion, six weeks of oral Mn exposure led to increased brain Mn that corresponded with locomotor and stereotypic behavior abnormalities suggesting a disturbance in circadian rhythm. Simultaneous changes in brain, plasma, and liver metabolites were also identified and associated with brain Mn accumulation. Together, these data provide a useful starting point to identify metabolite biomarkers that correspond with Mn toxicity in a more cost effective manner. Furthermore, it may be prudent to consider how shifts in multiple metabolites may relate to one another in Mn toxicity; for example, an indicator of brain Mn accumulation (plasma chenodeoxycholic acid predicts GP Mn) together with an indicator of Mn induced changes in the brain (plasma Mn predicts elevated brain desmosine) will better appraise the progression of neurotoxicity. GC/LC-TOFMS can be a powerful tool to identify potential biomarkers, and additional study paradigms (route of exposure and/or species) are warranted to identify consistent biomarkers using this technique.

Funding

This research was supported by the National Institutes of Health R15 NS061309-01 (KME)

CHAPTER V

**MANGANESE ACCUMULATION IN MEMBRANE FRACTIONS OF PRIMARY
ASTROCYTES IS ASSOCIATED WITH DECREASED γ -AMINOBUTYRIC ACID
(GABA) UPTAKE, AND IS EXACERBATED BY OLEIC ACID AND
PALMITATE**

Abstract

Overexposure to manganese (Mn) disrupts γ -aminobutyric acid (GABA) neurochemistry and has been associated with severe imbalances in the fatty acid profile of the brain. Evidence suggests that Mn increases extracellular GABA by interfering with GABA uptake mechanisms, but the effects of Mn on GABA transport proteins (GATs) have not been identified. The purpose of this study was to characterize how Mn neurotoxicity impairs GAT function in primary rat astrocytes. Based on our previous studies that showed significantly elevated brain fatty acid levels with Mn exposure, we exposed astrocytes to 500 μ M Mn for 24 hrs with or without co-treatments of oleic and palmitic acids (10 or 100 μ M) to ascertain the role of fatty acids on GABA uptake during Mn toxicity. Following exposure 3 H-GABA uptake was measured, and isolated astrocyte fractions (cytosolic and membrane) were examined for GAT3, protein kinase C (PKC), and phospho-PKC (pPKC) protein levels and metal content. 3 H-GABA uptake was significantly decreased by 24 hr Mn exposure ($p < 0.001$), an effect exacerbated

by co-treatment with 100 μ M oleic or palmitic acid. Increased pPKC levels were observed in the membrane fraction due to Mn and palmitic acid, but pPKC did not correspond with decreased membrane GAT3. Pretreatment with PKC inhibitors BIS II (10 μ M) and isorhamnetin (10 μ M) failed to restore uptake suggesting a diminished role of PKC in decreased GAT function. Oleic and palmitic acids (10 and 100 μ M) significantly elevated membrane Mn levels compared to Mn treatment alone ($p < 0.01$), and were negatively correlated with ^3H -GABA uptake ($r = -0.45$, $p = 0.011$). Furthermore, control cells exposed to Mn only during the experimental uptake had significantly reduced ^3H -GABA uptake, and the addition of 50 μ M GABA blunted cytosolic Mn accumulation. Together, these data indicate that reduced GAT function in astrocytes is not driven by PKC signaling, but is likely influenced by Mn and fatty acids interacting with the plasma membrane thereby inhibiting GABA uptake by GAT3.

Introduction

Manganese (Mn) neurotoxicity is associated with distinct neurochemical changes that contribute to extrapyramidal symptoms similar to Parkinson's disease. While most of the phenotypic changes resulting from prolonged Mn exposure are associated with changes in the dopamine system, evidence shows that Mn induced changes in the GABA neurotransmission exist prior to dopaminergic dysfunction (Gwiazda et al., 2002). GABA is the main inhibitory neurotransmitter in the brain that is responsible for modulating excitatory signals within the basal ganglia to help coordinate smooth motor function. Motor control

issues observed with Mn exposure (e.g. bradykinesia) and other artifacts of Mn accumulation, such as glutamate excitotoxicity, may result from disrupted GABA signaling. Specific mechanism as to how Mn alters GABA are unclear, but Mn appears to target GABA uptake mechanisms which are mediated by pre- and extra-synaptic GABA transport proteins GAT1 and GAT3, respectively (Kersanté et al., 2013). Astrocytes primarily express the GAT3 isoform and are integral to GABA uptake because of their relatively high K_m compared to neuronal GAT1 (33 μM versus 7 μM , respectively). The high K_m for GAT3 suggests that it plays a critical role in clearing GABA spillover from the synaptic cleft reducing the duration and intensity of inhibitory neurotransmission. Astrocytes also sequester Mn and other metals that pose a threat to the more vulnerable neurons (Aschner et al., 1992); however, as cellular Mn concentrations increase, the protective function of astrocytes including their role in GABA clearance may be jeopardized.

Several studies have shown that Mn exposure disrupts GABA levels in tissue and extracellular space of the striatum (Bonilla, 1978; Gianutsos and Murray, 1982; Gwiazda et al., 2002; Takeda et al., 2002, 2003; Anderson et al., 2008; Fordahl et al., 2010). Although these studies were conducted using various rodent models of Mn exposure, overall the findings indicate that Mn exposure decreases tissue GABA while increasing extracellular levels. The direct effect of Mn on GABA transporters, however, has only been measured in striatal synaptosomes using ^3H -GABA (Anderson et al., 2007a) and via *in vivo* microdialysis in Mn exposed rats after delivery of the GAT inhibitor nipecotic acid

(Fordahl et al., 2010). Striatal synaptosomes isolated from Mn exposed rats displayed a marked decline in ³H-GABA uptake than synaptosomes from control rats (Anderson et al., 2007a). Similarly, Mn exposure caused increased extracellular GABA compared to controls and blunted the expected rise in GABA after GAT inhibition by nipecotic acid (Fordahl et al., 2010). These data along with evidence that Mn exposure did not alter GAT protein or mRNA levels in Mn exposed rodents (Anderson et al., 2008) suggest a functional decline in GABA transport proteins due to Mn.

We hypothesize the decline in GABA transport is due to Mn altering cellular regulation of the GATs presumably through protein kinase C (PKC) signaling. PKC activation has been reported in dopaminergic N27 cells exposed to Mn (Latchoumycandane et al., 2005). Additionally, internalization of GATs from the plasma membrane to cytosolic vesicles is dependent on PKC phosphorylation of GATs (Gadea and Lopez-Colome, 2001; Quick et al., 2004). Data showing PKC activation with phorbol 12-myristate 13-acetate (PMA) reduced GABA uptake by 50% in human embryonic kidney cells, an effect that was blocked by PKC inhibitors (Sato et al., 1995). Moreover, other solute carrier family (Slc) transporters, like the glutamine transporter SNAT3, are impaired by Mn induced activation of PKC (Sidoryk-Wegrzynowicz et al., 2011).

Recently, data were published by our lab showing profound changes in brain lipid metabolism of Mn exposed rats (Fordahl et al., 2012). Significant

elevations of oleic acid (12 fold), palmitic acid (15 fold), and cholesterol (4 fold) were observed. These fatty acids are primary constituents of plasma membrane and membrane raft composition (Schumann et al., 2011), and oleic and palmitic acid have been independently associated with decreased GABA uptake and increased PKC activity (Troeger et al., 1984; Khan et al., 1992; Ragheb et al., 2009). Drastic changes in these fatty acids may contribute to GABA related dysfunction observed in Mn neurotoxicity; however to our knowledge this relationship has not been investigated.

The purpose of this project was to characterize how Mn decreases GABA uptake in primary astrocytes. Because astrocytes maintain the extracellular milieu around synaptic terminals, understanding how Mn and indirect consequences of Mn exposure (i.e. increased fatty acids) alter astrocyte GABA uptake is valuable to understand neurochemical changes associated with Mn neurotoxicity. For these reasons the goals of this study were to: 1) specifically examine GABA uptake and GAT3 protein levels in primary astrocytes after Mn exposure, 2) investigate the role of PKC signaling in GAT3 regulation with the use of a PKC inhibitor, isorhamnetin (ISO) (the primary quercetin metabolite found in the brain), and 3) characterize the effect of oleic acid and palmitic acid on GAT3 protein levels and function. We hypothesized that Mn directly regulates GAT3 proteins through PKC signaling leading to transporter internalization, similar to other transport proteins in the solute carrier family. Additionally, we hypothesized that oleic acid and palmitate would exacerbate Mn induced GAT3

dysfunction. Lastly, we wanted to quantify Mn accumulation in cytosolic and membrane fractions of astrocytes to identify if Mn distribution within these cellular fractions is associated with GAT3 localization, PKC signaling, or GABA uptake.

Materials and Methods

Cell Isolation and Culture

Cortical astrocytes were isolated from Sprague Dawley rat pups PND 1-3 (Harlan Laboratories) following the methods described by Allen et al., 2001 with slight modifications. Briefly, the pups were retrieved, cleaned using the antiseptic microbiocide Betadine, and swiftly decapitated. Using dissecting scissors and forceps the skull cap was detached and the brain was removed after carefully dissecting away any intact meninges to reduce fibroblast contamination. Once removed, well-defined cortices were carefully dissected apart from the rest of the brain and placed into serum free Dulbecco's minimal essential medium (D-MEM) (Sigma-Aldrich). The isolated tissue was minced by titration using a Pasteur pipette treated with Sigmacote® (Sigma-Aldrich) to prevent cell lysing. Astrocytes were dissociated using a 1:5 dilution of Trypsin 0.05% in serum free D-MEM. Dissociated cells were removed and placed in D-MEM containing 10% heat inactivated horse serum (Sigma-Aldrich) to neutralize the Trypsin. Cells were plated in 100mm dishes at a density of 7.5×10^5 or 6-well plates at a density of 1.0×10^5 and maintained in a humidified atmosphere of 95% air/5% CO₂ at 37 °C. Media was changed twice a week until cultures were 90% confluent. Culture purity was verified using immunocytochemistry where >95% stained positive for

the astroglial marker GFAP (Invitrogen). Experimental treatments were as follows: 500 μM Mn in the form of MnCl_2 was used for all Mn exposures unless otherwise indicated. This concentration of Mn falls in the symptomatic range of Mn neurotoxicity, 300 μM to 1000 μM , as measured in the brains of non-human primates (Suzuki et al., 1975). 10 μM Isorhamnetin (ISO) (Sigma-Aldrich), the methylated metabolite of quercetin and protein kinase C (PKC) inhibitor, was used as a pre- and co-treatment with Mn for uptake, western blot, and metal analyses. Isorhamnetin concentrations in rat plasma and brain have been reported at 15 μM and 200 nM, respectively (de Boer et al., 2005). Total GABA concentrations used in experiments were 50 μM representing physiologically relevant synaptic concentrations of GABA during inhibitory neurotransmission (Grabauskas, 2004). Logarithmic concentrations (10, 100, and 1000 μM) of albumin bound Oleic acid and palmitic acid (Sigma-Aldrich) were used for individual and co-treatment with Mn for all fatty acid experiments; however, decreased cell viability was observed during co-treatment of 1000 μM fatty acid and Mn so these data were not reported.

³H-GABA Uptake

Uptake of tritiated GABA (³H-GABA) was measured as described by Erikson and Aschner (2002). Astrocytes (90% confluent in 6-well plates) were incubated for 1, 6, or 24 hrs at 37°C with treatment media containing 0 or 500 μM Mn in the form of MnCl_2 . An additional group of control astrocytes received 500

μM Mn (CnMn) in the experimental buffer only for the duration of the uptake experiment. The CnMn group simulates Mn in the extracellular space, and was used to observe the interaction of Mn with extracellular GABA and GABA transport proteins. Cells were washed 3X with HEPES buffer [122 mM NaCl, 3.3 mM KCl, 0.4 mM MgSO₄, 1.3 mM CaCl₂, 1.2 mM KH₂PO₄, 10 mM glucose, and 25 mM N-2-hydroxy-ethylpiperanzine N-2-ethansulfonic acid, pH 7.4] and incubated for 1, 2, or 4 minutes with HEPES buffer containing 0.5 μCi ³H-GABA (PerkinElmer) and cold GABA (Sigma-Aldrich) resulting in a final concentration of 50 μM total GABA. The reaction was stopped by aspirating the tritiated HEPES and washing the cells 4X with cold (4°C) 290 mM mannitol buffer containing 0.5 mM calcium nitrate to maintain cell adhesion to the substrate. Cells were solubilized in 500 μL NaOH (1N) and 400 μL aliquots were neutralized with 33.3 μL HCl (12N) then used for β -counting with a Perkin Elmer liquid scintillation analyzer (PerkinElmer). The remaining 100 μL was used for protein determination using the bicinchoninic assay (BCA, Pierce Chemicals).

Cell Fractionation

Astrocyte cytosolic and membrane fractions were obtained through differential centrifugation. Astrocytes from two 100 mm plates were pooled into 1 mL phosphate buffered saline (PBS), centrifuged (1000 x g) to pellet, then rinsed with PBS and re-pelleted twice. The PBS was then aspirated and 100 μL cold 0.32 M sucrose pH 7.4 containing a protease inhibitor cocktail (Calbiochem) and

phosphatase inhibitors sodium orthovanadate, sodium fluoride, and β -glycerolphosphate (Sigma-Aldrich) was added to the final pellet to maintain membrane integrity. The pellet was sonicated on ice using ten one-second bursts. The remaining homogenate was centrifuged at 750 x g for 5 minutes to pellet nuclear material and any unbroken cells. The supernatant was decanted and centrifuged at 41,000 x g for 30 minutes at 4 °C. The resulting supernatant and pellet were separated and represent the cytosol and crude membrane fractions, respectively. The crude membrane fraction was solubilized in 100 μ L radioimmunoprecipitation assay (RIPA) lysis buffer (99 mL 1X PBS, 1 mL Nonidet 40, 0.1 g sodium dodecyl sulfate, 0.5 g sodium deoxycholate, pH 7.4). Cellular fractions of astrocytes were obtained from least three independent culture dates and used for Western blot and metal analyses.

Western Blot Analysis

Protein concentrations of cytosolic and plasma membrane samples were determined using BCA analysis. For western blots, 20 μ g of protein from each sample was loaded into NuPAGE® Bis-Tris precast gels, run with MES running buffer for 40 mins using NuPAGE® preset conditions on the PowerEase® 500 power supply system, and transferred to a Immobilon® PVDF membrane (Millipore) for 1 hr using the XCell II™ blot module in transfer buffer (All from Invitrogen). The following antibodies and dilutions were used for protein detection: GAT3 1:500 (Abcam), phospho-PKC (pan, β II Ser 660) 1:1000 (Cell

Signaling), PKC (pan, Thr 495) 1:1000 (Novus Biologicals), β -Actin 1:1000-1:5000 (Cell Signaling), and Anti-rabbit IgG HRP-linked secondary (Cell Signaling). Immunoblotting occurred overnight at 4 °C after membranes were blocked with tris-buffered saline containing tween (TBST, 2.42 g Tris, 8 g NaCl, 1 L deionized water, 500 μ L Tween 20, pH 7.6) and 5% instant milk. The membrane was then rinsed 4x with TBST and blocked again with 5% milk prior to being exposed to the secondary antibody for 2 hrs at room temperature. Protein detection was acquired using Western Lighting Chemiluminescence (PerkinElmer) on a BioRad Chemidoc imaging system, and the band signal intensity was assessed using QuantityOne software (BioRad).

Metal Analysis

Mn and Fe concentrations were measured with graphite furnace atomic absorption spectrometry (Varian AA240, Varian, Inc., USA). Aliquots of astrocyte cytosolic and plasma membrane homogenates (30 μ L) were digested in ultrapure nitric acid (1:2 v/v dilution) for 24-48 hours in a sand bath (60° C). Each sample was further diluted with a 2% nitric acid solution as need for analysis. A bovine liver (NBS Standard Reference Material, USDC, Washington, DC) (10 μ g Mn/g; 184 μ g Fe/g) was digested in ultrapure nitric acid and used as an internal standard for analysis (final concentration 5 μ g Mn/L and 92 μ g Fe/L). Metal data are expressed as μ M/mg protein.

Statistical Analyses

³H-GABA uptake and metal data were analyzed using SPSS v20 for Windows. Data were examined for the presence of outliers by boxplot analysis. Analysis of variance was conducted to identify mean differences between treatment groups for uptake and metal analyses with a significance threshold set at $p < 0.05$. Tukey's post hoc tests were conducted when a significant difference in means was detected to identify significant variations between individual treatments within the statistical model. Pearson's correlational analyses were then performed to examine relationships between metal concentrations and ³H-GABA uptake. The threshold of significance for all tests was set at $p < 0.05$.

Results

Manganese Decreases ³H-GABA Uptake in a PKC Independent Manner

A time dependent decrease in ³H-GABA uptake was observed in astrocytes exposed to 500 μ M Mn (Figure 1A). Mn significantly reduced GABA uptake after 24hrs of exposure ($p < 0.001$) and in astrocytes that were only exposed to Mn (CN Mn) during experimental conditions ($p = 0.025$), compared to control. The CN Mn group was added to identify the effect of extracellular Mn on GABA uptake. A time dependent increase in PKC phosphorylation (pPKC) was also observed with Mn exposure (Figure 1C); however, no appreciable changes in plasma membrane or cytosolic GAT3 protein levels resulted due to elevated pPKC, contrary to our hypothesis. To further investigate the involvement of PKC

in Mn reduced GABA transport we repeated the uptake experiments using the PKC inhibitors BIS II and isorhamnetin (ISO). Despite decreasing pPKC in the plasma membrane fraction (Figure 1D), pretreatment with 10 μ M ISO failed to restore Mn-impaired GABA uptake and further reduced uptake when Mn was present in the extracellular space (Figure 1B). Slight reductions in membrane bound GAT3 were observed with ISO treatment corroborating decreased uptake. ISO driven changes in membrane GAT3 are not likely due to PKC signaling because 24 hr Mn exposure did not yield similar results although pPKC was abundant. Moreover, treatment with the broad PKC inhibitor BIS II (10 μ M) did not restore Mn-impaired GABA uptake (Data not shown) further supporting a diminished role of PKC phosphorylation in Mn reduced GABA uptake.

Figure 5.1. ³H-GABA Uptake and GAT3 Protein Levels in Mn Exposed Astrocytes.

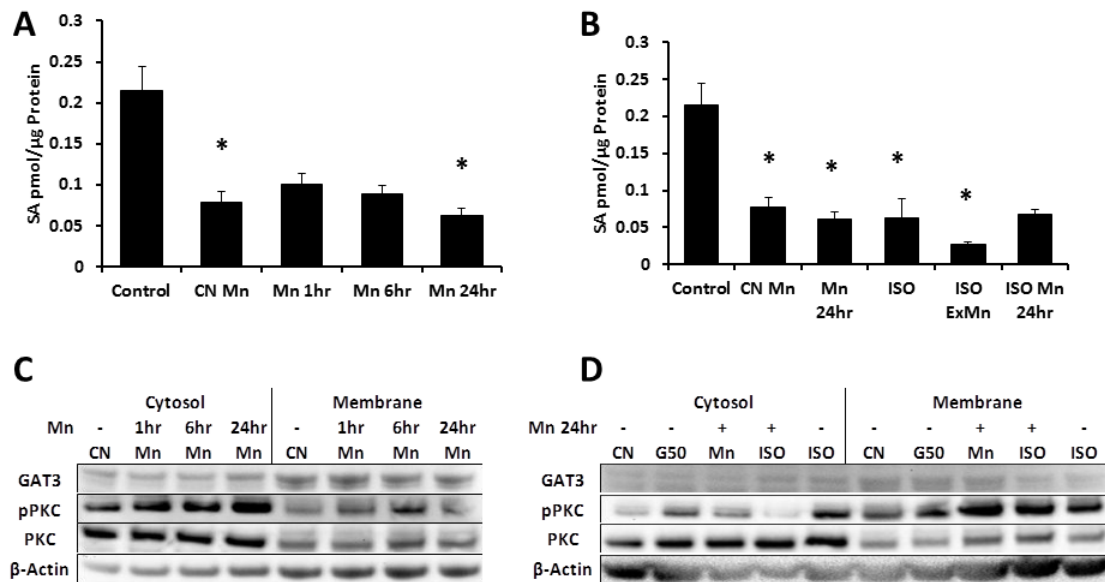


Figure 5.1. ³H-GABA Uptake and GAT3 Protein Levels in Mn Exposed Astrocytes. – Mn and isorhamnetin (ISO) significantly reduce ³H-GABA uptake independent of PKC phosphorylation. A) ³H-GABA uptake of astrocytes exposed for 2 min to an experimental buffer containing 0.5 μCi ³H-GABA (total GABA concentration, 50 μM). Prior to uptake astrocytes were exposed to 500 μM Mn for 0 (Control), 1, 6, or 24 hrs. An additional group of control astrocytes were exposed experimental buffer containing ³H-GABA and 500 μM Mn (CN Mn) to simulate extracellular Mn. B) 2 min uptake of ³H-GABA in astrocytes pretreated for 72hr with 10μM ISO, ISO plus extracellular Mn (ISO ExMn), and 24 hr Mn exposure after ISO pretreatment (ISO Mn 24hr). All uptake data represent three sample replicates from three independent culture dates (n=9) and are expressed as mean specific activity normalized to protein ± SEM. C and D) Western blot analysis on cytosolic and plasma membrane fractions of cells exposed to 500 μM Mn for 0, 1, 6, or 24 hrs (C), or 24 hr exposure to Mn after pretreatment with ISO (D). An additional group of cells were treated with 50 μM GABA (G50) (D) to control for protein expression changes due to the uptake experimental conditions. Analysis of variance was performed on uptake data, and when applicable, Tukey's post hoc analysis was conducted to determine significant differences between treatment groups, p ≤ 0.05.

Membrane GAT3 May be Influenced by Cellular Manganese Localization

Metal analysis of membrane and cytosolic fractions provide novel data that suggest Mn and ISO induced changes in GABA uptake may be associated with cellular Mn localization. Astrocytes exposed to 500 μ M Mn rapidly accumulate cytosolic Mn by 600 fold within one hour of exposure, followed by drastic Mn efflux resulting in a \sim 100 fold increase in cytosolic Mn at 24 hrs compared to control (Figure 2A). Interestingly, ISO pretreatment blunted cytosolic Mn accumulation by 60% after one and six hours of Mn exposure, but cytosolic Mn normalized after 24 hrs (Figures 2A, 2B). Cytosolic and membrane Mn levels were significantly elevated from controls after 24 hrs of Mn exposure ($p = 0.003$ and 0.005 , respectively), corresponding with significantly reduced GABA uptake but stable membrane GAT3 levels. Decreased Mn uptake in the ISO treatment group, and a near significant ($p = 0.06$) reduction in membrane Mn levels compared to the Mn alone treatment, may allow for proper GAT3 membrane recycling.

Figure 5.2. Astrocyte Mn Accumulation after Mn Exposure and ISO Pretreatment.

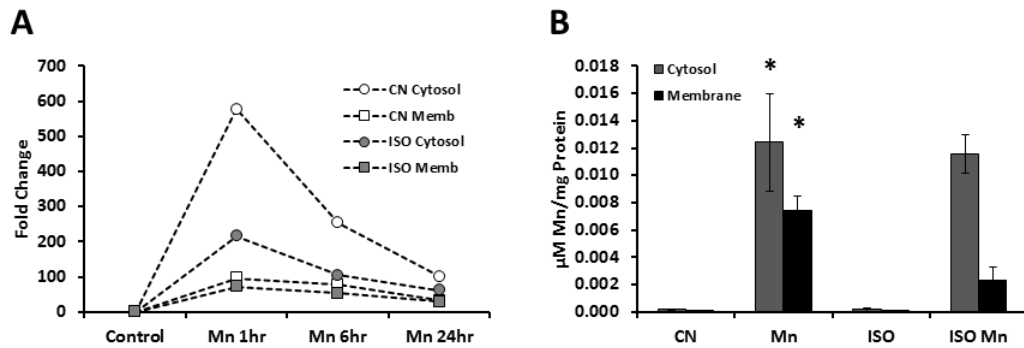


Figure 5.2. Astrocyte Mn Accumulation after Mn Exposure and ISO Pretreatment. – A) Astrocytes exposed to 500 μM Mn responded with rapid accumulation of cytosolic Mn after 1hr of exposure but retained less cytosolic Mn with longer term exposure. The Mn content in plasma membrane fractions of astrocytes responded similarly over time with less magnitude of change. After 24 hrs of Mn exposure, cytosolic and membrane Mn concentrations were significantly elevated compare to control (B). Pretreatment with ISO blunted the initial cytosolic accumulation of Mn (A), and caused a near significant ($p = 0.06$) reduction in plasma membrane Mn content after 24 hrs of Mn exposure (B). Analysis of variance was performed on metal analysis data, and when applicable, Tukey’s post hoc analysis was conducted to determine significant differences between treatment groups, $p \leq 0.05$.

Oleic Acid and Palmitic Acid Exacerbate Manganese Accumulation Resulting in Decreased GABA Uptake

Administration of oleic acid and palmitic acid to astrocyte cultures resulted in concentration dependent changes in GABA uptake (Figure 3A). Low concentrations (10 μM) of either fatty acid had little effect on GABA uptake but a logarithmic increase in fatty acid dose reduced uptake. Mn exposure compounded this effect significantly impairing GABA uptake with 10 or 100 μM

treatment of either fatty acid (Figure 3A). Moreover, the application of fatty acids enhanced Mn accumulation in cytosolic and membrane fractions of astrocytes (Figure 4B). Co-application of oleic acid and Mn significantly increased membrane Mn content (O10 Mn, $p = 0.001$; O100 Mn, $p = 0.013$) over Mn treatments alone (Figure 4B). Similarly, combined palmitic acid and Mn applications significantly elevated membrane Mn levels over Mn treatments alone (P10 Mn and P100 Mn, $p < 0.001$), but palmitic acid also exacerbated Mn uptake leading to significantly greater cytosolic Mn concentrations than Mn treatment alone ($p < 0.001$) (Figure 4D). Correlational analysis revealed significant inverse relationships between GABA uptake and both cytosolic (Figure 4C, $p = 0.010$) and membrane (Figure 4D, $p = 0.011$) Mn concentrations. Decreased uptake and augmented Mn accumulation with oleic acid and palmitic acid were not associated with changes in GAT3 protein levels (Figures 3B, 3C).

Figure 5.3. ^3H -GABA Uptake and Western Blot Analysis of Astrocytes Exposed to Oleic and Palmitic Acids.

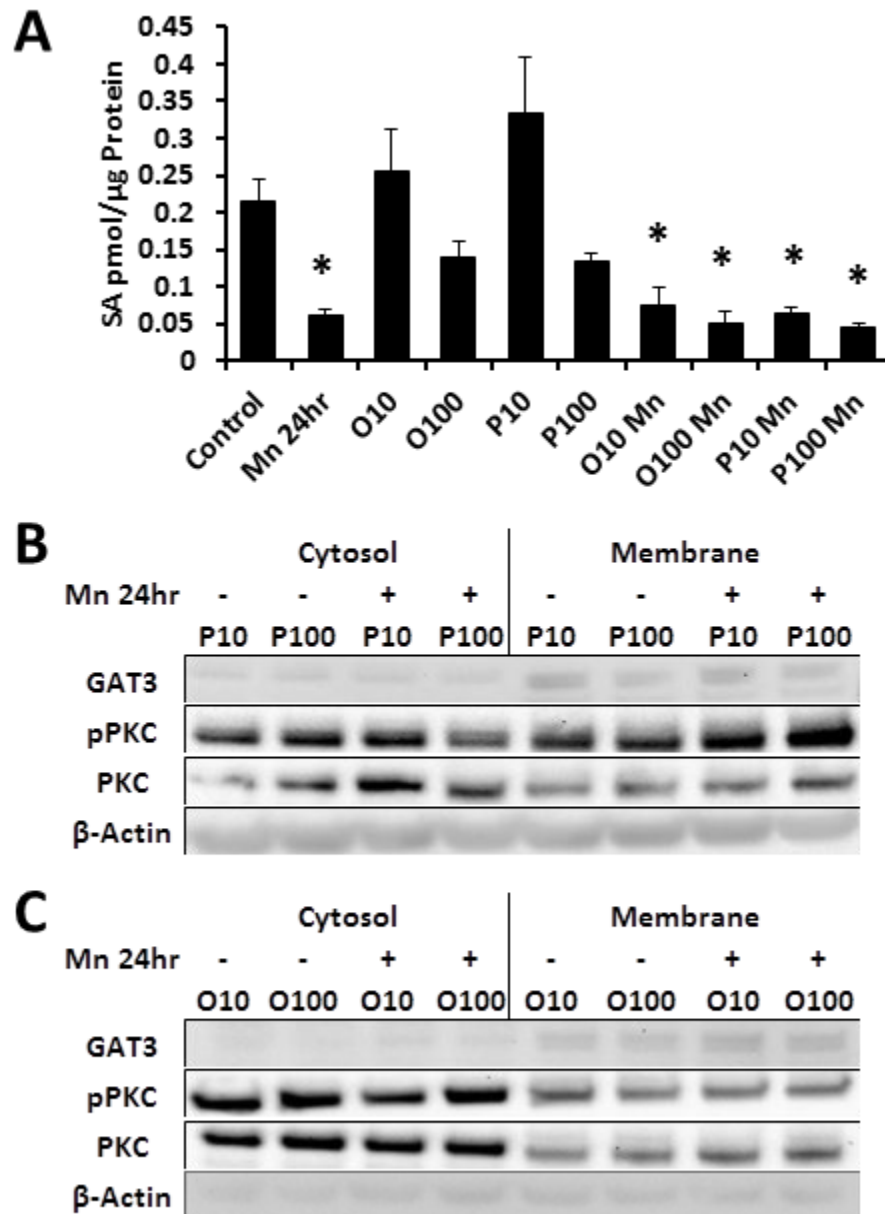


Figure 5.3. ^3H -GABA Uptake and Western Blot Analysis of Astrocytes Exposed to Oleic and Palmitic Acids. – Astrocytes were exposed to oleic acid or palmitate (10 μM (P10 and O10) or 100 μM (P100 and O100)) for 24 hrs with or without 500 μM Mn. Uptake and western blot analyses were performed on astrocytes from three independent culture dates. Uptake samples ($n = 9$) and western blots are representative of protein changes from the three culture dates. A) Oleic acid and palmitate significantly decrease ^3H -GABA uptake when combined with Mn exposure, but not independently. B) Changes in ^3H -GABA uptake did not correspond with changes in plasma membrane GAT3 content or PKC phosphorylation. Analysis of variance was performed on uptake data, and when applicable, Tukey's post hoc analysis was conducted to determine significant differences between treatment groups, $p \leq 0.05$.

Figure 5.4. Cytosolic and Plasma Membrane Metal Content of Astrocytes Exposed to Oleic and Palmitic Acids.

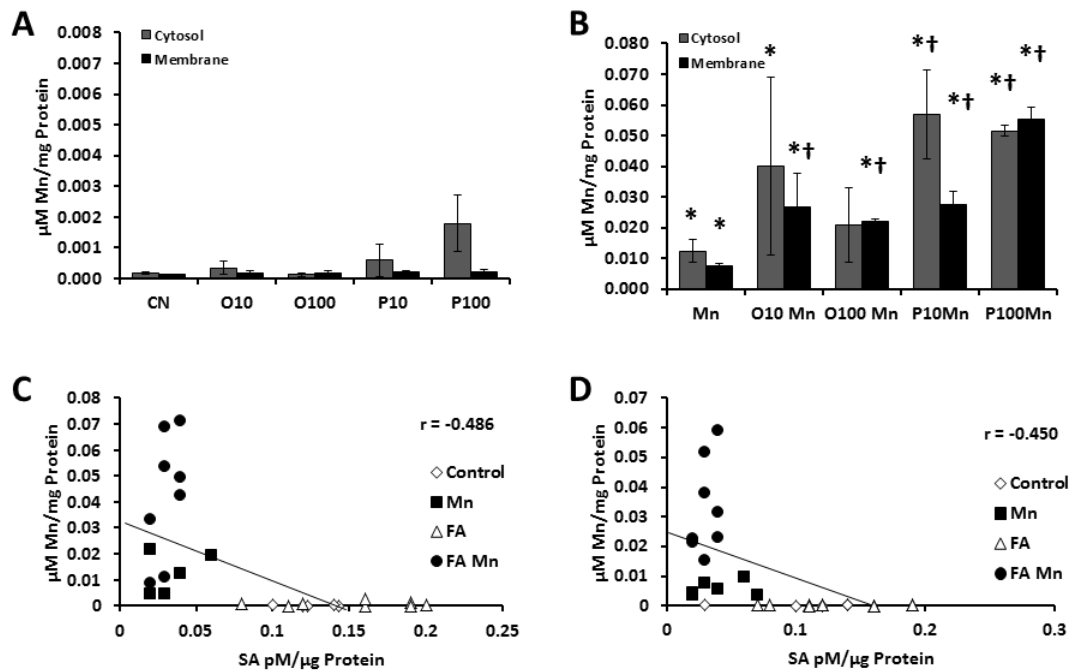


Figure 5.4. Cytosolic and Plasma Membrane Metal Content of Astrocytes Exposed to Oleic and Palmitic Acids. – Exposure to oleic acid and palmitate exacerbate Mn accumulation due to 500 μM Mn exposure in cytosolic and membrane fractions, and was negatively correlated with ^3H -GABA uptake. Data represent samples from two independent culture dates and are expressed as μM Mn normalized to sample protein \pm SEM. A) Mn concentrations of cytosolic and

membrane fractions of cells exposed to 10 or 100 μM fatty acid. B) Co-treatment with 500 μM Mn and fatty acids enhance Mn accumulation in both cell fractions compared to control (*) and Mn exposure (†) alone. C) Cytosolic Mn concentrations of Mn and fatty acid (FA) exposures had a significant negative correlation with ^3H -GABA uptake. D) A significant negative correlation was also observed between plasma membrane Mn content and ^3H -GABA uptake of Mn and FA exposed astrocytes. Analysis of variance with Tukey's post hoc analysis was used to determine significant differences in Mn content between treatment groups, and Pearson's correlational analysis was conducted to elucidate the relationship between ^3H -GABA uptake and Mn accumulation, $p \leq 0.05$.

Iron Deficiency Decreases GABA Uptake

Iron deficiency has been shown to down regulate DAT function by promoting transporter internalization (Wiesinger et al., 2007). For this reason we wanted to investigate if iron deficiency regulated GABA uptake and GAT3 in a similar fashion. Using the iron chelator desferrioxamine (DFO), iron deficiency suppressed GABA uptake to the same extent as Mn exposure (Figure 6A). While DFO treatment had no effect on cellular Mn levels, it depleted cytosolic Fe and doubled the Fe content found in the plasma membrane fraction compared to controls (Data not shown). Iron deficiency decreased GABA uptake, but it did not reduce membrane GAT3 levels.

Figure 5.5. Dose Response: Cytosolic and Membrane Mn Concentrations with Increasing Mn and GABA.

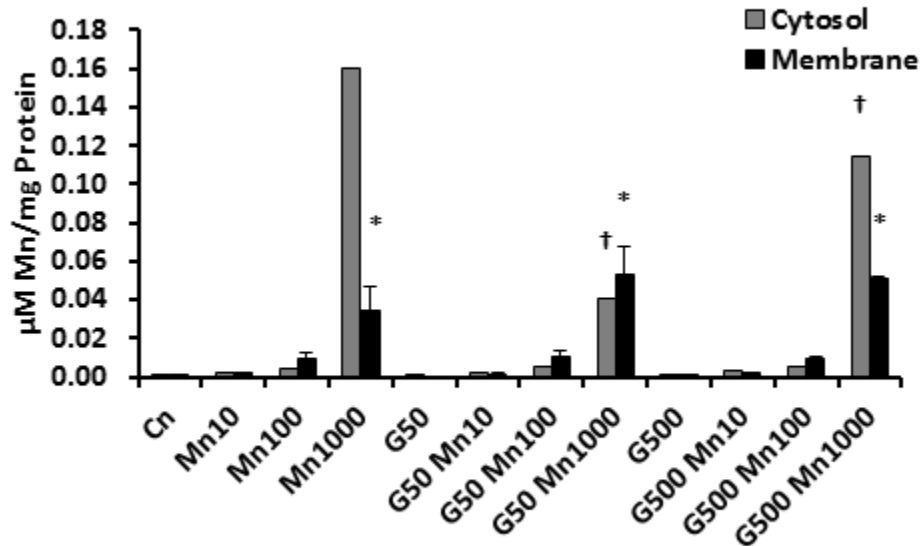


Figure 5.5. Dose Response: Cytosolic and Membrane Mn Concentrations with Increasing Mn and GABA. – These data represent cytosolic and membrane Mn concentrations of astrocytes exposed to logarithmic increases in Mn (10, 100, and 1000 µM) and GABA (50 and 500 µM) independent or in combination for 24hrs. These data represent experiments from two independent culture dates. Analysis of variance with Tukey’s post hoc analysis were applicable was used for statistical analysis. (*) represents a significant change from control and (†) represents a significant change from Mn 1000, $p \leq 0.05$.

Figure 5.6. Iron Deficiency Reduces ^3H -GABA Uptake in Cultured Astrocytes.

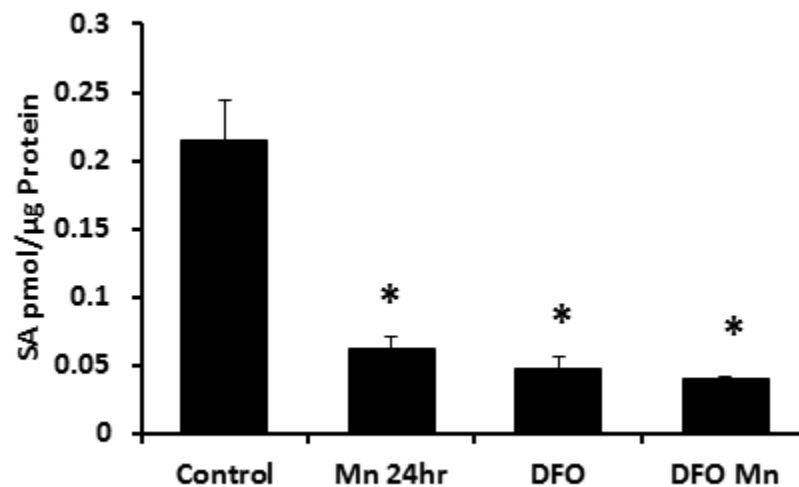


Figure 5.6. Iron Deficiency Reduces ^3H -GABA Uptake in Cultured Astrocytes. – To determine the effect of iron deficiency on GABA uptake we induced iron deficiency using the iron chelator desferrioxamine (DFO) 200 μM with or without 500 μM Mn for 24 hrs. Iron deficiency significantly reduced uptake compared to control, as determined by analysis of variance with Tukey's post hoc test, $p \leq 0.05$.

Extracellular Manganese and GABA Interact Reducing Their Transport Into Cells

Astrocytes exposed to Mn only during the uptake experiment (CN Mn) had reduced GABA uptake similar to astrocytes that were exposed to Mn for 24 hrs (Figure 1A). Additionally, extracellular Mn reduced GABA uptake in the ISO treatment group versus the ISO treatment without Mn in the experimental buffer (Figure 1C). These data show that extracellular Mn decreases GABA uptake. Next we tested whether increasing concentrations of GABA had the same effect on Mn uptake. Astrocytes exposed to 10, 100, and 1000 μM Mn had significantly

elevated cytosolic Mn compared to control (Figure 5); however concomitant administration of 50 μ M or 500 μ M GABA with 1000 μ M Mn significantly decreased cytosolic Mn concentrations compared with 1000 μ M Mn alone ($p < 0.001$) (Figure 5).

Discussion

These data corroborate previous findings of impaired GABA uptake (Anderson et al., 2008; Takeda et al., 2002; 2003) extending to primary astrocytes and novel evidence that mechanisms driving this impairment involve Mn interacting with the plasma membrane. Additionally, our results show that increases in brain fatty acid levels associated with Mn neurotoxicity exacerbate the effect of Mn on GABA uptake by enhancing Mn accumulation in the membrane fraction of astrocytes.

We hypothesized that Mn would decreased GABA uptake in astrocytes via PKC phosphorylation and internalization of GAT3. This assumption was based on data indicating that Mn activates PKC (Latchoumycandane et al., 2005; Kitazawa et al., 2005), PKC mediates membrane recycling of GAT1 (Wang and Quick, 2005), and that Mn induced PKC activation led to internalization of other transporters in the Slc6 family (Sidoryk-Wegrzynowicz et al., 2011). We observed a time dependent increase in PKC phosphorylation with Mn exposure; however, this increase did not correspond with internalization of GAT3 protein. There is abundant evidence in the literature supporting the role of PKC in the regulation of

GAT1 (Whitworth and Quick, 2001; Quick et al., 2004; Wang and Quick, 2005), but a paucity of experimental studies examining GAT3 regulation. We measured both GAT1 (data not shown) and GAT3 in our primary astrocytes, but only detected the presence of GAT3. It is possible that GAT3 regulation functions through different mechanisms, or that GAT3 does not recycle as dynamically as GAT1 to and from the plasma membrane. Because GAT3 transporters have a higher K_m (33 μM vs 7 μM for GAT1), are primarily extrasynaptic, and function to clear synaptic GABA overflow, it is likely that membrane levels of GAT3 remain more stable. Alternatively, increased pPKC in astrocytes promotes SNARE protein interactions with GAT1 (and likely GAT3), which has been shown to stabilize GAT1 on the membrane, but due to conformational changes, decreases GAT function (Quick, 2006; Wang et al., 2003). However, because the PKC inhibitors Bis II and ISO did not restore GABA uptake in our study, and the addition of Mn to the experimental buffer decreased uptake in control astrocytes, we feel that Mn interacts directly with the plasma membrane and possibly the GAT proteins. Mn binding GATs could reduce GABA transport similar to decreased dopamine transporter (DAT) function upon zinc binding to extracellular loops of DATs (Norregaard et al., 1998).

Mn is chaperoned by intra- and extra-cellular transport proteins, but once the need for Mn in metalloenzymes is met and storage mechanisms become overwhelmed, excess Mn can impair cellular respiration, induce lipid peroxidation, and initiate apoptosis (Malecki, 2001; Yiin et al., 1996, Yoon et al.,

2011). The unbound species of Mn (Mn^{3+}) is highly reactive and will quickly bind to sulfhydryl moieties of amino acid residues (Fisher and Jones, 1981) or scavenge electrons initiating oxidative damage. The production of F_2 -isoprostanes and increase of prostaglandin E_2 due to Mn exposure demonstrates this reactivity (Milatovic et al., 2009), but also provides evidence that Mn interacts with the plasma membrane. Our data confirm that Mn content in the membrane fraction of astrocytes is significantly elevated with Mn exposure, and was also associated with decreased GABA uptake. Sulfhydryl containing cysteine residues on the short extracellular loop four of the GABA transporters are fundamental to sodium and GABA ligand binding for translocation to the cytosol (Zomot and Kanner, 2003). Mn interfering with these sulfhydryl residues is a putative mechanism for decreased GABA uptake in primary astrocytes. Additionally, the DAT (of the same, largely conserved, Slc6 transporter family) was identified to play a role in Mn transport in striatal synaptosomes and the globus pallidus of Mn exposed rats (Anderson et al., 2007b). We observed that adding physiological concentrations of GABA (50 μ M) to astrocyte cultures decreased cytosolic Mn accumulation. We speculate that Mn interacts with extracellular GABA or competes as a ligand for GATs.

The effect of fatty acid treatment on GABA uptake observed in our study was less than previously reported (Troeger et al., 1984; Rhoads et al., 1982). A significant decline in GABA uptake was only achieved when oleic acid or palmitate were co-administered with Mn. Again, PKC associated internalization of

GAT3 did not occur with either fatty acid alone or combined fatty acid/Mn treatments. Changes in the amount of these fatty acids, specifically the saturated fatty acid palmitate, may compromise the membrane fluidity and impair protein mediated transport (Hulbert et al., 2005). Oleic acid is one of the most abundant fatty acids in the plasma membrane, and oleic and palmitic acids are the predominant fatty acids found in membrane lipid rafts (Schumann et al., 2011). Disrupting lipid composition in membrane rafts resulted in a 50% decrease in transport rate by GATs (North and Fleischer, 1982; Allen et al., 2007). We speculate that the debilitating effect of fatty acids and Mn on GABA uptake is due to altered lipid raft composition. Our speculation is based on studies showing that GATs are associated with lipid raft micor-domains (Allen et al., 2007). Moreover, oleic and palmitic acids significantly elevated Mn accumulation in membrane fractions over Mn exposure alone. It is unclear whether decreased GABA uptake is primarily affected by Mn directly or Mn induced changes in fatty acids, but our data show a synergistic relationship between the two.

Due to the reciprocal relationship between Mn toxicity and iron deficiency, the influence of iron deficiency on DAT function (Erikson et al., 2000), and PKC mediated trafficking of DATs induced by iron deficiency (Wiesinger et al., 2007), we also examined whether iron deficiency contributed to the observed decline in GABA transport. Induced iron deficiency in astrocyte cultures significantly reduced GABA uptake similar to Mn exposure and combined iron deficient/Mn treatments. Iron deficiency did not decrease plasma membrane concentrations of

GAT3 as was observed with DAT in iron deficient rats (Erikson et al., 2000). The use of DFO depleted cytosolic iron as expected, but interestingly resulted in a doubling of the iron content in the membrane fraction (Data not shown). Membrane iron accumulation is presumably an artifact of elevated extracellular iron in the culture medium due to the DFO treatments; however, increased extracellular iron may interact with the plasma membrane akin to extracellular Mn. It is noteworthy that extracellular iron has been reported to decrease in the striatum of Mn exposed rats while extracellular Mn is significantly elevated (Fordahl et al., 2010; Anderson et al., 2009). Further studies need to be conducted to confirm direct binding of Mn or Fe to GATs. Binding could be identified using structural modeling to predict metal binding sites, similar to the elucidation of the zinc/DAT binding site. In conjunction with structural modeling, immunoprecipitation of GATs from Mn exposed cells followed by metal analysis of the eluted protein could identify metal/GAT binding.

In conclusion, contrary to our hypothesis, it appears that Mn exposure does not alter cellular GAT 3 in primary astrocytes, specifically via PKC signaling. It is possible that endoplasmic reticular stress compromises post translational modification of neurotransmitter transporters, but results from this and previous studies from our lab suggest that Mn exposure alters membrane structure/function as evidenced by the oleic acid, palmitic acid, and cholesterol changes *in vivo* with Mn exposure (Fordahl et al., 2012) and their influence on *in vitro* GABA uptake (North and Fleischer, 1982; Allen et al., 2007). These

changes may influence membrane dynamics, and our data suggest that elevations of these fatty acids augment Mn aggregation at the membrane where Mn is available to interact with transmembrane proteins or instigate oxidative damage. Further characterizing the effects of Mn accumulation on membrane integrity will provide valuable information on how Mn neurotoxicity affects GABA and other neurotransmitter systems within the basal ganglia. While direct binding of Mn to GATs needs to be confirmed, we provide evidence that an interaction between Mn and these transmembrane proteins may exist

CHAPTER VI

EPILOGUE

Exposure to environmental manganese (Mn) is associated with dire neurological consequences. Inhalation of Mn airborne particulate or ingestion of Mn contaminated water each contributes to documented cases of Mn neurotoxicity; however, pathologies for these sources of exposure are quite different. Diagnosis of inhalation exposure is often associated with motor control issues (Meyer-Baron et al., 2009), whereas ingestion results in more subtle cognitive impairments (Wasserman et al., 2006; Khan et al., 2011). Length and severity of Mn exposure in either scenario influence the extent of neurotoxic damage, but a common theme to the overall etiology of Mn neurotoxicity is disrupted dopamine and γ -aminobutyric acid (GABA) signaling in the basal ganglia. Changes in brain GABA levels have been reported prior to changes in dopamine (Gwiazda et al., 2002), and results from this dissertation suggest that Mn altered GABA is associated with GABA transporter function. Additionally, our findings identify biomarkers that correspond with Mn accumulation. Prior to the studies herein, reliable biomarkers and mechanisms involved with GABA dysregulation were unknown. These data serve as a foundation for future studies to further characterize the effects of Mn neurotoxicity, and to develop tests for the candidate biomarkers we have identified.

A goal of this project was to characterize how Mn interfered with GABA neurotransmission. The impact of Mn on GABA was examined specifically by: 1) measuring the clearance of extracellular GABA in Mn exposed rats using *in vivo* microdialysis, and 2) testing the effect of Mn on GABA transport proteins (GATs) using the GAT inhibitor nipecotic acid (NA). These experiments were based on previous studies in our lab showing increased extracellular GABA levels in the striatum of Mn exposed rats with minimal effect on transport proteins (Anderson et al., 2008). Results from this study corroborated our previous observations of elevated striatal GABA with Mn exposure, but several novel findings appeared after blocking GAT mediated GABA clearance with NA. In control animals, administration of NA was followed by a significant rise in extracellular GABA, as expected. This effect was absent in Mn exposed rats indicating that the function of GAT proteins was already impaired due to Mn. These data confirmed our hypothesis that Mn impairs GABA uptake by attenuating GAT protein function, instead of altering protein or mRNA expression. Additionally, Mn nearly abolished extracellular taurine and mitigated the taurine release that followed extraneous synaptic GABA. We speculated that the taurine efflux was a compensatory response to regulate GABA release through GABA_B receptor activation (Chen and vanden Pol, 1998), or to stabilize the inhibitory tone of the striatum due to increased GABA_A receptor activation (del Olmo et al., 2000; Jua et al., 2008). Altered extracellular GABA and taurine in the striatum due to Mn is likely to affect

neurochemical coordination with other brain regions and neurotransmitter systems.

Because the microdialysis data indicated a functional decline in GAT proteins, and previous reports indicate minimal change in protein expression (Anderson et al., 2008), cellular experiments were designed to investigate whether internalization of GAT proteins contributed to the loss of function. Primary astrocytes were used to examine cellular Mn accumulation and the protein kinase C signaling pathway which is critical to membrane recycling of GAT proteins (Quick et al., 2004). We hypothesized that Mn decreased membrane density of the astrocyte specific GAT isoform, GAT3, through PKC activation and subsequent GAT3 internalization. Surprisingly, membrane levels of GAT3 were largely unaffected in Mn exposed astrocytes despite increased PKC phosphorylation and a significant decline in ^3H -GABA uptake. Instead, decreased uptake was correlated with Mn accumulation in the membrane fractions of astrocytes. Moreover, extracellular Mn alone markedly reduced ^3H -GABA uptake and dose response studies with Mn and GABA revealed that physiological concentrations of GABA reduce the binding affinity of Mn to membrane fractions. We speculate that under conditions of Mn neurotoxicity, free extracellular Mn either binds to GAT proteins as an allosteric or non-competitive inhibitor decreasing GABA transport, or aggregates with extracellular GABA blocking reuptake via GATs. These hypotheses are based on the allosteric regulation of zinc on dopamine receptors (Schetz and Sibley, 1997).

To further characterize the involvement of PKC signaling with Mn accumulation, ³H-GABA uptake and western analyses were repeated in astrocytes pretreated with isorhamnetin (ISO), a blood brain permeable quercetin metabolite and PKC inhibitor. ISO slightly decreased PKC phosphorylation, but did not improve membrane GAT3 protein levels or ³H-GABA uptake in Mn exposed cells. To confirm a diminished role of PKC in GAT3 regulation of GABA uptake in Mn exposed astrocytes, cells were treated with the potent PKC inhibitor bisindolylmaleimide (BIS II) prior to the uptake experiments. We expected BIS II to improve ³H-GABA uptake in Mn exposed cells by reducing PKC mediated internalization of GAT3. BIS II ablated PKC phosphorylation but did not restore ³H-GABA uptake. BIS II actually decreased uptake compared to controls, similar to ISO. GAT3 protein levels were also unaffected by BIS II, suggesting that GAT3 mediated GABA uptake is regulated by mechanisms other than PKC signaling.

Results from our studies on GAT3 regulation in astrocytes differ from previous research on GAT1 regulatory mechanisms in neurons and GAT1 transfected cell lines. Using primary astrocytes as a model to characterize GAT mechanisms may account for the differences observed, and may provide a limitation to characterize Mn induced GAT regulation. Knowing that maturation of the rat brain GABA neurotransmitter system happens between post natal days (PND) 10-30 (Kilb, 2012), our model may have been developmentally mistimed since the astrocytes isolated for our studies were harvested between PND 1-3; however, isolation of astrocytes beyond PND 3 substantially diminishes astrocyte

viability and increases the likelihood of neuronal, microglial, and fibroblast contamination (Allen et al., 2001). GAT3 protein levels were detectable, but regulatory mechanisms may differ in these cells compared to astrocytes isolated from a GABA mature environment. GABA release is a key factor to GABAergic development *in vivo* (Bernstein and Quick, 1999). For that reason we fortified our media to contain 50 μ M GABA while in culture prior to experimental treatments. GABA fortification modestly improved GAT3 protein levels, and we suspect that this aided astrocyte GAT regulation. It is important to note that this model is still appropriate to characterize the impact of Mn neurotoxicity. Because astrocytes are the primary metal handling cells of the brain, early neurochemical changes presumably result when the metal sequestering capacity of these cells is exhausted, and astrocyte function begins to diminish. Astrocyte impairment not only leaves neurons vulnerable to metals and other toxic molecules, but reduces the ability of astrocytes to modulate the extracellular space by clearing excess neurotransmitters. Moreover, we observed a functional decline in uptake with Mn accumulation despite internalization of GAT3. This observation demonstrates that the effect of Mn on GABA neurotransmission extends beyond our initial hypothesis of altered cellular signaling and membrane recycling of GAT proteins.

Future studies need to be conducted to examine whether Mn directly interacts with membrane proteins, specifically GAT3. Our results suggest that Mn may compete with extracellular GABA as a ligand for GATs, or allosterically inhibit GAT3 protein function. A logical next step would be to immunoprecipitate

(IP) GAT1 and GAT3 from Mn exposed cells, then conduct metal analysis on the eluted protein. If Mn directly binds to the protein, it will be detectable in the IP fraction. Alternatively, the use of structural modeling to predict metal binding sites of GAT1 and GAT3, similar to the elucidation of the zinc/dopamine transporter (DAT) binding site, could be used to identify putative binding sites.

Another aim of this project was to identify biomarkers that correspond with Mn neurotoxicity. Metabolomic analysis was conducted on plasma, liver, and brain samples from rats that were exposed to waterborne Mn for six weeks, and behavior changes were assessed using 24 hr video surveillance. Mn neurotoxicity was confirmed when stereotypic behaviors that are known to correspond with neurotoxicity became present. Brain, plasma, and liver Mn content was significantly elevated in Mn exposed rats compared to control, and a total of 98 metabolites were significantly altered between these three compartments. Plasma homogentisic acid, aspartic acid, and chenodeoxycholic acid emerged as potential biomarkers of neurotoxicity, each significantly correlating with Mn accumulation in the striatum and globus pallidus. The most notable metabolic shift due to Mn exposure was found in fatty acid metabolism. In the brain, oleic and palmitic acids were significantly elevated after Mn exposure (12 and 15 fold change, respectively), and were strongly correlated with plasma Mn ($r > 0.75$). Oleic acid was similarly altered in the liver along with significantly decreased ketone body formation suggesting altered lipid metabolism.

Several behavioral changes were observed in Mn exposed rats. Twenty-four hour surveillance of the home cage environment identified a decrease in stereotypic behaviors during the dark cycle, but light cycle activity increased. The overall increase in activity was strongly correlated with brain and systemic Mn levels; however, a reversal of circadian rhythm has also been associated with iron deficiency (Youdim et al., 1980). We speculate that this reversal in circadian clock is influenced by Mn induced changes in striatal dopamine and GABA, which are known to fluctuate in a circadian fashion (Castaneda et al., 2004) and influence proteins critical to circadian regulation (Hood et al., 2010). The ability to identify consistent behaviors that correspond with Mn neurotoxicity in rodents may be useful to develop indices for early diagnosis in Mn exposed humans.

A possible limitation to this study was that the striatum and globus pallidus were not able to be used for metabolomic analysis. These target regions of Mn accumulation were dissected out for metal and other biochemical analyses, leaving the remainder of the brain available for metabolomic analysis. Because of this, a global shift in brain metabolism could be discerned, but future studies are warranted to examine specific metabolic shifts in the striatum and globus pallidus. Characterizing metabolic changes in brain regions routinely affected by Mn accumulation would shed light onto mechanisms that affect neurochemistry.

The significant changes in brain oleic and palmitic acids identified with metabolomic analysis, along with notable alterations in cholesterol and

desmosine suggest that structural damage or membrane remodeling may occur with Mn accumulation. These changes could affect membrane fluidity and alter the function of transmembrane proteins. Oleic acid and palmitate are primary constituents of plasma membranes and lipid raft domains (Schumann et al., 2011), and have been linked with decreased GABA uptake (Troeger et al., 1984; Rhoads et al., 1982). For this reason experiments were conducted to examine whether these Mn induced metabolic changes influenced GABA dysfunction in primary astrocytes. Oleic and palmitic acids synergistically reduced GABA uptake with Mn exposure. This effect was accompanied by a significant increase in plasma membrane Mn accumulation compared to Mn exposed astrocytes alone. Mechanisms that contribute to the effect of fatty acids on membrane Mn accumulation are unclear, but altered membrane composition and palmitoylation of membrane proteins likely contribute to impaired ^3H -GABA uptake. Palmitoylation has been shown to regulate DAT kinetics and prevent PKC mediated regulation of the protein thereby stabilizing DAT at the plasma membrane (Foster and Vaughan, 2011). GAT3 could be modified by palmitoylation in a similar manner. Alternatively, if lipid raft micro domains are compromised by high concentrations of saturated fatty acids, GAT3 proteins associated with these domains could be affected. Further studies are warranted to address these questions. Employing methodology from Foster and Vaughan (2011), palmitoylation of GATs could be confirmed using ^3H -pamitatic acid to label palmitoylated membrane proteins, IP GATs of interest, confirm

palmitoylated protein with electrophoretic migration, using hydroxylamine treatments as a negative control. Hydroxylamine cleaves fatty acylated thioester bonds, which would remove the radiolabelled palmitate. These experiments would address questions that arose from our studies, and further characterize how metabolic shifts influence cell function.

The etiology of Mn neurotoxicity is diverse depending on route, length, and magnitude of exposure. Mechanisms that contribute to neurotoxicity are still under investigation, but it is clear that Mn accumulates in distinct regions of the brain, inflicts cellular damage, and modifies neurochemical signaling. The chronology of these events and how they influence one another needs to be further characterized; however, data from this dissertation provide evidence that altered fatty acid metabolism and cellular compartmentalization of Mn affect GABA neurotransmission. Understanding how Mn compromises cellular function and alters metabolism is essential to develop treatments that target pathways capable of restoring the neurochemical imbalances associated with Mn exposure. Such breakthroughs would be applicable to similar neurodegenerative diseases, like Parkinson's disease, or other neurological disorders affected by metal homeostasis (e.g. copper and Wilson's disease).

REFERENCES

Ade KK, Janssen MJ, Otrinski PI, Vicini S. Differential tonic GABA conductances in striatal medium spiny neurons. *J Neurosci*. 2008; 28(5): 1185-1197.

Ali SF, Dunhart HM, Newport GD, Lipe GW, Slikker W. Manganese-induced reactive oxygen species: comparison between Mn^{+2} and Mn^{+3} . *Neurodegeneration*. 1995; 4 (3): 329-34.

Allen JW, Mutkus LA, Aschner M. 2001. Isolation of Neonatal Rat Cortical Astrocytes for Primary Cultures. *Current Protocols in Toxicology*. 4:12.4.1-12.4.15.

Allen JA, Halverson-Tamboli RA, Rasenick MM. Lipid raft microdomains and neurotransmitter signaling. *Nat Rev Neurosci* 2007; 8 (2): 128-140.

Anderson JG, Cooney PT, Erikson KM. Brain Manganese Accumulation is Inversely Related to γ -Amino Butyric Acid Uptake in Male and Female Rats. *Toxicol. Sci*. 2007; 95 (1): 188-195.

Anderson JG, Cooney PT, Erikson KM. Inhibition of DAT function attenuates manganese accumulation in the globus pallidus. *Environ Tox Pharmacol* 2007; 23: 179-184.

Anderson JG, Fordahl SC, Cooney PT, Weaver TL, Colyer CL, Erikson KM.

Manganese exposure alters extracellular GABA, GABA receptor and transporter protein and mRNA levels in the developing rat brain. *NeuroToxicology* 2008; 29: 1044-1053.

Anderson JG, Fordahl SC, Cooney PT, Weaver TL, Colyer CL, Erikson KM.

Extracellular norepinephrine, norepinephrine receptor and transporter protein and mRNA levels are differentially altered in the developing rat brain due to dietary iron deficiency and manganese exposure. *Brain Res.* 2009; 1281: 1-14.

Arduino DM, Esteves AR, Dominques AF, Pereira CM, Cardoso SM, Oliveira CR.

ER-mediated stress induces mitochondrial-dependent caspases activation in NT2 neuron-like cells. *BMB Rep.* 2009; 42 (11): 719-724.

Aschner M, Gannon M, Kimelberg HK. Manganese uptake and efflux in cultured

rat astrocytes. *J Neurochem* 1992; 58 (2): 730-735.

Aschner M, Vrana KE, Zheng W. Manganese uptake and distribution in the

central nervous system (CNS). *NeuroTox.* 1999; 20 (3):173-80.

Aschner M, Erikson KM, Dorman DC. Manganese dosimetry: species differences

and implications for neurotoxicity. *Crit. Rev. Tox.* 2005; 35: 1-32.

Aschner JL, Aschner M. Nutritional aspects of manganese homeostasis. *Mol*

Aspects Med. 2005; 26 (4-5): 353-362.

Aschner M, Guilarte TR, Schneider JS, Zheng W. Manganese: Recent advances in understanding its transport and neurotoxicity. *Toxicol App Pharmacol* 2007; 221 (2): 131-47.

Aschner M, Gannon M. Manganese (Mn) transport across the rat blood-brain barrier: storable and transferrin-dependent transport mechanism. *Brain Res Bull* 1994; 33 (3): 345-9.

ATSDR. (2008). Agency for Toxic Substances and Disease Registry. (U.S. Department of Health and Human Services, Public Health Service) Retrieved August 2013, from Toxicological Profile for Manganese:
<http://www.atsdr.cdc.gov/substances/toxsubstance.asp?toxid=23>

Baquer NZ, Nothersall JS, Greenbaum AL, McLean P. The modifying effect of manganese on the enzymic profiles and pathways of carbohydrate metabolism in rat liver and adipose tissue during development. *Biochim. Biophys. Res. Comm.* 1974; 62 (3): 634-641.

Barbeau A. Manganese and extrapyramidal disorders (a critical review and tribute to Dr. George C. Cotzias). *NeuroTox* 1984; 5 (1): 13-35.

Beard JL, Chen Q, Connor J, Jones BC. Altered monamine metabolism in caudate-putamen of iron-deficient rats. *Pharmacol Biochem Behav.* 1994; 48(3): 621-624.

Beckman ML, Bernstein EM, Quick MW. Multiple G protein-coupled receptors initiate protein kinase C redistribution of GABA transporters in hippocampal neurons. *J Neurosci* 1999; 19: RC9.

Bernstein EM, Quick MW. Regulation of gamma-aminobutyric acid (GABA) transporters by extracellular GABA. *J Biol Chem*. 1999; 274 (2): 889-895.

Bitoun M, Tappaz M. Taurine Down-Regulates Basal and Osmolarity-Induced Gene expression of Its Transporter, but Not the Gene Expression of Its Biosynthetic Enzymes, in Astrocyte Primary Cultures. *J Neurochem* 2000; 75: 919-924.

Bonilla E. Increased GABA content in caudate nucleus of rats after chronic manganese chloride administration. *J Neurochem* 1978; 31: 551-552.

Bouchard MF, Laforest F, Vandelac L, Bellinger D, Mergler D. Hair Manganese and Hyperactive Behaviors: Pilot Study of School-Age Children Exposed through Tap Water. *EHP* 2007; 115 (1): 122-127.

Bouchard MF, Sauve S, Barbeau B, Legrand M, Brodeur M, Bouffard T, Limoges E, Bellinger DC, Mergler D. Intellectual Impairment in School-Age Children Exposed to Manganese from Drinking Water. *EHP* 2011; 119 (1): 138-143.

Brenneman KA, Wong BA, Buccellato MA, Costa ER, Gross EA, Dorman DC. Direct olfactory transport of inhaled manganese ((MnCl₂)-Mn-54) to the rat brain:

Toxicokinetic investigations in a unilateral nasal occlusion model. *Toxicol App Pharmacol* 2000; 169 (3): 238-48.

Brock AA, Chapman SA, Ulman EA, Wu G. Dietary Manganese Deficiency Decreases Rat Hepatic Arginase Activity. *J. Nutr.* 1994; 124 (3): 340-344.

Brooks DJ. Neuroimaging in Parkinson's disease. *NeuroRx* 2004; 1 (2): 243-254.

Bureau MH, Olsen RW. Taurine acts on a subclass of GABAA receptors in mammalian brain in vitro. *Eur J Pharmacol Mol Pharmacol* 1991; 1: 9-16.

Burton NC, Schneider JS, Syversen T, Guilarte TR. Effects of chronic manganese exposure on glutamatergic and GABAergic neurotransmitter markers in the nonhuman primate brain. *Tox Sci* 2009; 111 (1): 131-139.

Butterworth RF, Spahr L, Fontaine S, Layrarques GP. Manganese toxicity, dopaminergic dysfunction and hepatic encephalopathy. *Metab Brain Dis* 1995; 10 (4): 259-267.

Cai T, Che H, Yao T, Chen Y, Huang C, Zhang W, Du K, Zhang J, Cao Y, Chen J, Luo W. Manganese induces tau hyperphosphorylation through the activation of ERK MAPK pathway in PC12 cells. *Toxicol. Sci.* 2011 119 (1): 169-177.

Calabresi P, Ammassari-Teule M, Gubellin P, Sancesario G, Morello M, Centonze D, Marfia GA, Saulle E, Passino E, Picconi B, Bernardi G. A synaptic

mechanism underlying the behavioral abnormalities induced by manganese intoxication. *Neurobiol Dis* 2001; 8:419-432.

Calne DB, Chu NS, Huang CC, Lu CS, Olanow W. Manganese and idiopathic parkinsonism: similarities and differences. *Neurology* 1994; 44(9): 1583–1586.

Carlsson M, Carlsson A. Interactions between glutamatergic and monoaminergic systems within the basal ganglia-implications for schizophrenia and Parkinson's disease. *Trends Neurosci.* 1990; 13: 272-276.

Castaneda TR, de Prado BM, Prieto D, Francisco M. Circadian rhythms of dopamine, glutamate and GABA in the striatum and nucleus accumbens of the awake rat: modulation by light. *J. Pineal Res* 2004; 177-185.

Cersosimo MG, Koller WC. The diagnosis of manganese-induced parkinsonism. *NeuroToxicology* 2006; 27: 340-346.

Chandra SV, Malhotra KM, Shukla GS. GABAergic neurochemistry in manganese exposed rats. *Acta Pharmacol Toxicol (Copenh)* 1982; 51 (5): 456-458.

Chen Q, Beard JL, Jones BC. Abnormal rat brain monoamine metabolism in iron deficiency anemia. *J Nutr Biochem* 1995; 6(9): 486-493.

Chen G, van den Pol AN. Presynaptic GABAB Autoreceptor Modulation of P/Q-Type Calcium Channels and GABA Release in Rat Suprachiasmatic Nucleus Neurons. *J Neurosci* 1998; 78(5): 1913-1922.

Chen MK, Lee JS, McGlothan JL, Furukawa E, Adams RJ, Alexander M, Wong DF, Guilarte TR. Acute manganese administration alters dopamine transporter levels in the non-human primate striatum. *NeuroTox* 2006; 27: 229-236.

Chen Z, Wu J, Baker GB, Parent M, Dovichi NJ. Application of capillary electrophoresis with laser-induced fluorescence detection to the determinations of biogenic amines and amino acids in brain microdialysate and homogenate samples. *J Chromatography A* 2001; 914: 293-298.

Chua AC, Morgan EH. Effects of iron deficiency and iron overload on manganese uptake and deposition in the brain and other organs of the rat. *Biol Trace Elem Res.* 1996; 55(1-2): 39-54.

Chua AC, Morgan EH. Manganese metabolism impaired in the Belgrade laboratory rat. *J Comp Physiol B.* 1997; 167 (5): 361-9.

Chun HS, Lee H, Son JH. Manganese induces endoplasmic reticulum (ER) stress and activates multiple caspases in nigral dopaminergic neuronal cells, SN4741. *Neurosci. Letters* 2001; 316: 5-8.

Copeland B, Vogelsberg V, Neff NH, Hadjiconstantinou M. Protein kinase C activation decreases dopamine uptake into striatal synaptosomes. *J Pharmacol Exp Ther* 1996; 277: 1527-1532.

Cowan DM, Zheng W, Zou Y, Shi X, Chen J, Rosenthal FS, Fan Q. Manganese exposure among smelting workers: relationship between blood manganese-iron

ratio and early onset neurobehavioral alterations. *NeuroToxicology* 2009; 30(6): 1214-1222.

Critchfield JW, Keen CL. Manganese +2 exhibits dynamic binding to multiple ligands in human plasma. *Metabolism* 1992; 41: 1087-1092.

Crossgrove JS, Allen DD, Bukaveckas BL, Rhineheimer SS, Yokel RA. Manganese distribution across the blood-brain barrier. I. Evidence for carrier-mediated influx of manganese citrate as well as manganese and manganese transferrin. *NeuroTox* 2003; 24 (1): 3-13.

Crossgrove J, Zheng W. Manganese toxicity upon overexposure. *NMR Biomed.* 2004; 17: 544-553.

Crossgorve JS, Yokel RA. Manganese distribution across the blood-brain barrier. IV. Evidence for brain influx through store-operated calcium channels. *NeuroTox* 2005; 26 (3): 297-307.

Davis CD, Greger JL. Longitudinal changes of manganese-dependent superoxide dismutase and other indexes of manganese and iron status in women. *Am. J. Clin. Nutr.* 1992; 55 (3): 747-752.

de Boer VCJ, Dihal AA, van der Woude H, Arts ICW, Wolffram S, Alink GM, Rietjens IMCM, Keijer J, Hollman PCH. Tissue Distribution of Quercetin in Rats and Pigs. *J Nutr* 2005; 135: 1617-1618.

de Haas R, Nijdam A, Westra TA, Kas MJH, Westenberg HGM. Behavioral pattern analysis and dopamine release in quinpirole-induced repetitive behavior in rats. *J Psychopharmacol* 2010; 0 (0): 1-8.

Defazio G, Soleo L, Zefferino R, Livrea P. Manganese toxicity in serumless dissociated mesencephalic and striatal primary culture. *Brain Res Bull* 1996; 40 (4): 257-262.

del Olmo N, Bustamante J, del Rio RM, Solis JM. Taurine activates GABA(A) but not GABA(B) receptors in rat hippocampal CA1 area. *Brain Res.* 2000; 864(2): 298-307.

del Olmo N, Suarez LM, Orensanz LM, Suarez F, Bustamante J, Duarte JM, Martin del Rio R, Solis JM. Role of taurine uptake on the induction of long-term synaptic potentiation. *Eur j Neurosci.* 2004; 19(7): 1875-1886.

Demougeot C, Garnier PI, Mossiat C, Bertrand N, Giroud M, Beley A, Marie C. N-Acetylaspartate, a marker of both cellular dysfunction and neuronal loss: its relevance to studies of acute brain injury. *J. Neurochem.* 2001; 77 (2): 408-415.

Dobson AW, Erikson KM, Aschner M. Manganese neurotoxicity. *Ann NY Acad Sci* 2004; 1012: 115-128.

Dorman DC, Struve MF, James RA, McManus BE, Marshall MW, Wong BA. Influence of dietary manganese on the pharmacokinetics of inhaled manganese sulfate in male CD rats. *Toxicol Sci* 2001; 60: 242-251.

Dorman DC, Brenneman KA, McElveen AM, Lynch SE, Roberts KC, Wong BA. Olfactory transport: A direct route of delivery of inhaled manganese phosphate to the rat brain. *J Toxicol and Environ Health* 2002; 65 (20): 1493-1511.

Dorman CD, Struve MF, Wong AW, Dye JA, Robertson ID. Correlation of Brain Magnetic Resonance Imaging Changes with Pallidal Manganese Concentrations in Rhesus Monkeys Following Subchronic Manganese Inhalation. *Toxicol. Sci.* 2006; 92 (1): 219-227.

Dorman CD, Struve MF, Norris A, Higgings AJ. Metabolomic Analyses of Body Fluids after Subchronic Manganese Inhalation in Rhesus Monkeys. *Toxicol. Sci.* 2008; 106 (1): 46-54.

Duffy KB, Spangler EL, Devan BD, Shukitt-Hale B, Joseph JA, Ingram DK. A blueberry-enriched diet provides cellular protection against oxidative stress and reduces a kainate-induced learning impairment in rats. *Neurobiology of Aging* 2008; 37: 304-317.

Erikson KM, Jones BC, Beard JL. Iron deficiency alters dopamine transporter functioning in rat striatum. *J Nutr* 2000; 130 (11): 2831-2837.

Erikson KM, Aschner M. Manganese causes differential regulation of glutamate transporter (GLAST) taurine transporter and metallothionein in cultured rat astrocytes. *NeuroToxicology* 2002; 23: 595-602.

Erikson KM, Shihabi ZK, Aschner JL, Aschner M. Manganese accumulates in iron deficient rat brain regions in a heterogeneous fashion and is associated with neurochemical alterations. *Biolog Trace Elem Res* 2002; 87: 143-156.

Erikson KM, Syversen T, Steinnes E, Aschner M. Globus pallidus: a target brain region for divalent metal accumulation associated with dietary iron deficiency. *J Nutr Biochem*. 2004; 15(6): 335-341.

Erikson KM, John CE, Jones SR, Aschner M. Manganese accumulation in striatum of mice exposed to toxic doses is dependent upon a functional dopamine transporter. *Environ Toxicol and Pharmacol*. 2005; 20(3): 390-4.

Erikson KM, Dorman DC, Lash LH, Aschner M. Manganese Inhalation by Rhesus Monkeys is Associated with Brain Regional Changes in Biomarkers of Neurotoxicity. *Toxicol. Sci*. 2007; 97 (2): 459-466.

Eriksson H, Gillberg PG, Aquilonius SM, Dedstrom KG, Heilbronn E. Receptor alterations in manganese intoxicated monkeys. *Arch Toxicol* 1992; 66 (5): 359-364.

Farias AC, Cunha A, Benko CR, McCracken JT, Costa MT, Farias LG, Cordeiro ML. Manganese in Children with Attention-Deficit/Hyperactivity Disorder: Relationship with Methylphenidate Exposure. *J Child Adolesc Psychopharmacol* 2010; 20 (2):113-118.

Ferriola PC, Cody V, Middleton Jr. E. Protein kinase C inhibition by plant flavonoids: Kinetic mechanisms and structure-activity relationships. *Bio Pharmacol* 1989; 38 (10): 1617-1624.

Finley JW. Manganese absorption and retention by young women is associated with serum ferritin concentration. *Am J Clin Nutr* 1999; 70: 37-43.

Finley JW. Does environmental exposure to manganese pose a health risk to healthy adults? *Nutr Rev*. 2004; 62 (4): 148-153.

Fisher NS, Jones GJ. Heavy metals and marine phytoplankton: Correlation of toxicity and sulfhydryl-binding. *J Phycol* 1981; 17: 108-111.

Fishman JB, Rubin JB, Handrahan JV, Connor JR, Fine RE. Receptor-mediated transcytosis of transferrin across the blood-brain-barrier. *J Neurosci Res* 1987; 18 (2): 299-304.

Fitsanakis VA, Au C, Erikson KM, Aschner M. The effects of manganese on glutamate, dopamine and γ -aminobutyric acid regulation. *Neurochem Int* 2006; 48: 426-433.

Fitsanakis VA, Zhang N, Anderson JG, Erikson KM, Avison MJ, Gore JC, Aschner M. Measuring brain manganese and iron accumulation in rats following 14 weeks of low-dose manganese treatment using atomic absorption spectroscopy and magnetic resonance imaging. *Toxicol Sci*. 2008; 103(1): 116-124.

Flagel SB, Robinson TE. Quantifying the psychomotor activating effects of cocaine in the rat. *Behav Pharmacol* 2007; 18:297-302.

Fordahl SC, Anderson JG, Cooney PT, Weaver TL, Colyer CL, Erikson KM. Manganese exposure inhibits the clearance of extracellular GABA and influences taurine homeostasis in the striatum of developing rats. *NeuroTox* 2010; 31: 639-646.

Fordahl S, Cooney P, Qiu Y, Xie G, Jia W, Erikson KM. Waterborne manganese exposure alters plasma, brain, and liver metabolites accompanied by changes in stereotypic behaviors. *Neurotoxicol Teratol* 2012; 34: 27-36.

Foster JD, Vaughan RA. Palmitoylation controls dopamine transporter kinetics, degradation, and protein kinase C-dependent regulation. *J Biol Chem.* 2011; 286 (7): 5175-5186

Freeland-Graves JH, Turnlund JR. Deliberations and evaluations of the approaches, endpoints and paradigms for manganese and molybdenum dietary recommendations. *J of Nutr* 1996; 126 (9): S2435-40.

Gadea A, López-Colomé AM. Glial transporters for glutamate, glycine, and GABA: II. GABA transporters. *J Neurosci Res* 2001; 63:461-468.

Garcia SJ, Gellein K, Syversen T, Aschner M. A manganese enhanced diet alters brain metals and transporters in the developing rat. *Tox Sci* 2006; 92: 516-525.

Garcia et al SJ, Gellein K, Syversen T, Aschner M. Iron deficient and manganese supplemented diets alter metals and transporters in the developing rat brain. *Toxicol Sci* 2007; 95: 205-214.

Garrick MD, Dolan KG, Horbinski C, Ghio AJ, Higgins D, Porubcin M, Moore EG, Hainsworth LN, Umbreit JN, Conrad ME, Feng L, Lis A, Roth JA, Singleton S, Garrick LM. DMT1: a mammalian transporter for multiple metals. *BioMetals* 2003; 16: 41-54.

Gianutsos G, Murray MT. Alterations in brain dopamine and GABA following inorganic or organic manganese administration. *NeuroToxicology* 1982; 3: 75-81.

Gianutsos G, Seltzer MD, Saymeh R, Wu MW, Michel RG. Brain manganese accumulation following systemic administration of different forms. *Arch Toxicol* 1985; 57: 272-275.

Gibson RS. Content and bioavailability of trace elements in vegetarian diets. *Am J Clin Nutr* 1994; 59: 1223s-1232s.

Grabauskas G. Time course of GABA in the synaptic clefts of inhibitory synapses in the rostral nucleus of the solitary tract. *Neurosci Letters* 2005; 373: 10-15.

Guilarte TR, McGlothlan JL, Degaonkar M, Chen MK, Barker PB, Syversen T, Schneider JS. Evidence for Cortical Dysfunction and Widespread Manganese Accumulation in the Nonhuman Primate Brain following Chronic Manganese Exposure: A ¹H-MRS and MRI Study. *Toxicol. Sci.* 2006; 94 (2): 351-358.

Gunshin H, Allerson CR, Polycarpou-Schwarz M, Rofts A, Rogers JT, Kishi F, Hentze MW, Rouault TA, Andrews NC, Hediger MA. Iron-dependent regulation of the divalent metal ion transporter. *FEBS Lett* 2001; 509: 309-316.

Gunter TE, Yule DI, Gunter KK, Eliseev RA, Salter JD. Calcium and Mitochondria. *FEBS Lett.* 2004; 567 (1): 96-102.

Gwiazda RH, Lee D, Sheridan J, Smith DR. Low cumulative manganese exposure affects striatal GABA but not dopamine. *NeuroToxicology* 2002; 23: 69-76.

Halket JM, Waterman D, Przyborowska AM, Patel RKP, Fraser PD, Bramley PM. Chemical derivatization and mass spectral libraries in metabolic profiling by GC/MS and LC/MS/MS. *J. Exp. Botany* 2005; 56 (410): 219-243.

Harkness JE, Wagner JE 1989, *The Biology and Medicine of Rabbits and Rodents*; 3rd Edition, Lea and Febiger, Philadelphia

Hernandes MS, Troncone LRP. Glycine as a neurotransmitter in the forebrain: a short review. *J Neural Transm* 2009; 116: 1551-1560.

Hernandez EH, Discalzi G, Valentini C, Venturi F, Chio A, Carmellino C, Rossi L, Sacchetti A, Pira E. Follow-up of patients affected by manganese-induced Parkinsonism after treatment with CaNa₂-EDTA. *Neurotoxicology* 2006; 27: 333-9.

HMDB (2011). Human Metabolome Database Web site. <http://www.hmdb.ca/>

Accessed: January 18, 2011.

Hochberg F, Miller G, Valenzuela R, McNelis S, Crump KS, Covington T, Valdivia G, Hochberg B, Trustman JW. Late motor deficits of Chilean manganese miners: A blinded control study. *Neurology* 1996; 47(3): 788-95.

Hood S, Cassidy P, Cossette MP, Weigl Y, Verwey M, Robinson B, Stewart J, Amir S. Endogenous Dopamine Regulates the Rhythm of Expression of Clock Protein PER2 in the Rat Dorsal Striatum via Daily Activation of D₂ Dopamine Receptors. *J Neurosci.* 2010; 30 (40): 14016-14058.

Huang CC, Weng YH, Lu CS, Chu NS, Yen TC. Dopamine transporter binding in chronic manganese intoxication. *Neurology* 2003; 250 (11): 1335-1339.

Hulbert AJ, Turner N, Storlein LH, Else P. Dietary fats and membrane function: implications for metabolism and disease. *Biol Reviews* 2005; 80 (1): 155-169.

Hurley LS, Keen CL. Manganese, in *Trace Elements in Human Health and Animal Nutrition*, E. Underwood and W. Mertz, eds., Academic, New York, pp. 185-223 (1987).

Hurrell RF. Phytic acid degradation as a means of improving iron absorption. *Int J for Vit and Nutr Res* 2004; 74 (6): 445-52.

Ingersol RT, Montgomery EB Jr, Aposhian HV. Central nervous system toxicity of manganese. II: Cocaine or reserpine inhibit manganese concentration in the rat brain. *NeuroTox* 1999; 20 (2-3): 467-476.

Iversen LL. Role of Transmitter Uptake Mechanisms in Synaptic Neurotransmission. *British Journal of Pharmacology* 1971; 41: 571–591.

Jia F, Yue M, Chandra D, Keramidas A, Goldstein PA, Homanics GE, Harrison NL. Taurine is a potent activator of extrasynaptic GABA(A) receptors in the thalamus. *J Neurosci*. 2008; 28(1): 106-115.

Jiang YM, Mo XA, Du FQ, Fu X, Zhu XY, Gao HY, Xie JL, Liao FL, Pira E, Zheng W. Effective Treatment of Manganese-Induced Occupational Parkinsonism With p-Aminosalicylic Acid: A Case of 17-Year Follow-Up Study. *J Occup Environ Med*. 2006; 48: 644-49.

Jin HL, Jones EE. Studies on the Purification and Partial Characterization of Cysteinesulfinic Acid Decarboxylase from Porcine Liver. *J Biochem Mol Biol*. 1996; 29(4): 335-342.

Kamisaki Y, Maeda K, Ishimura M, Omura H, Itoh T. Effects of taurine on depolarization-evoked release of amino acids from rat cortical synaptosomes. *Brain Res*. 1993; 627(2): 181-185.

Kawamura R, Ikuta H, Fukuzumi S, Yamada R, Tsubaki S. Intoxication by manganese in well water. *Kitasato Arch Exp Med* 1941; 18:145-171.

Kern CH, Smith DR. Prewaning Mn exposure leads to prolonged astrocyte activation and lasting effects of dopaminergic system in adult male rats. *Synapse* 2011; 65: 532-544.

Kern CH, Stanwood GD, Smith DR. Prewaning Manganese Exposure causes Hyperactivity, Disinhibition, and Spatial Learning and Memory Devicits Associated With Altered Dopamine Receptor and Transporter Levels. *Synapse* 2010; 64: 363-378.

Kersanté F, Rowley SC, Pavlov I, Gutiérrez-Macinas M, Semyanov A, Reul J M.H.M, Walker MC, Linthorst A C.E. A functional role for both GABA transporter-1 and GABA transporter-3 in the modulation of extracellular GABA and GABAergic tonic conductances in the rat hippocampus. *J Physiol* 2012; 591 (10): 2429-2441.

Kessler KR, Wunderlich G, Hefter H, Seitz RJ. Secondary progressive chronic manganism associated with markedly decreased striatal D2 receptor density. *Mov Disord* 2003; 18 (2): 217-218.

Khan WA, Blobe GC, Hannun YA. Activation of Protein Kinase C by Oleic Acid. *J Biol Chem* 1992; 267 (6): 3605-3612.

Kim JW, Kim Y, Cheong HK, Ito K. Manganese induced parkinsonism: A case report. *J Korean Med Sci* 1998; 13: 437-439.

Kim Y, Kim JW, Ito K, Hisanaga N, Cheong HK, Kim KS, Moon Y. Positron Emission Tomography (PET) in Differentiating Manganism from Idiopathic Parkinsonism. *J Occup Health* 1999; 41: 91-94.

Kim YS, Maruvada P, Milner JA. Metabolimics in biomarker discovery: future uses for cancer prevention. *Future Oncol.* 2008; 4 (1): 93-102.

Kitazawa M, Anantharam V, Yang Y, Hirata Y, Kanthasamy A, Kanthasamy AG. Activation of protein kinase C δ by proteolytic cleavage contributes to manganese-induced apoptosis in dopaminergic cells: protective role of Bcl-2. *Biochem Pharmacol* 2005; 69: 133-146.

Koch GL. The endoplasmic reticulum and calcium storage. *Bioessays* 1990; 12 (11): 527-531.

Kong WX, Chen SW, Li YL, Zhang YJ, Wang R, Min L, Mi X. Effects of taurine on rat behaviors in three anxiety models. *Pharmacol Biochem Behav.* 2006; 83 (2): 271-276.

Kovacosova M, Barta A, Parohova J, Vrankova S, and Pechanova O. Neuroprotective Mechanisms of Natural Polyphenolic Compounds. *Act Nerv Super Rediviva* 2010; 52 (3): 181-186.

Kris-Etherton PM, Hecker KD, Bonanome A, Coval SM, Binkoski AE, Hilpert KF, Griel AE, Etherton TD. Bioactive Compounds in Foods: Their Role in the

Prevention of Cardiovascular Disease and Cancer. *Am J Med.* 2002; 113 (9B): 71S-88S.

Krogsgaard-Larsen P. Inhibitors of the GABA uptake systems. *Mol Cell Biochem.* 1980; 31 (2): 105-121.

Krogsgaard-Larsen P, Frolund B, Frydenvang K. GABA uptake inhibitors. Design, molecular pharmacology and therapeutic aspects. *Curr Pharm Des.* 2000; 6(12): 1193-1209.

Lambert IH. Regulation of the Cellular Content of the Organic Osmolyte Taurine in Mammalian Cells *Neurochem Res.* 2004; 29(1): 27-63.

Lang F. Mechanisms and significance of cell volume regulation. *J Am Coll Nutr.* 2007; 26 (5suppl): 613S-623S

Latchoumycandane C, Anantharam V, Kitazawa M, Yang Y, Kanthasamy A, Kanthasamy AG. Protein kinase C δ is a key downstream mediator of manganese-induced apoptosis in dopaminergic neuronal cells. *J Pharmacol Exper Therap* 2005; 313:46-55.

Leavens TL, Rao D, Andersen ME, Dorman DC. Evaluating transport of manganese from olfactory mucosa to striatum by pharmacokinetic modeling. *Toxicol Sci* 2007; 97 (2): 265-78.

Li R, Peng N, Li X, Le W. (-)-Epigallocatechin gallate regulates dopamine transporter internalization via protein kinase C-dependent pathway. *Brain Res.* 2006; 1097: 85-89.

Lipe GW, Duhart H, Newport GD, Slikker W Jr., Ali SF. Effect of manganese on the concentration of amino acids in different regions of the rat brain. *J Environ Sci Health* 1999; B34 (1): 119-132.

Liu HM, Tsai SJ, Chen FC, Chung SY. Determination of trace manganese in the brain of mice subjected to manganese deposition by graphite furnace atomic absorption spectrometry. *Analytica Chimica Acta* 2000; 405: 197-203.

Loder MK, Melikian HE. The dopamine transporter constitutively internalizes and recycles in a protein kinase C-regulated manner in stably transfected PC12 cell lines. *J Biol Chem* 2003; 278: 22168-22174.

Malecki EA. Manganese toxicity is associated with mitochondrial dysfunction and DNA fragmentation in rat primary striatal neurons. *Brain Res Bulletin* 2001; 55 (2): 225-228.

Mandela P, Ordway GA. The norepinephrine transporter and its regulation. *J Neurochem* 2006; 97:310-33.

Meyer-Baron M, Knapp G, Schäper M, van Thriel C. Performance alterations associated with occupational exposure to manganese – a meta-analysis. *Neurotoxicology* 2009; 30 (4): 487-496.

McDougall SA, Reichel CM, Farley CM, Flesher MM, Der-Ghazarian T, Cortez AM, Wacan JJ, Martinez CE, Varela FA, Butt AE, Crawford CA. Postnatal manganese exposure alters dopamine transporter function in adult rats: potential impact on nonassociative and associative processes. *Neurosci* 2008; 154: 848-860.

McDougall SA, Der-Ghazarian T, Britt CE, Varela FA, Crawford CA. Postnatal manganese exposure alters the expression of D2L and D2S receptor isoforms: Relationship to PKA activity and Akt levels. *Synapse* 2011; 65 (7): 583-591.

Milatovic D, Yin Z, Gupta RC, Sidoryk M, Albrecht J, Aschner JL, Aschner M. Manganese Induces Oxidative Impairment in Cultured Rat Astrocytes. *Tox Sci* 2007; 98 (1): 198-205.

Milatovic D, Zaja-Milatovic S, Gupta RC, Yu Y, Aschner M. Oxidative damage and neurodegeneration in manganese-induced neurotoxicity. *Toxicol App Pharmacol* 2009; 240: 219-225.

Melikian HE. Neurotransmitter transporter trafficking: endocytosis, recycling, and regulation. *Pharmacology & Therapeutics* 2004; 104: 17-27.

Melikian HE, Buckley KM. Membrane trafficking regulates the activity of the human dopamine transporter. *J Neurosci* 1999; 19: 7699-7710.

Minelli A, Brecha NC, Karschin C, DeBiasi S, Conti F. GAT-1, a high-affinity GABA plasma membrane transporter, is localized to neurons and astroglia in the cerebral cortex. *J Neurosci* 1995; 15 (11): 7734-7746.

Molchanova S, Oja SS, Saransaari P. Characteristics of basal taurine release in the striatum measured by microdialysis. *Amino Acids* 2004; 27(3-4): 261-268.

Mongin AA, Reddi JM, Charniga C, Kimelberg H. [3H]taurine and D-[3H]aspartate release from astrocyte cultures are differently regulated by tyrosine kinases. *Am J Physiol Cell Physiol* 1999; 276: 1226-1230.

Mortensen OV, Larsen MB, Prasad BM, Amara SG. Genetic Complementation Screen Identifies a Mitogen-activated Protein Kinase Phosphatase, MKP3, as a Regulator of Dopamine Transporter Trafficking. *Mol Biol of the Cell* 2008; 19: 2818-2829.

Mustafa SJ, Chandra SV. Levels of 5-hydroxytryptamine, dopamine and norepinephrine in whole brain of rabbits in chronic manganese toxicity. *J Neurochem* 1971; 18 (6): 931-933.

Nam J, Kim K. Abnormal motor function and the expression of striatal dopamine D2 receptors in manganese-treated mice. *Biol Pharm Bull* 2008; 31 (10): 1894-1897.

Namima M, Okamoto K, Sakai Y. Taurine acts on presynaptic autoreceptors for GABA in the cerebellum: Effects on Ca²⁺ influx and GABA release. *Japan. J. Pharmacol.* 1982; 32: 746-749.

Namima M, Okamoto K, Sakai Y. Modulatory Action of Taurine on the Release of GABA in Cerebellar Slices of the Guinea Pig. *J Neurochem.* 1983; 40: 1-9.

National Academy of Science, 2002. Dietary Reference Intakes for Vitamin A, Vitamin K, Arsenic, Boron, Chromium, Copper, Iodine, Iron, Manganese, Molybdenum, Nickel, Silicon, Vanadium, Zinc. Available at www.nap.edu/books/0309072794/html/.

Natsume Y, Ito S, Satsu H, Shimizu M. Protective effect of quercetin on ER stress caused by calcium dynamics dysregulation in intestinal epithelial cells. *Toxicology* 2009; 258: 164-175.

Neff NH, Barrett RE, Costa E. Selective depletion of caudate nucleus dopamine and serotonin during chronic manganese dioxide administration to squirrel monkeys. *Experientia* 1969; 25 (11): 1140-1141.

Nelson C, Erikson K, Pinero DJ, Beard JL. In vivo dopamine metabolism is altered in iron-deficient anemic rats. *J Nutr.* 1997; 127(12): 2282-2288.

Norregaard L, Frederiksen D, Nielsen EØ, Gether U. Delineation of an endogenous zinc-binding site in the human dopamine transporter. *EMBO J* 1998; 17 (15): 4266-4273.

North P, Fleischer S. Alteration of Synaptic Membrane Cholesterol/Phospholipid Ratio Using a Lipid Transfer Protein. *J Biol Chem* 1982; 258 (2): 1242-1253.

NTP. (1993). Toxicology and carcinogenesis studies of manganese (II) sulfate monohydrate in F344/N rats and B6C3F1 mice (feed study). National Toxicology Program. Technical Report Series 428. RISKLINE 94030007.

O'Donoghue JL. Clinical Neurologic Indices of Toxicity in Animals. *Environ Health Perspect* 1996; 104 (Suppl 2): 323-330.

Oertel WH, Mungnaini E. Immunocytochemical studies of GABAergic neurons in the rat basal ganglia and their relations to other neuronal systems. *Neurosci Lett*. 1984; 47(3): 233-238.

Oh HL, Seok JY, Kwon CH, Kang SK, Kim YK. Role of MAPK in ceramide-induced cell death in primary cultured astrocytes from mouse embryonic brain. *NeuroToxicology*. 2006; 27 (1): 31-38.

Oresic M, Vidal-Puig A, Hanninen V. Metabolomic approaches to phenotype characterization and applications to complex diseases. *Expert Rev. Mol. Diagn.* 2006; 6 (4): 575-585.

Pal PK, Samii A, Calne DB. Manganese neurotoxicity: a review of clinical features, imaging and pathology. *Neurotoxicology* 1999; 20: 227-238.

Pan L, Qiu Y, Chen T, Lin J, Chi Y, Su M, Zhao A, Jia W. An optimized procedure for metabonomic analysis of rat liver tissue using gas chromatography/time-of-flight mass spectrometry. *J. Pharm. Biomed. Anal.* 2010; 52 (4), 589–596.

Pasquali-Ronchetti I, Baccarani-Contri M. Elastic fiber during development and aging. *Microsc. Res. Techniq.* 1997; 38 (4): 428-435.

Patil S, Melrose J, Chan C. Involvement of astroglial ceramide in palmitic acid-induced Alzheimer-like changes in primary neurons. *Europ. J. Neurosci.* 2007; 26: 2131-2141.

Patil S, Balu D, Melrose J, Chan C. Brain region-specificity of palmitic acid-induced abnormalities associated with Alzheimer's disease. *BMC Res. Notes* 2008; 1: 20.

Paulke A, Eckert GP, Schubert-Zsilavec M, Wurglics M. Isoquercitrin provides better bioavailability than quercetin: comparison of quercetin metabolites in body tissue and brain sections after six days administration of isoquercitrin and quercetin. *Pharmazie.* 2012; 67 (12) 991-996.

Paxinos G, Watson C. *The rat brain in stereotaxic coordinates.* Academic Press Inc, San Diego, CA. 1998.

Perl DP, Olanow CW. The neuropathology of manganese-induced Parkinsonism. *J Neuropathol Exp Neurol.* 2007; 66(8): 675-682.

Powell PR, Ewing AG. Recent advances in the application of capillary electrophoresis to neuroscience. *Anal Bioanal Chem.* 2005; 382(3): 581-591.

Pradat PF, Dib M. Biomarkers in amyotrophic lateral sclerosis: facts and future horizons. *Mol. Diagn. Therapy* 2009; 13 (2): 115-125.

Qiu Y, Cai G, Su M, Chen T, Zheng X, Xu Y, Ni Y, Zhao A, Xu LX, Cai S, Jia W. Serum metabolite profiling of human colorectal cancer using GC-TOFMS and UPLC-QTOFMS. *J. Proteome Res.* 2009; 8 (10), 4844–4850.

Quick MW, Corey JL, Davidson N, Lester HA. Second messengers, trafficking-related proteins, and amino acid residues that contribute to the functional regulation of the rat brain GABA transporter GAT1. *J Neurosci* 1997; 17: 2967-2979.

Quick MW, Hu J, Wang D, Zhang HY. Regulation of a γ -Aminobutyric Acid Transporter by Reciprocal Tyrosine and Serine Phosphorylation. *J Biol Chem* 2004; 279 (16), 15961-15967.

Quick MW. The role of SNARE proteins in trafficking and function of neurotransmitter transporters. *Handb Exp Pharmacol* 2006; 175: 181-196.

Ragheb R, Shanab GML, Medhat AM, Seoudi DM, Adeli D, Fantus IG. Free fatty acid-induced muscle insulin resistance and glucose uptake dysfunction: Evidence for PKC activation and oxidative stress-activated signaling pathways. *Biochim Biophys Res Comm* 2009; 389: 211-216.

Rama Rao K, Norenberg MD. Manganese Induces the Mitochondrial Permeability Transition in Cultured Astrocytes. *J of Biol Chem.* 2004; 279 (31): 32333-38.

Rhoads DE, Kaplan MA, Peterson NA, Raghupathy E. Effects of Free Fatty Acids on Synaptosomal Amino Acid Uptake Systems. *J Neurochem* 1982; 38: 1255-1260.

Robinson MB. Regulated trafficking of neurotransmitter transporters: common notes but different melodies. *J Neurochem* 2002; 80: 1-11.

Ronchetti IP, Contri MB. Elastic Fiber During Development and Aging. *Microsc Res Tech* 1997; 38: 428-435.

Reghunandanan V, Reghunandanan R. Neurotransmitters of the suprachiasmatic nuclei. *J Circadian Rhythm* 2006; 4 (2): 1-20.

Sahni V, Léger Y, Panaro L, Allen M, Giffin S, Fury D, and Hamm N. Case report: a metabolic disorder presenting as pediatric manganism. *Environ Health Perspect* 2007; 115: 1176-9.

Sato K, Betz H, Schloss P. The recombinant GABA transporter GAT1 is downregulated upon activation of protein kinase C. *FEBS Letters* 1995; 375(1-2): 99-102.

Scalbert A, Williamson G. Dietary intake and bioavailability of polyphenols. *J Nutr.* 2000; 130 (8S Suppl): 2073S-2085S.

Schetz JA, Sibley DR. Zinc Allosterically Modulates Antagonist Binding to Cloned D₁ and D₂ Dopamine Receptors. *J Neurochem* 1997; 68: 1990-1997.

Schneider JS, Decamp E, Koser AJ, Fritz S, Gonczi H, Syversen T, Guilarte TR. Effects of Chronic Manganese Exposure on Cognitive and Motor Functioning in Non-Human Primates. *Brain Res.* 2006; 1118 (1): 222-231

Schumann J, Leichtle A, Thiery J, Fuhrmann H. Fatty Acid and Peptide Profiles in Plasma membrane and Membrane Rafts of PUFA Supplemented RAW264.7 Macrophages. *PLOS One* 2011; 6 (8): e24066.

Scorpio RM, Masoro EJ. Differences between Manganese and Magnesium Ions with Regard to Fatty Acid Biosynthesis, Acetyl-Coenzyme A Carboxylase Activity and Malonyl-Coenzyme A Decarboxylation. *Biochim. J.* 1970; 118: 391-399.

Scheer FA, Kalsbeek A, Buijs RM. Cardiovascular control by the suprachiasmatic nucleus: neural and neuroendocrine mechanisms in human and rat. *Biol Chem* 2003; 384: 697-709.

Shobab LA, Hsiung GYR, Feldman HH. Cholesterol in Alzheimer's disease. *Lancet Neurol.* 2005; 4: 841-852.

Sidoryk-Wegrzynowicz M, Lee E, Mingwei N, Aschner M. Disruption of Astrocytic Glutamine Turnover by Manganese Is Mediated by the Protein Kinase C Pathway. *Glia* 2011; 59: 1732-1743.

Sriram K, Lin GX, Jefferson AM, Roberts JR, Chapman RS, Chen BT, Soukup JM, Ghio AJ, Antonini JM. Dopaminergic neurotoxicity following pulmonary exposure to manganese-containing welding fumes. *Arch Toxicol* 2010; 84: 521-540.

Steele AD, Jackson WS, King OD, Lindquist S. The power of automated high-resolution behavior analysis revealed by its application to mouse models of Huntington's and prion diseases. *PNAS* 2007; 104:1983-1988.

Suzuki K, Miyamoto M, Miyamoto T, Iwanami M, Hirata K. Sleep disturbances associated with Parkinson's Disease. *Parkinsons Dis.* 2011 (219056): 1-10.

Suzuki Y, Mouri T, Suzuki Y, Nishiyama K, Fujii N. Study of subacute toxicity of manganese dioxide in monkeys. *Tokushima J Exp Med.* 1975; 22: 5-10.

Takeda A, Sotogaku N, Oku N. Manganese influences the levels of neurotransmitters in synapses in rat brain, *Neurosci* 2002; 114: 669-674.

Takeda A, Sotogaku N, Oku N. Influence of manganese on the release of neurotransmitters in rat striatum. *Brain Res.* 2003; 965: 279-282.

Tang WX, Hsu CC, Sun Y, Wu E, Yang CY, Wu JY. Multiplicity of Brain Cysteine Sulfinic Acid Decarboxylase – Purification, Characterization and Subunit Structure. *J Biomed Sci.* 1996; 3: 442-453.

Tantral L, Malathi K, Kohyama S, Silane M, Berenstein A, Jayaraman T. Intracellular calcium release is required for caspase-3 and -9 activation. *Cell Biochem Funct.* 2004; 22 (1): 35-40.

Tappaz M, Almarghini K, Legay F, Remy A. Taurine Biosynthesis Enzyme Cysteine Sulfinic Acid Decarboxylase (CSD) from Brain : The Long Tricky Trail to Identification. *Neurochem Res.* 1992; 17(9): 849-859.

Tjalkens RB, Zoran MJ, Mohl B, Barhoumi R. Manganese suppresses ATP-dependent intercellular calcium waves in astrocyte networks through alteration of mitochondrial and endoplasmic reticulum calcium dynamics. *Brain Res.* 2006; 1113: 210-219.

Tong-un T, Muchimapura S, Wattanathorn J, Phachonpai W. Nasal Administration of Quercetin Liposomes Improves Memory Impairment and Neurodegeneration in Animal Model of Alzheimer's Disease. *American Journal of Agricultural and Biological Sciences* 2010; 5 (3): 286-293.

Torres GE, Gainetdinov RR, Caron MG. Plasma membrane monoamine transporters: structure, regulation and function. *Nat Rev Neurosci* 2003; 4 (1): 13-25.

Troeger MB, Rafalowska U, Erecińska M. Effect of Oleate on Neurotransmitter Transport and Other Plasma Membrane Functions in Rat Brain Synaptosomes. *J Neurochem* 1984; 42: 1735-1742.

Uchino A, Noguchi T, Nomiyama K, Takase Y, Nakazono T, Nojiri J, Kudo S. Manganese accumulation in the brain: MR imaging. *Neuroradiology* 2007; 49: 715-720.

Vacher CM, Gassmann M, Desrayaud S, Challet E, Bradaia A, Hoyer D, Waldmeier P, Kaupmann K, Pevert P, Bettler B. Hyperdopaminergia and altered locomotor activity in GABAB1-deficient mice. *J Neurochem* 2006; 97: 979-991.

Verkhatsky A. Endoplasmic reticulum calcium signaling in nerve cells. *Riol Res.* 2004; 37 (4): 693-699.

Wagner S, Sagiv N, Yarom Y. GABA-induced current and circadian regulation of chloride in neurones of the rat suprachiasmatic nucleus. *J Physiol* 2001; 537.3: 853-869.

Wang D, Deken SL, Whitworth TL, Quick MW. Syntaxin 1A Inhibits GABA Flux, Efflux, and Exchange Mediated by the Rat Brain GABA Transporter GAT1. *Mol Pharmacol* 2003; 64 (4): 905-913.

Wang D, Quick MW. Trafficking of the plasma membrane GABA transporter GAT1: Size and rates of an acutely recycling pool. *J Biol Chem* 2005; 280 (19): 18703-18709.

Wang DD, Bordey A. The astrocyte odyssey. *Prog Neurobiol.* 2008; 86(4): 342-367.

Wasserman GA, Liu X, Parvez F, Ahsan H, Levy D, Factor-Litvak P, Kline J, van Geen A, Slavkovich V, Lolocono NJ, Cheng Z, Zheng Y, and Graziano JH. Water Manganese Exposure and Children's Intellectual Function in Araihaazar, Bangladesh. *Health Perspect* 2006; 114: 124-129.

Whitworth TL, Quick MW. Substrait-induced Regulation of γ -Aminobutyric Acid Transporter Trafficking Requires Tyrosine Phosphorylation. *J Biol Chem* 2001; 276 (46), 42932-42937.

Wiesinger JA, Buwen JP, Cifelli CJ, Unger EL, Jones BC, Beard JL. Down-regulation of dopamine transporter by iron chelation in vitro is mediated by altered trafficking, not synthesis. *J Neurochem* 2007; 100: 167-179.

Witholt R, Gwiazda RH, Smith DR. The neurobehavioral effects of subchronic manganese exposure in the presence and absence of pre-parkinsonism. *Neurotox Teratol* 2000; 22: 851-61.

Xu H, Wang W, Tang ZQ, Xu TL, Chen L. Taurine acts as a glycine receptor agonist in slices of rat inferior colliculus. *Hearing Research* 2006; 220: 95-105.

Yiin SJ, Lin TH, Shih TS. Lipid peroxidation in workers exposed to manganese. *Scand J Work Environ Health* 1996; 22 (5): 381-386.

Yoon H, Kim DS, Lee GH, Kim KW, Kim HR, Chae HJ. Apoptosis Induced by Manganese on Neuronal SK-N-MC Cell Line: Endoplasmic Reticulum (ER) Stress and Mitochondria Dysfunction. *Environ Health Tox* 2011; 26: e2011017.

Youdim MB, Green AR, Bloomfield MR, Mitchell BD, Heal DJ, Grahame-Smith DG. The effects of iron deficiency on brain biogenic monoamine biochemistry and function in rats. *Neuropharmacol* 1980; 19: 259-267.

Youdim MB, Yehuda S. Iron Deficiency Induces Reversal of Dopamine Dependent Circadian Cycles: Differential Resonse to d-Amphetamine and TRH. *Peptides* 1985; 6: 851-855.

Zhang S, Fu J, Zhou. In vitro effect of manganese chloride exposure on reactive oxygen species generation and respiratory chain complexes activities of mitochondria isolated from rat brain. *Toxicol In Vitro*. 2004; 18 (1): 71-7

Zoller H, Pietrangelo A, Vogel W, Weiss G. Duodenal metal-transporter (DMT-1, NRAMP-2) expression in patients with hereditary haemochromatosis. *Lancet* 1999; 353 (9170); 2120-3.

Zomot E, Kanner BI. The Interaction of the γ -Aminobutyric Acid Transporter GAT-1 with the Neurotransmitter Is Selectively Impaired by Sulfhydryl Modification of a Conformationally Sensitive Cysteine Residue Engineered into Extracellular Loop IV. *J Biol Chem* 2003; 278: 42950-42958.

APPENDIX A
COPYRIGHT LICENSES

**SPRINGER LICENSE
TERMS AND CONDITIONS**

Aug 02, 2013

This is a License Agreement between Steve Fordahl ("You") and Springer ("Springer") provided by Copyright Clearance Center ("CCC"). The license consists of your order details, the terms and conditions provided by Springer, and the payment terms and conditions.

All payments must be made in full to CCC. For payment instructions, please see information listed at the bottom of this form.

License Number	3200920214821
License date	Aug 02, 2013
Licensed content publisher	Springer
Licensed content publication	Springer eBook
Licensed content title	The Neurochemical Alterations Associated with Manganese Toxicity
Licensed content author	Steven C. Fordahl
Licensed content date	Jan 1, 2012
Type of Use	Thesis/Dissertation
Portion	Full text
Number of copies	5
Author of this Springer article	Yes and you are the sole author of the new work
Order reference number	
Title of your thesis / dissertation	Manganese neurotoxicity and the (gamma)-aminobutyric acid (GABA) transport system.
Expected completion date	Dec 2013
Estimated size(pages)	150
Total	0.00 USD
Terms and Conditions	

Introduction

The publisher for this copyrighted material is Springer Science + Business Media. By clicking "accept" in connection with completing this licensing transaction, you agree that

the following terms and conditions apply to this transaction (along with the Billing and Payment terms and conditions established by Copyright Clearance Center, Inc. ("CCC"), at the time that you opened your Rightslink account and that are available at any time at <http://myaccount.copyright.com>).

Limited License

With reference to your request to reprint in your thesis material on which Springer Science and Business Media control the copyright, permission is granted, free of charge, for the use indicated in your enquiry.

Licenses are for one-time use only with a maximum distribution equal to the number that you identified in the licensing process.

This License includes use in an electronic form, provided its password protected or on the university's intranet or repository, including UMI (according to the definition at the Sherpa website: <http://www.sherpa.ac.uk/romeo/>). For any other electronic use, please contact Springer at (permissions.dordrecht@springer.com or permissions.heidelberg@springer.com).

The material can only be used for the purpose of defending your thesis, and with a maximum of 100 extra copies in paper.

Although Springer holds copyright to the material and is entitled to negotiate on rights, this license is only valid, subject to a courtesy information to the author (address is given with the article/chapter) and provided it concerns original material which does not carry references to other sources (if material in question appears with credit to another source, authorization from that source is required as well).

Permission free of charge on this occasion does not prejudice any rights we might have to charge for reproduction of our copyrighted material in the future.

Altering/Modifying Material: Not Permitted

You may not alter or modify the material in any manner. Abbreviations, additions, deletions and/or any other alterations shall be made only with prior written authorization of the author(s) and/or Springer Science + Business Media. (Please contact Springer at (permissions.dordrecht@springer.com or permissions.heidelberg@springer.com))

Reservation of Rights

Springer Science + Business Media reserves all rights not specifically granted in the combination of (i) the license details provided by you and accepted in the course of this licensing transaction, (ii) these terms and conditions and (iii) CCC's Billing and Payment terms and conditions.

Copyright Notice:Disclaimer

You must include the following copyright and permission notice in connection with any reproduction of the licensed material: "Springer and the original publisher /journal title, volume, year of publication, page, chapter/article title, name(s) of author(s), figure number(s), original copyright notice) is given to the publication in which the material was originally published, by adding; with kind permission from Springer Science and Business Media"

Warranties: None

Example 1: Springer Science + Business Media makes no representations or warranties with respect to the licensed material.

Example 2: Springer Science + Business Media makes no representations or warranties with respect to the licensed material and adopts on its own behalf the limitations and disclaimers established by CCC on its behalf in its Billing and Payment terms and conditions for this licensing transaction.

Indemnity

You hereby indemnify and agree to hold harmless Springer Science + Business Media and CCC, and their respective officers, directors, employees and agents, from and against any and all claims arising out of your use of the licensed material other than as specifically authorized pursuant to this license.

No Transfer of License

This license is personal to you and may not be sublicensed, assigned, or transferred by you to any other person without Springer Science + Business Media's written permission.

No Amendment Except in Writing

This license may not be amended except in a writing signed by both parties (or, in the case of Springer Science + Business Media, by CCC on Springer Science + Business Media's behalf).

Objection to Contrary Terms

Springer Science + Business Media hereby objects to any terms contained in any purchase order, acknowledgment, check endorsement or other writing prepared by you, which terms are inconsistent with these terms and conditions or CCC's Billing and Payment terms and conditions. These terms and conditions, together with CCC's Billing and Payment terms and conditions (which are incorporated herein), comprise the entire agreement between you and Springer Science + Business Media (and CCC) concerning this licensing transaction. In the event of any conflict between your obligations established by these terms and conditions and those established by CCC's Billing and Payment terms and conditions, these

terms and conditions shall control.

Jurisdiction

All disputes that may arise in connection with this present License, or the breach thereof, shall be settled exclusively by arbitration, to be held in The Netherlands, in accordance with Dutch law, and to be conducted under the Rules of the 'Netherlands Arbitrage Instituut' (Netherlands Institute of Arbitration). **OR:**

All disputes that may arise in connection with this present License, or the breach thereof, shall be settled exclusively by arbitration, to be held in the Federal Republic of Germany, in accordance with German law.

Other terms and conditions:

v1.3

If you would like to pay for this license now, please remit this license along with your payment made payable to "COPYRIGHT CLEARANCE CENTER" otherwise you will be invoiced within 48 hours of the license date. Payment should be in the form of a check or money order referencing your account number and this invoice number RLNK501082127.

Once you receive your invoice for this order, you may pay your invoice by credit card. Please follow instructions provided at that time.

**Make Payment To:
Copyright Clearance Center
Dept 001
P.O. Box 843006
Boston, MA 02284-3006**

For suggestions or comments regarding this order, contact RightsLink Customer

Support: customercare@copyright.com or +1-877-622-5543 (toll free in the US) or +1-978-646-2777.

Gratis licenses (referencing \$0 in the Total field) are free. Please retain this printable license for your reference. No payment is required.

**ELSEVIER LICENSE
TERMS AND CONDITIONS**

Aug 02, 2013

This is a License Agreement between Steve Fordahl ("You") and Elsevier ("Elsevier") provided by Copyright Clearance Center ("CCC"). The license consists of your order details, the terms and conditions provided by Elsevier, and the payment terms and conditions.

All payments must be made in full to CCC. For payment instructions, please see information listed at the bottom of this form.

Supplier	Elsevier Limited The Boulevard, Langford Lane Kidlington, Oxford, OX5 1GB, UK
Registered Company Number	1982084
Customer name	Steve Fordahl
Customer address	824 Leichester Square Ct. KERNERSVILLE, NC 27284
License number	3200911329037
License date	Aug 02, 2013
Licensed content publisher	Elsevier
Licensed content publication	NeuroToxicology
Licensed content title	Manganese exposure inhibits the clearance of extracellular GABA and influences taurine homeostasis in the striatum of developing rats
Licensed content author	Steve C. Fordahl, Joel G. Anderson, Paula T. Cooney, Tara L. Weaver, Christa L. Colyer, Keith M. Erikson
Licensed content date	December 2010
Licensed content volume number	31
Licensed content issue number	6
Number of pages	8
Start Page	639
End Page	646
Type of Use	reuse in a thesis/dissertation
Intended publisher of new work	other
Portion	full article
Format	both print and electronic
Are you the author of this Elsevier article?	Yes

Will you be translating?	No
Order reference number	
Title of your thesis/dissertation	Manganese neurotoxicity and the (gamma)-aminobutyric acid (GABA) transport system.
Expected completion date	Dec 2013
Estimated size (number of pages)	150
Elsevier VAT number	GB 494 6272 12
Permissions price	0.00 USD
VAT/Local Sales Tax	0.00 USD
Total	0.00 USD
Terms and Conditions	

INTRODUCTION

1. The publisher for this copyrighted material is Elsevier. By clicking "accept" in connection with completing this licensing transaction, you agree that the following terms and conditions apply to this transaction (along with the Billing and Payment terms and conditions established by Copyright Clearance Center, Inc. ("CCC"), at the time that you opened your Rightslink account and that are available at any time at <http://myaccount.copyright.com>).

GENERAL TERMS

2. Elsevier hereby grants you permission to reproduce the aforementioned material subject to the terms and conditions indicated.

3. Acknowledgement: If any part of the material to be used (for example, figures) has appeared in our publication with credit or acknowledgement to another source, permission must also be sought from that source. If such permission is not obtained then that material may not be included in your publication/copies. Suitable acknowledgement to the source must be made, either as a footnote or in a reference list at the end of your publication, as follows:

“Reprinted from Publication title, Vol /edition number, Author(s), Title of article / title of chapter, Pages No., Copyright (Year), with permission from Elsevier [OR APPLICABLE SOCIETY COPYRIGHT OWNER].” Also Lancet special credit - “Reprinted from The Lancet, Vol. number, Author(s), Title of article, Pages No., Copyright (Year), with permission from Elsevier.”

4. Reproduction of this material is confined to the purpose and/or media for which permission is hereby given.

5. Altering/Modifying Material: Not Permitted. However figures and illustrations may be

altered/adapted minimally to serve your work. Any other abbreviations, additions, deletions and/or any other alterations shall be made only with prior written authorization of Elsevier Ltd. (Please contact Elsevier at permissions@elsevier.com)

6. If the permission fee for the requested use of our material is waived in this instance, please be advised that your future requests for Elsevier materials may attract a fee.

7. Reservation of Rights: Publisher reserves all rights not specifically granted in the combination of (i) the license details provided by you and accepted in the course of this licensing transaction, (ii) these terms and conditions and (iii) CCC's Billing and Payment terms and conditions.

8. License Contingent Upon Payment: While you may exercise the rights licensed immediately upon issuance of the license at the end of the licensing process for the transaction, provided that you have disclosed complete and accurate details of your proposed use, no license is finally effective unless and until full payment is received from you (either by publisher or by CCC) as provided in CCC's Billing and Payment terms and conditions. If full payment is not received on a timely basis, then any license preliminarily granted shall be deemed automatically revoked and shall be void as if never granted. Further, in the event that you breach any of these terms and conditions or any of CCC's Billing and Payment terms and conditions, the license is automatically revoked and shall be void as if never granted. Use of materials as described in a revoked license, as well as any use of the materials beyond the scope of an unrevoked license, may constitute copyright infringement and publisher reserves the right to take any and all action to protect its copyright in the materials.

9. Warranties: Publisher makes no representations or warranties with respect to the licensed material.

10. Indemnity: You hereby indemnify and agree to hold harmless publisher and CCC, and their respective officers, directors, employees and agents, from and against any and all claims arising out of your use of the licensed material other than as specifically authorized pursuant to this license.

11. No Transfer of License: This license is personal to you and may not be sublicensed, assigned, or transferred by you to any other person without publisher's written permission.

12. No Amendment Except in Writing: This license may not be amended except in a writing signed by both parties (or, in the case of publisher, by CCC on publisher's behalf).

13. Objection to Contrary Terms: Publisher hereby objects to any terms contained in any purchase order, acknowledgment, check endorsement or other writing prepared by you, which terms are inconsistent with these terms and conditions or CCC's Billing and

Payment terms and conditions. These terms and conditions, together with CCC's Billing and Payment terms and conditions (which are incorporated herein), comprise the entire agreement between you and publisher (and CCC) concerning this licensing transaction. In the event of any conflict between your obligations established by these terms and conditions and those established by CCC's Billing and Payment terms and conditions, these terms and conditions shall control.

14. **Revocation:** Elsevier or Copyright Clearance Center may deny the permissions described in this License at their sole discretion, for any reason or no reason, with a full refund payable to you. Notice of such denial will be made using the contact information provided by you. Failure to receive such notice will not alter or invalidate the denial. In no event will Elsevier or Copyright Clearance Center be responsible or liable for any costs, expenses or damage incurred by you as a result of a denial of your permission request, other than a refund of the amount(s) paid by you to Elsevier and/or Copyright Clearance Center for denied permissions.

LIMITED LICENSE

The following terms and conditions apply only to specific license types:

15. **Translation:** This permission is granted for non-exclusive world **English** rights only unless your license was granted for translation rights. If you licensed translation rights you may only translate this content into the languages you requested. A professional translator must perform all translations and reproduce the content word for word preserving the integrity of the article. If this license is to re-use 1 or 2 figures then permission is granted for non-exclusive world rights in all languages.

16. **Website:** The following terms and conditions apply to electronic reserve and author websites:

Electronic reserve: If licensed material is to be posted to website, the web site is to be password-protected and made available only to bona fide students registered on a relevant course if:

This license was made in connection with a course,

This permission is granted for 1 year only. You may obtain a license for future website posting,

All content posted to the web site must maintain the copyright information line on the bottom of each image,

A hyper-text must be included to the Homepage of the journal from which you are licensing at <http://www.sciencedirect.com/science/journal/xxxxx> or the Elsevier homepage for books at <http://www.elsevier.com> , and

Central Storage: This license does not include permission for a scanned version of the material to be stored in a central repository such as that provided by Heron/XanEdu.

17. **Author website** for journals with the following additional clauses:

All content posted to the web site must maintain the copyright information line on the bottom of each image, and the permission granted is limited to the personal version of your paper. You are not allowed to download and post the published electronic version of your article (whether PDF or HTML, proof or final version), nor may you scan the printed edition to create an electronic version. A hyper-text must be included to the Homepage of the journal from which you are licensing at <http://www.sciencedirect.com/science/journal/xxxxx> . As part of our normal production process, you will receive an e-mail notice when your article appears on Elsevier's online service ScienceDirect (www.sciencedirect.com). That e-mail will include the article's Digital Object Identifier (DOI). This number provides the electronic link to the published article and should be included in the posting of your personal version. We ask that you wait until you receive this e-mail and have the DOI to do any posting.

Central Storage: This license does not include permission for a scanned version of the material to be stored in a central repository such as that provided by Heron/XanEdu.

18. **Author website** for books with the following additional clauses:

Authors are permitted to place a brief summary of their work online only.

A hyper-text must be included to the Elsevier homepage at <http://www.elsevier.com> . All content posted to the web site must maintain the copyright information line on the bottom of each image. You are not allowed to download and post the published electronic version of your chapter, nor may you scan the printed edition to create an electronic version.

Central Storage: This license does not include permission for a scanned version of the material to be stored in a central repository such as that provided by Heron/XanEdu.

19. **Website** (regular and for author): A hyper-text must be included to the Homepage of the journal from which you are licensing at <http://www.sciencedirect.com/science/journal/xxxxx> . or for books to the Elsevier homepage at <http://www.elsevier.com>

20. **Thesis/Dissertation**: If your license is for use in a thesis/dissertation your thesis may be submitted to your institution in either print or electronic form. Should your thesis be published commercially, please reapply for permission. These requirements include permission for the Library and Archives of Canada to supply single copies, on demand, of the complete thesis and include permission for UMI to supply single copies, on demand, of the complete thesis. Should your thesis be published commercially, please reapply for permission.

21. **Other Conditions**: Permission is granted to submit your article in electronic format. This license permits you to post this Elsevier article online if it is embedded within your

thesis. You are also permitted to post your Author Accepted Manuscript online however posting of the final published article is prohibited. Please refer to Elsevier's Posting Policy for further information: <http://www.elsevier.com/wps/find/authors.authors/postingpolicy>

v1.6

If you would like to pay for this license now, please remit this license along with your payment made payable to "COPYRIGHT CLEARANCE CENTER" otherwise you will be invoiced within 48 hours of the license date. Payment should be in the form of a check or money order referencing your account number and this invoice number RLNK501082123. Once you receive your invoice for this order, you may pay your invoice by credit card. Please follow instructions provided at that time.

**Make Payment To:
Copyright Clearance Center
Dept 001
P.O. Box 843006
Boston, MA 02284-3006**

For suggestions or comments regarding this order, contact RightsLink Customer Support: customercare@copyright.com or +1-877-622-5543 (toll free in the US) or +1-978-646-2777.

Gratis licenses (referencing \$0 in the Total field) are free. Please retain this printable license for your reference. No payment is required.

**ELSEVIER LICENSE
TERMS AND CONDITIONS**

Aug 02, 2013

This is a License Agreement between Steve Fordahl ("You") and Elsevier ("Elsevier") provided by Copyright Clearance Center ("CCC"). The license consists of your order details, the terms and conditions provided by Elsevier, and the payment terms and conditions.

All payments must be made in full to CCC. For payment instructions, please see information listed at the bottom of this form.

Supplier	Elsevier Limited The Boulevard, Langford Lane Kidlington, Oxford, OX5 1GB, UK
Registered Company Number	1982084
Customer name	Steve Fordahl
Customer address	824 Leichester Square Ct. KERNERSVILLE, NC 27284
License number	3195990505271
License date	Jul 25, 2013
Licensed content publisher	Elsevier
Licensed content publication	Neurotoxicology and Teratology
Licensed content title	Waterborne manganese exposure alters plasma, brain, and liver metabolites accompanied by changes in stereotypic behaviors
Licensed content author	Steve Fordahl, Paula Cooney, Yunping Qiu, Guoxiang Xie, Wei Jia, Keith M. Erikson
Licensed content date	January–February 2012
Licensed content volume number	34
Licensed content issue number	1
Number of pages	10
Start Page	27
End Page	36
Type of Use	reuse in a thesis/dissertation
Portion	full article
Format	both print and electronic
Are you the author of this Elsevier article?	Yes
Will you be translating?	No

Order reference number	
Title of your thesis/dissertation	Manganese neurotoxicity and the (gamma)-aminobutyric acid (GABA) transport system.
Expected completion date	Dec 2013
Estimated size (number of pages)	150
Elsevier VAT number	GB 494 6272 12
Permissions price	0.00 USD
VAT/Local Sales Tax	0.00 USD / 0.00 GBP
Total	0.00 USD
Terms and Conditions	

INTRODUCTION

1. The publisher for this copyrighted material is Elsevier. By clicking "accept" in connection with completing this licensing transaction, you agree that the following terms and conditions apply to this transaction (along with the Billing and Payment terms and conditions established by Copyright Clearance Center, Inc. ("CCC"), at the time that you opened your Rightslink account and that are available at any time at <http://myaccount.copyright.com>).

GENERAL TERMS

2. Elsevier hereby grants you permission to reproduce the aforementioned material subject to the terms and conditions indicated.

3. Acknowledgement: If any part of the material to be used (for example, figures) has appeared in our publication with credit or acknowledgement to another source, permission must also be sought from that source. If such permission is not obtained then that material may not be included in your publication/copies. Suitable acknowledgement to the source must be made, either as a footnote or in a reference list at the end of your publication, as follows:

“Reprinted from Publication title, Vol /edition number, Author(s), Title of article / title of chapter, Pages No., Copyright (Year), with permission from Elsevier [OR APPLICABLE SOCIETY COPYRIGHT OWNER].” Also Lancet special credit - “Reprinted from The Lancet, Vol. number, Author(s), Title of article, Pages No., Copyright (Year), with permission from Elsevier.”

4. Reproduction of this material is confined to the purpose and/or media for which permission is hereby given.

5. Altering/Modifying Material: Not Permitted. However figures and illustrations may be altered/adapted minimally to serve your work. Any other abbreviations, additions,

deletions and/or any other alterations shall be made only with prior written authorization of Elsevier Ltd. (Please contact Elsevier at permissions@elsevier.com)

6. If the permission fee for the requested use of our material is waived in this instance, please be advised that your future requests for Elsevier materials may attract a fee.

7. Reservation of Rights: Publisher reserves all rights not specifically granted in the combination of (i) the license details provided by you and accepted in the course of this licensing transaction, (ii) these terms and conditions and (iii) CCC's Billing and Payment terms and conditions.

8. License Contingent Upon Payment: While you may exercise the rights licensed immediately upon issuance of the license at the end of the licensing process for the transaction, provided that you have disclosed complete and accurate details of your proposed use, no license is finally effective unless and until full payment is received from you (either by publisher or by CCC) as provided in CCC's Billing and Payment terms and conditions. If full payment is not received on a timely basis, then any license preliminarily granted shall be deemed automatically revoked and shall be void as if never granted. Further, in the event that you breach any of these terms and conditions or any of CCC's Billing and Payment terms and conditions, the license is automatically revoked and shall be void as if never granted. Use of materials as described in a revoked license, as well as any use of the materials beyond the scope of an unrevoked license, may constitute copyright infringement and publisher reserves the right to take any and all action to protect its copyright in the materials.

9. Warranties: Publisher makes no representations or warranties with respect to the licensed material.

10. Indemnity: You hereby indemnify and agree to hold harmless publisher and CCC, and their respective officers, directors, employees and agents, from and against any and all claims arising out of your use of the licensed material other than as specifically authorized pursuant to this license.

11. No Transfer of License: This license is personal to you and may not be sublicensed, assigned, or transferred by you to any other person without publisher's written permission.

12. No Amendment Except in Writing: This license may not be amended except in a writing signed by both parties (or, in the case of publisher, by CCC on publisher's behalf).

13. Objection to Contrary Terms: Publisher hereby objects to any terms contained in any purchase order, acknowledgment, check endorsement or other writing prepared by you, which terms are inconsistent with these terms and conditions or CCC's Billing and Payment terms and conditions. These terms and conditions, together with CCC's Billing

and Payment terms and conditions (which are incorporated herein), comprise the entire agreement between you and publisher (and CCC) concerning this licensing transaction. In the event of any conflict between your obligations established by these terms and conditions and those established by CCC's Billing and Payment terms and conditions, these terms and conditions shall control.

14. **Revocation:** Elsevier or Copyright Clearance Center may deny the permissions described in this License at their sole discretion, for any reason or no reason, with a full refund payable to you. Notice of such denial will be made using the contact information provided by you. Failure to receive such notice will not alter or invalidate the denial. In no event will Elsevier or Copyright Clearance Center be responsible or liable for any costs, expenses or damage incurred by you as a result of a denial of your permission request, other than a refund of the amount(s) paid by you to Elsevier and/or Copyright Clearance Center for denied permissions.

LIMITED LICENSE

The following terms and conditions apply only to specific license types:

15. **Translation:** This permission is granted for non-exclusive world **English** rights only unless your license was granted for translation rights. If you licensed translation rights you may only translate this content into the languages you requested. A professional translator must perform all translations and reproduce the content word for word preserving the integrity of the article. If this license is to re-use 1 or 2 figures then permission is granted for non-exclusive world rights in all languages.

16. **Website:** The following terms and conditions apply to electronic reserve and author websites:

Electronic reserve: If licensed material is to be posted to website, the web site is to be password-protected and made available only to bona fide students registered on a relevant course if:

This license was made in connection with a course,

This permission is granted for 1 year only. You may obtain a license for future website posting,

All content posted to the web site must maintain the copyright information line on the bottom of each image,

A hyper-text must be included to the Homepage of the journal from which you are licensing at <http://www.sciencedirect.com/science/journal/xxxxx> or the Elsevier homepage for books at <http://www.elsevier.com> , and

Central Storage: This license does not include permission for a scanned version of the material to be stored in a central repository such as that provided by Heron/XanEdu.

17. **Author website** for journals with the following additional clauses:

All content posted to the web site must maintain the copyright information line on the bottom of each image, and the permission granted is limited to the personal version of your paper. You are not allowed to download and post the published electronic version of your article (whether PDF or HTML, proof or final version), nor may you scan the printed edition to create an electronic version. A hyper-text must be included to the Homepage of the journal from which you are licensing at <http://www.sciencedirect.com/science/journal/xxxxx>. As part of our normal production process, you will receive an e-mail notice when your article appears on Elsevier's online service ScienceDirect (www.sciencedirect.com). That e-mail will include the article's Digital Object Identifier (DOI). This number provides the electronic link to the published article and should be included in the posting of your personal version. We ask that you wait until you receive this e-mail and have the DOI to do any posting.

Central Storage: This license does not include permission for a scanned version of the material to be stored in a central repository such as that provided by Heron/XanEdu.

18. **Author website** for books with the following additional clauses:

Authors are permitted to place a brief summary of their work online only.

A hyper-text must be included to the Elsevier homepage at <http://www.elsevier.com>. All content posted to the web site must maintain the copyright information line on the bottom of each image. You are not allowed to download and post the published electronic version of your chapter, nor may you scan the printed edition to create an electronic version.

Central Storage: This license does not include permission for a scanned version of the material to be stored in a central repository such as that provided by Heron/XanEdu.

19. **Website** (regular and for author): A hyper-text must be included to the Homepage of the journal from which you are licensing at <http://www.sciencedirect.com/science/journal/xxxxx>. or for books to the Elsevier homepage at <http://www.elsevier.com>

20. **Thesis/Dissertation**: If your license is for use in a thesis/dissertation your thesis may be submitted to your institution in either print or electronic form. Should your thesis be published commercially, please reapply for permission. These requirements include permission for the Library and Archives of Canada to supply single copies, on demand, of the complete thesis and include permission for UMI to supply single copies, on demand, of the complete thesis. Should your thesis be published commercially, please reapply for permission.

21. **Other Conditions**:

v1.6

If you would like to pay for this license now, please remit this license along with your payment made payable to "COPYRIGHT CLEARANCE CENTER" otherwise you will be invoiced within 48 hours of the license date. Payment should be in the form of a check or money order referencing your account number and this invoice number RLNK501075051.

Once you receive your invoice for this order, you may pay your invoice by credit card. Please follow instructions provided at that time.

**Make Payment To:
Copyright Clearance Center
Dept 001
P.O. Box 843006
Boston, MA 02284-3006**

For suggestions or comments regarding this order, contact RightsLink Customer

Support: customercare@copyright.com or +1-877-622-5543 (toll free in the US) or +1-978-646-2777.

Gratis licenses (referencing \$0 in the Total field) are free. Please retain this printable license for your reference. No payment is required.
